Charles University

Faculty of Science

Study programme: Molecular and Cellular Biology, Genetics and Virology

Mgr. Martina Dvořáková

Functional role of SOX2 in inner ear neurosensory development

Funkční role SOX2 v neurosenzorickém vývoji vnitřního ucha

Doctoral thesis

Supervisor: RNDr. Gabriela Pavlínková, Ph.D.

Prague, 2020

Prohlášení:

Prohlašuji, že jsem závěrečnou práci zpracovala samostatně. Všechny použité informační zdroje a literatura jsou řádně citovány. Tato práce ani její podstatná část nebyla využita k získání jiného nebo stejného akademického titulu.

V Praze, 19. 5. 2020

Mgr. Martina Dvořáková

Acknowledgement

Foremost, I would like to thank my supervisor RNDr. Gabriela Pavlínková, Ph.D. for her continuous support, friendly and helpful guidance and inspiring environment she offered me in her laboratory group. I also thank all the members of the Laboratory of Molecular Pathogenetics for being always ready and willing to help and for being such friendly colleagues. I am grateful to our collaborators from other institutions and groups who contributed to this work.

Many thanks belong to my family for supporting me throughout all my studies.

Abstract

The main functional cells of the inner ear are neurons and sensory cells that are formed from a common embryonic epithelial neurosensory domain. Discovering genes important for specification and differentiation of sensory cells and neurons in the inner ear is a crucial basis for understanding the pathophysiology of hearing loss. Some of these factors are necessary not only for the inner ear but also for the development of other neurosensory systems such as the visual and olfactory system.

The aim of this work was to reveal functions of transcription factor SOX2 in inner ear development by using mouse models with different conditional deletions of *Sox2* gene. *Sox2* gene was deleted by *cre-loxP* recombination.

In *Isl1-cre, Sox2 CKO* mutant, reduced number of hair cells differentiated only in some inner ear organs (utricle, saccule and cochlear base) and not in others (cristae and cochlear apex). Early forming inner ear neurons in the vestibular ganglion and neurons innervating the cochlear base developed in these mutants but died by apoptosis due to the lack of neurotrophic support from sensory cells. Late forming neurons in the cochlear apex never formed.

In *Foxg1-cre, Sox2 CKO* mutant, only rudimental ear with no sensory cells was formed. The initial formation of vestibular ganglion with peripheral and central projections was unaffected, whereas only a few transient neurons of the spiral ganglion were detected. The near-normal formation of early neurons in these mutants suggests that SOX2 is not necessary for early ear neurogenesis. In the absence of SOX2, the early ear placode development proceeded normally but the development of lens and olfactory placodes was abolished.

Neurod1-cre mediated deletion of *Sox2* in *Neurod1-cre, Sox2 CKO* mice did not cause any changes in neurosensory development of the inner ear or hearing functions, suggesting that SOX2 is not necessary for inner ear neuronal development.

Key words: *Sox2*, *Isl1*, *Foxg1*, *Neurod1*, mouse conditional deletion, inner ear development, spiral ganglion, vestibular ganglion

Abstrakt

Neurony a senzorické buňky, které jsou hlavními funkčními buňkami vnitřního ucha, vznikají ze společné embryonální epiteliální neurosenzorické domény. K pochopení patofyziologie ztráty sluchu je klíčové identifikovat geny, které se podílí na specifikaci a diferenciaci senzorických buněk a neuronů ze společného prekurzoru. Některé z těchto faktorů jsou nezbytné nejen pro vnitřní ucho, ale také pro vývoj dalších smyslů, jako jsou zrakový a čichový systém.

Cílem této práce bylo popsat důležitost jednoho z těchto faktorů, transkripčního faktoru SOX2, ve vývoji vnitřního ucha za použití myšího modelu s různými podmíněnými delecemi genu *Sox2*. Gen *Sox2* byl deletován pomocí rekombinačního systému *cre-loxP*.

V myší linii *Isl1-cre, Sox2 CKO* vznikalo pouze malé množství vláskových buněk v některých orgánech vnitřního ucha (utrikulus, sakulus a báze kochley), zatímco ve zbývajících orgánech se vláskové buňky nediferencovaly vůbec (kristy a apex kochley). Časně se diferencující neurony vestibulárního ganglia a neurony inervující bázi kochley krátce po vzniku apopticky zanikly v důsledku chybějících neurotrofických faktorů produkovaných senzorickými buňkami. Naopak pozdně vznikající neurony v apexu kochley se u tohoto mutanta vůbec netvořily.

Delece *Sox2* u *Foxg1-cre, Sox2 CKO* způsobila vznik velmi redukovaného vnitřního ucha bez senzorických buněk. Počáteční vznik vestibulárního ganglia s periferními a centrálními neurálními projekcemi nebyl mutací ovlivněn, kdežto spirální ganglium bylo tvořeno pouze několika málo neurony s krátkou životností. Téměř normální vznik raně se vyvíjejících neuronů u tohoto mutanta ukazuje, že SOX2 není nezbytný pro časnou neurogenezi. Časný vývoj sluchové plakody probíhal při absenci SOX2 normálně, ale naopak, vývoj oční čočky a čichového systému byl zastaven.

Delece *Sox2* v neuronech vnitřního ucha pomocí *Neurod1-cre* u *Neurod1-cre, Sox2 CKO* myší neměla vliv na vývoj orgánů vnitřního ucha ani na sluchové funkce, což naznačuje, že transkripční faktor SOX2 není nezbytný pro vývoj neuronů vnitřního ucha.

Klíčová slova: *Sox2*, *Isl1*, *Foxg1*, *Neurod1*, podmíněné delece u myší, vývoj vnitřního ucha, spirální ganglium, vestibulární ganglium

List of abbreviations

Abbreviations used in the text

ABR	Auditory brainstem response
AC	Anterior crista
ASC	Anterior semicircular canal
ATOH1	Atonal homolog 1
ATP	Adenosine triphosphate
BDNF	Brain-derived neurotrophic factor
bHLH	Basic helix-loop-helix
BMP	Bone morphogenic protein
bp	Base pair
BrdU	5-bromo-2'-deoxyuridine
cDNA	Complementary DNA
CKO	Conditional knockout
DLL1	Delta-like protein1
DPOAE	Distortion product otoacoustic emissions
DSHB	Developmental Studies Hybridoma Bank
E	Embryonic day
EdU	5-ethynyl-2'-deoxyuridine
EYA1	Eyes absent homolog 1
F	Forward
f/f	Floxed/floxed
FGF	Fibroblast growth factor
FOX	Forkhead box

GBX2	Gastrulation brain homeobox 2
GER	Greater epithelial ridge
GnRH	Gonadotropin releasing hormone
HMG	High mobility group
IgG	Immunoglobulin G
IPCs	Inner pillar cells
IRX3	Iroquois homeobox 3
ISL1	Insulin gene enhancer protein ISL-1
JAG	Jagged
Lcc	Light coat and circling
LIM	LIN11, ISL1, MEC-3
MET	Mechanoelectrical transducer
MSBB	Methyl salicylate, benzyl benzoate
MYO7A	Myosin VIIA
NCC	Neural crest cells
NEC	Neuroepithelial cells
NeuN	Neuronal nuclei
NEUROD1	Neuronal differentiation 1
NF200	Neurofilament 200
NGN1	Neurogenin1
NTF3	Neurotrophin3
OTX2	Orthodenticle homeobox 2
P	Postnatal day
$P27^{Kip1}$	Cyclin-dependent kinase inhibitor 1B

P75	Low-affinity nerve growth factor receptor
PAX	Paired-box gene
PBS	Phosphate buffered saline
PCR	Polymerase chain reaction
PFA	Paraformaldehyde
PPR	Preplacodal region
R	Reverse
SD	Standard deviation
SHH	Sonic hedgehog
SIX	Sineoculis homeobox homolog
SOX	SRY-related HMG box
SRY	Sex determining region Y
SSC	Saline sodium citrate
TRK	Tyrosine receptor kinase
WNT	Wingless/Integrated
Ysb	Yellow submarine

Abbreviations used only in figures

AA	Anterior ampulla
CB	Cerebellum
CD	Cochlear duct
CE	Contralateral inner ear efferents
CN	Cochlear nucleus
ED	Endolymphatic duct

FN	Facial nerve
G	Ganglion
GG	Geniculate ganglion
H/Cl	Hensen/Claudius cells
HC	Horizontal crista
HCs	Hair cells
IE	Inner ear efferents
IHC	Inner hair cell
IN	Intermediate nerve
LA	Lateral ampulla
LSC	Lateral semicircular canal
LV	Lens vesicle
mut	Mutant
NR	Neural retina
OC	Organ of Corti
OHC	Outer hair cell
OlfP	Olfactory placode
OpV	Optic vesicle
PA	Posterior ampulla
PC	Posterior crista
PLE	Presumptive lens ectoderm
pLP	Pre-lens placode
PSC	Posterior semicircular canal
r2, r4, r6	Rhombomere 2, 4, 6

RPE	Retinal pigment epithelium
S	Saccule
SCs	Supporting cells
SG	Spiral ganglion
SPL	Sound pressure level
tel	Telencephalon
U	Utricle
VG	Vestibular ganglion
VN	Vestibular nerve
wt	Wild type
V	Trigeminal nerve (Cranial nerve V)
VIII	Vestibulocochlear nerve
IX	Glossopharyngeal nerve
X	Vagus nerve

Table of contents

1. INTRODUCTION

The main interest of this thesis is the development of the inner ear neurosensory system in the absence of Sex determining region Y (SRY) related high mobility group (HMG) box protein SOX2 (SOX2). However, the development of other neurosensory systems, such as visual and olfactory system, is similar in many aspects in requirements for SOX2. Therefore, these organs are briefly described in order to report more complexly on the distinct roles of SOX2 in neurosensory development.

1.1. Anatomy of sensory organs

1.1.1. The visual system: an overview

The mammalian eye is a spherical organ with three layers (Králíček, 2004). The outermost layer is white sclera, which is in the anterior part of the eye turning into transparent cornea (Figure 1). The middle layer, uvea, is forming iris with the round opening called pupil. Lens is positioned behind the iris. The innermost layer is called retina. Retina consists of specialized sensory neurons (rod and cone photoreceptors) forming the outer nuclear layer; interneurons (horizontal, bipolar and amacrine) that form the inner nuclear layer; and projection ganglion cells forming the ganglion cell layer (Heavner and Pevny, 2012). Together, they accomplish tasks of vision: image detection, processing and transmission.

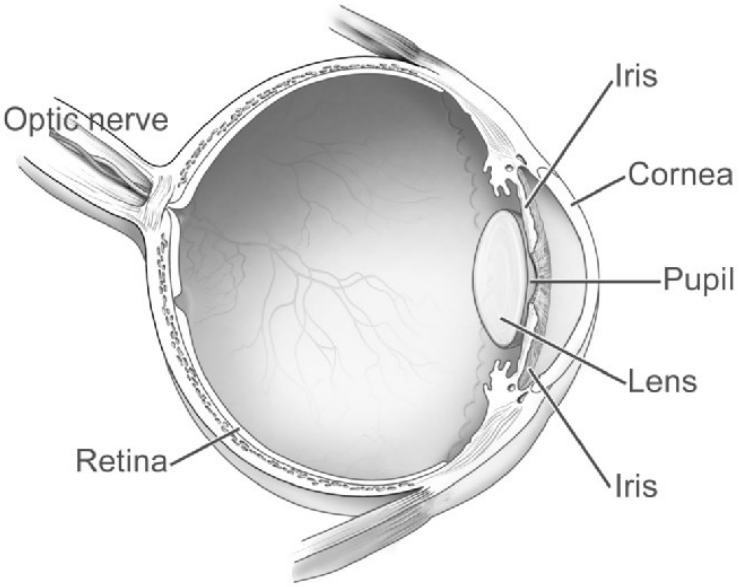

Figure 1: Eye diagram (National Eye Institute, National Institutes of Health (NationalEyeInstitute, 2012))

The observed object is projected on the retina and the light energy is transformed into electrochemical signals by photoreceptor cells (Králíček, 2004). The photoreceptor sensory cell converts light energy into a neuronal signal that is passed through the bipolar and amacrine cells to the retina ganglion cell (Remington, 2012). The axons of ganglion cells leave the retina via the optic nerve. Optic nerves from both eyes cross each other in the optic chiasm and terminate on the opposite side of the brain. Visual information is then carried to the lateral geniculate nucleus and terminates in the visual cortex of the occipital lobe.

The eyeball and its associated muscles and nerves are situated in the orbital cavity (Králíček, 2004). The extrinsic eye muscles are innervated by the oculomotor nerve and are responsible for movements of the eye, for the control of the eyelid and also for the pupillary constriction.

1.1.2. The olfactory system: an overview

Olfaction is the oldest sense (López-Elizalde *et al.*, 2018). Its afferent nerve is the only cranial nerve that lacks a precortical connection to the thalamus.

The olfactory epithelium is directly responsible for detecting odorants, chemicals diffused in the air (Králíček, 2004). These chemicals are dissolved in the mucous membrane during the sense of smell. The olfactory epithelium lies on the top of the nasal cavity and contains three types of cells: olfactory receptor cells, sustentacular (supporting) cells and basal cells (Mombaerts, 1999) (Figure 2).

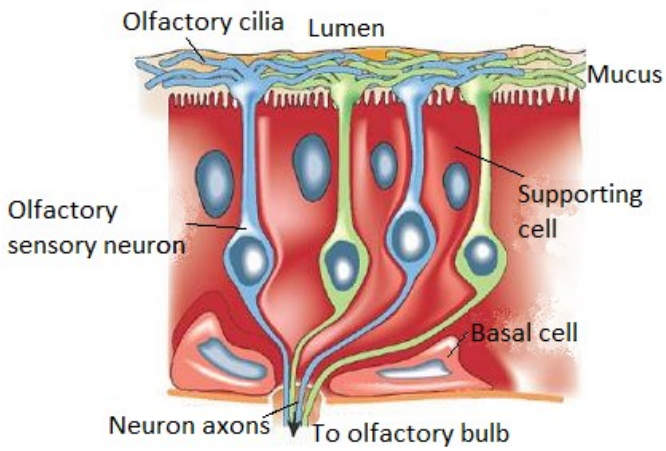

Figure 2: Olfactory epithelium (modified from (OpenWetWare, 2006))

Olfactory receptors themselves are the cells responsible for sensing smell (Králíček, 2004). They are actually modified bipolar neurons with non-motile cilia on their short dendrites (Mombaerts, 1999; Králíček, 2004). The cilia protrude from the epithelium into the airspace and detect odorants. The long unbranched, unmyelinated axons of olfactory neurons together form the olfactory nerve and terminate in the olfactory bulb of the telencephalon. Olfactory receptor cells die after several days and new receptors differentiate from the basal cells of the epithelium. Secondary neuron (mitral and tufted cells) and interneuron (periglomerular and granule cells) synapses with the olfactory nerve in the olfactory bulb and relays information to the olfactory cortex (Figure 3). The network of the olfactory system is distributed into several cortical regions and subcortical structures (Milardi *et al.*, 2017).

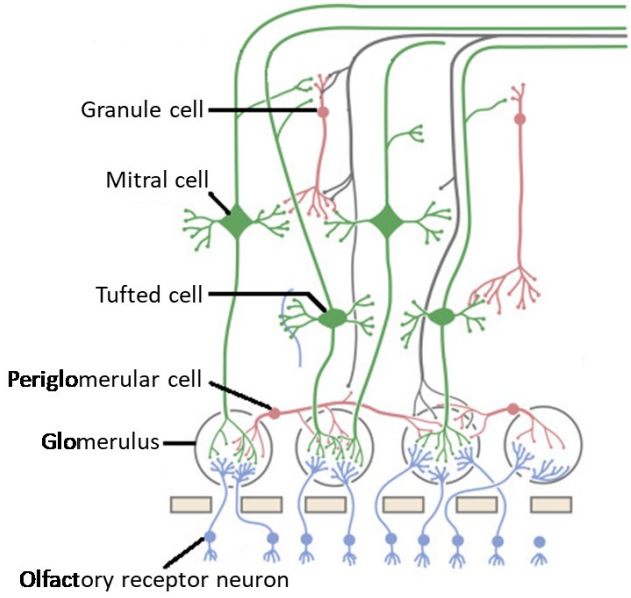

Figure 3: Schematic drawing of the olfactory bulb (modified from (Simpson, 2018))

1.1.3. The auditory and vestibular systems: an overview

The vertebrate ear is the organ which sends information about sound and movement of the head to the brain (Králíček, 2004). The ear can be generally divided into three regions with distinct functions: the outer, middle and inner ear (Anthwal and Thompson, 2016). The outer ear and the middle ear, which are not found in all vertebrates, enhance hearing. They work together to transform sound in free air to sound pressure and volume changes in the fluid of the inner ear (Rosowski, 2003). The inner ear is found in all vertebrates and contains neurosensory cells that convert sound- or movement-evoked mechanical stimuli into an electrical response, which is then processed by the central nervous system.

In mammals, the ear comprises all three parts: the outer, middle and inner ear (Anthwal and Thompson, 2016) (Figure 4).

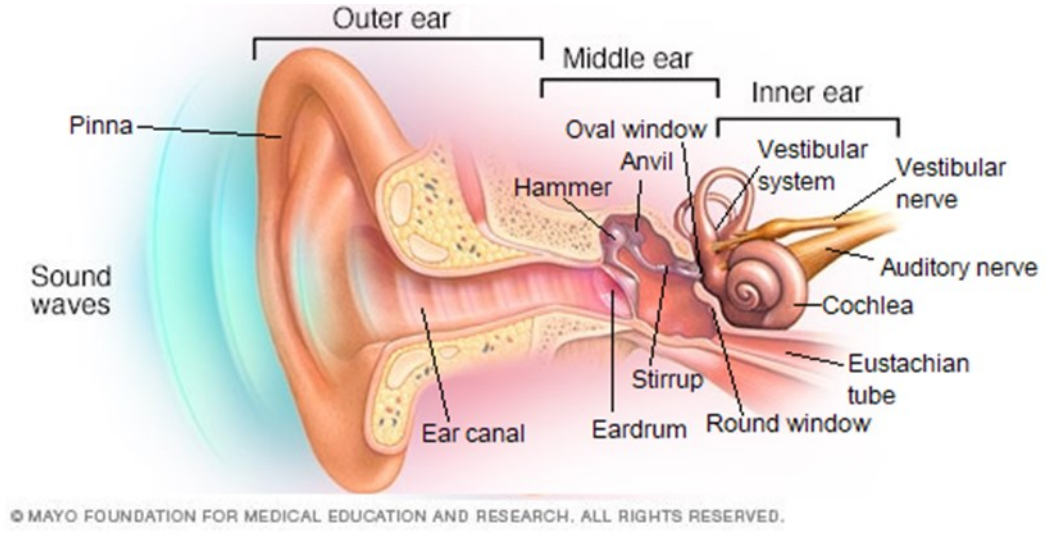

Figure 4: Outer, middle and inner ear (modified from (MayoClinic))

The outer ear comprises the pinna, which captures the sound and propagates it through the auditory meatus (ear canal) to the tympanic membrane (eardrum) (Králíček, 2004). Pinna, auditory meatus and the eardrum can function as a resonator of tones of specific frequencies.

The middle ear cavity is filled with the air and consists of three bones, the oval window, the round window and the Eustachian tube (Králíček, 2004; Anthwal and Thompson, 2016; Thompson and Tucker, 2013). The three bones are the *malleus* (hammer), *incus* (anvil) and *stapes* (stirrup). The pressure from sound waves vibrates the eardrum; the vibrations are further transmitted via the three bones to the oval window. The round and oval windows vibrate in opposite phase allowing the fluid in the cochlea to move. The middle ear and the nasopharynx are connected via the Eustachian tube which is normally closed and opens only during swallowing, chewing or yawning. The function of the Eustachian tube is to equilibrate the air pressure on both sides of the eardrum.

The inner ear consists of the cochlea, the vestibular system and the auditory and vestibular nerves (Králíček, 2004).

The whole auditory system consists of the peripheral part (the outer, middle and inner ear) and of the central part (the central auditory pathway with its corresponding brain areas) (Králíček, 2004). Auditory hair cells are connected to the cochlear nuclei in brainstem by spiral ganglion neurons whose central axons form the auditory nerve

(Kandler, Clause and Noh, 2009). Next auditory center is the superior olivary complex and then the inferior colliculus which is the most important relay station of the auditory pathway (Nieuwenhuys, Voogd and van Huijzen 1988). A last relay before the auditory cortex is the medial geniculate body in the thalamus.

The vestibular end organs communicate with the brainstem and the cerebellum that process the information about head position and movement (Purves *et al.*, 2001). The vestibular organs are innervated by vestibular neurons that reside in the vestibular ganglion. Central processes of the vestibular nerves project via the vestibular branch of the eighth (VIIIth) cranial nerve to the vestibular nuclei and also directly to the cerebellum.

1.2. Mouse model in inner ear research

About 278 million people in the world suffer from mild or severe hearing loss in both ears (Chatterjee and Lufkin, 2011). Any defect in the outer and middle ear can lead to conductive hearing loss, while defects in the inner ear cause sensorineural hearing loss (Anthwal and Thompson, 2016). Hereditary sensorineural hearing loss is the most common hereditary disorder; its prevalence is 1 in 1000 children (Friedman, Dror and Avraham, 2007). Understanding the causes of hearing loss to possibly treat the affected individuals is thus an important task.

Studies of sensorineural hearing loss in humans are limited by the inability to follow inner ear development (Friedman, Dror and Avraham, 2007). However, mouse models allow studies of deafness-related genes *in vivo*. Mutant mouse models manifesting hereditary hearing loss due to inner ear defects may help to identify factors important for the development or function of the inner ear.

Laboratory mice (*Mus musculus*) have become the major model in inner ear research, including gene discovery and characterization (Ohlemiller, Jones and Johnson, 2016). Previously, the majority of information about mammalian hearing was known from cats, rats and guinea pigs. However, *Mus musculus* surpassed and exceeded all other models due to the availability of mouse inbred strains with nearly eliminated uncontrolled genetic variance.

1.3. Mouse inner ear structure

The inner ear is composed of six sensory receptor epithelia: three ampullae containing sensory cristae, saccule and utricle containing maculae and cochlea with the organ of Corti (Raft and Groves, 2015). The vestibular system (ampullae, saccule and utricle) is responsible for movement sensing and the auditory system (cochlea) is responsible for hearing (Králíček, 2004; Raft and Groves, 2015; Kopecky *et al.*, 2012a). Both the vestibular and the auditory systems are located in the bony labyrinth of the temporal bone.

The membranous labyrinth contains a fluid called endolymph (Králíček, 2004; Raft and Groves, 2015; Torres and Giráldez, 1998). Between the membranous and the bony labyrinth is a fluid called perilymph. Perilymph and endolymph have unique ionic composition suited to their functions in regulating electrochemical impulses of hair cells (Králíček, 2004; Torres and Giráldez, 1998). The perilymph is similar to the extracellular fluid with the high concentration of sodium cations and low concentration of potassium cations. In contrast, endolymph is similar to the intracellular fluid and has a low concentration of sodium and a high concentration of potassium cations. The endolymph is produced by a specialized highly vascularized epithelium in the cochlear duct called *stria vascularis* and is drained by the endolymphatic duct. The endolymphatic duct is a continuation of the utriculosaccular duct and ends in the endolymphatic sac.

The membranous vestibular system placed in the vestibular bony labyrinth is composed of three semicircular canals beginning with three ampullae and of two pouches: the saccule and the utricle (Králíček, 2004; Raft and Groves, 2015) (Figure 5). The semicircular canals are oriented orthogonally to each other and end in the utricle. The utricle is connected with the saccule by the utriculosaccular duct. There is a connection between the saccule and the cochlear duct made by *ductus reuniens*.

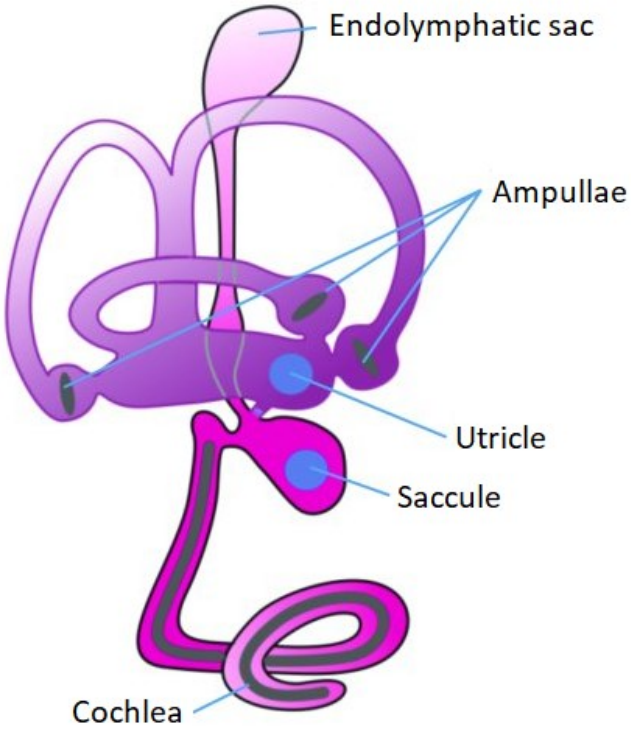

Figure 5: Mouse inner ear (modified from (Choi *et al.*, 2011))

The semicircular canals detect the rotation movement of the head (angular acceleration) (Raft and Groves, 2015). The sensory receptor itself is located in each of the ampullae and is called *crista ampullaris* (Figure 6). *Crista ampullaris* contains two types of cells: sensory-transducing hair cells and supporting cells (Torres and Giráldez, 1998). Each hair cell has several thin stereocilia and one long central kinocilium on its apical surface (Králíček, 2004). Stereocilia and kinocilia are immersed in the gelatinous mass, the cupula, which can be deflected on either side of the canal in response to the angular acceleration of the head. The bases of hair cells are connected by chemical synapses to bipolar neurons. The bodies of bipolar neurons form the vestibular ganglion.

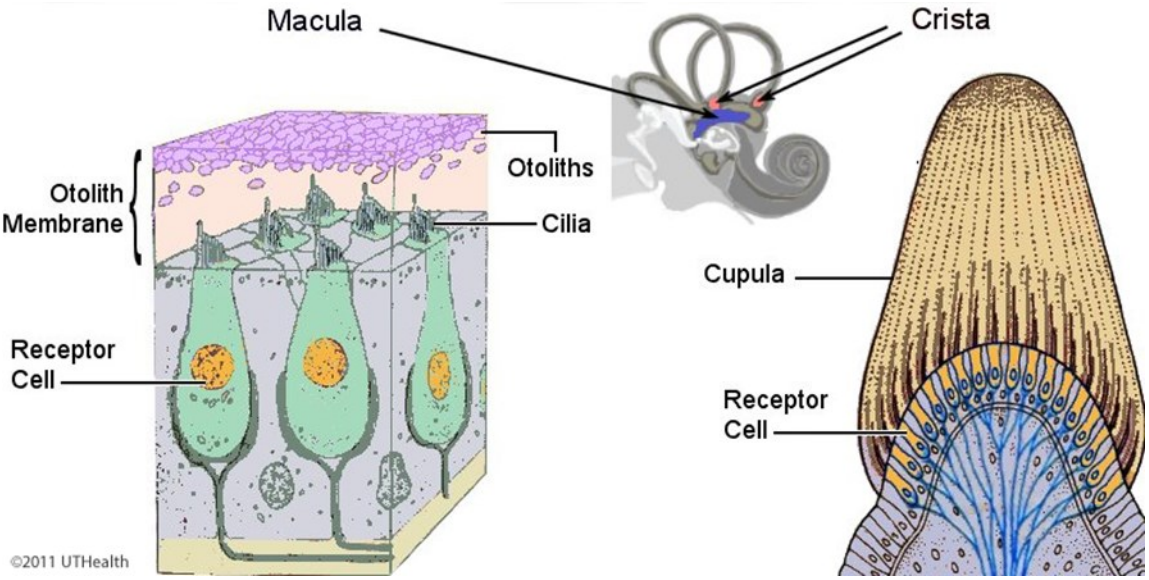

Figure 6: Vestibular organs: Macular organs and *crista ampullaris* (UTHealth, 2011)

The utricle and saccule sense the position of the head and the linear accelerations (Králíček, 2004; Torres and Giráldez, 1998). Sensory hair cells and supporting cells are organized in the utricular or saccular macula, which are perpendicular to each other. Hair cells are topped with stereocilia and kinocilia and embedded in a gelatinous otolith membrane (Figure 6). The orientation of the stereocilia within the sensory epithelium is determined by the striola, a narrow central area of the utricular or saccular macula. Here, the orientation of the tallest cilia changes. In the utricle, the kinocilia are oriented toward the striola and in the saccule they are oriented away from it. Otoliths are calcium carbonate crystals lying above the otolith membrane. They get displaced during linear acceleration, which in turn deflects the hair cells' stereocilia and produces a sensory signal. The action potential is then triggered in bipolar neurons of the vestibular ganglion.

The membranous auditory system (cochlea) is placed inside the bony labyrinth and forms a spiral-shaped cavity turning around the bony cone-shaped modiolus (Králíček, 2004). The cochlear duct is triangle-shaped on its cross section with the basilar membrane on the lower side, Reissner's membrane on the upper and *stria vascularis* on the peripheral side (Bok, Chang and Wu, 2007) (Figure 7). The bony labyrinth above the cochlear duct is called *scala vestibuli*, below is *scala tympani*. These two cavities are interconnected in the cochlear apex by a small gap, the helicotrema. The space inside the cochlear duct is

called *scala media*. *Scala media* is filled with endolymph, *scala vestibuli* and *scala tympani* contain perilymph (Fariñas *et al.*, 2001).

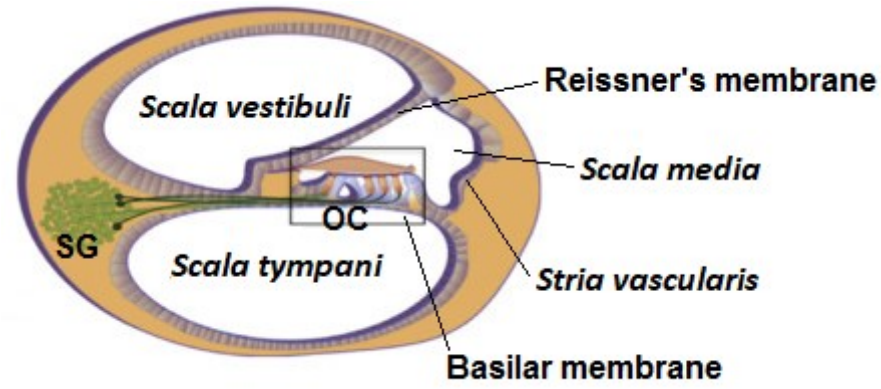

Figure 7: Cross section of the auditory bony labyrinth (modified from (Delacroix and Malgrange, 2015)); SG spiral ganglion, OC organ of Corti

The sensory organ of hearing is the organ of Corti (Králíček, 2004). The organ of Corti sits on the thin basilar membrane and is distributed along the coiled cochlear duct (Figure 8). It transforms the mechanic signal produced by sound into the electric one by receptor hair cells surrounded by supporting cells. Sensory hair cells are arranged into three rows of outer and one row of inner hair cells (Lim, 1986). Several microvilli and one central kinocilium are found on the apical surface of hair cells during development. As the microvilli elongate and form stereocilia, the kinocilium regresses. The stereocilia are covered by the tectorial membrane. The bearing skeleton of the organ of Corti is made of two rows of pillar cells which are a subtype of supporting cells (Králíček, 2004). The supporting phalangeal cells (three outer are also called Deiters' cells) hold the base of the hair cells and send a phalangeal projection up, towards the top of the organ of Corti. Medially, next to the inner phalangeal cells, there is one row of border cells which changes into the low epithelium of the inner supporting cells. Hensen cells are located laterally to the outer phalangeal cells.

Bipolar neurons are connected to hair cells by chemical synapses (Raft and Groves, 2015). The neuronal bodies are located inside the modiolus and form the spiral ganglion (Králíček, 2004).

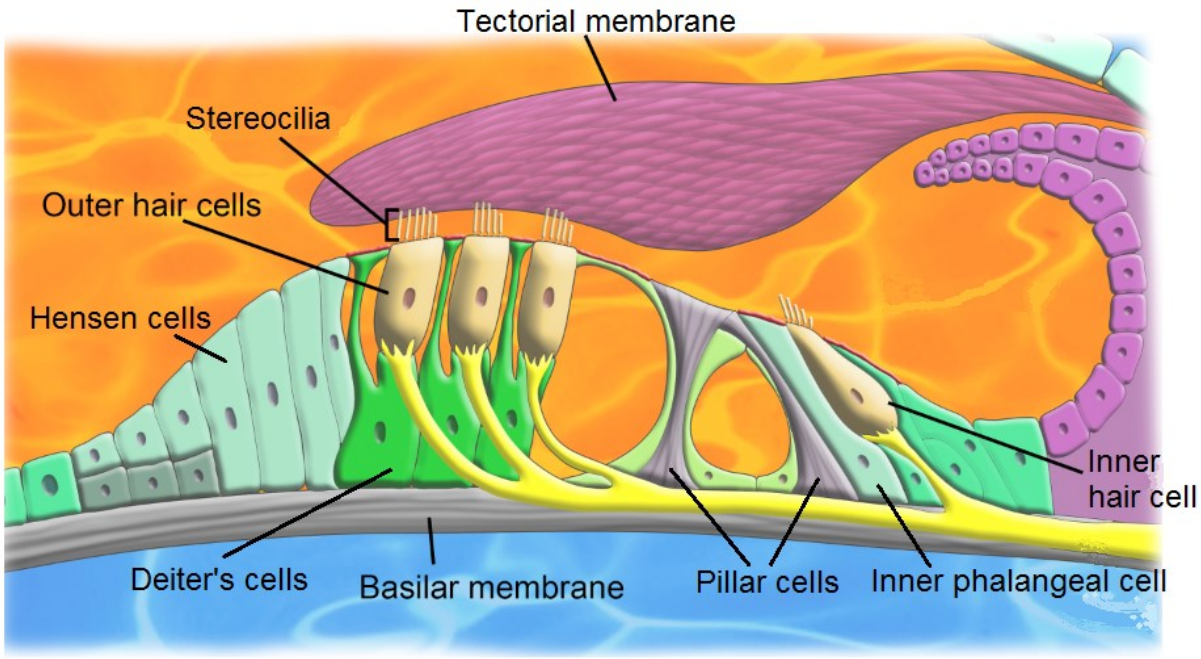

Figure 8: Organ of Corti (modified from Anatomy and Physiology, BIO 264 Textbook (BYU-Idaho))

1.3.1. Hair cells in the organ of Corti

The cellular organization, innervation patterns and function of inner and outer hair cells are distinctly different (Zheng *et al.*, 2000; Lim, 1986). However, both inner and outer hair cells show some similarities, such as the organization of stereocilia and growing stereociliary height along the length of the cochlea (Lim, 1986). The gradation of stereociliary height and changes of the tectorial and basilar membrane stiffness along the cochlear length determine the area that is maximally stimulated by the traveling waves created by a given stimulating frequency. Therefore, a hair cell responds best to a specific frequency, which is maximally tuned to. Hair cells in the base give their largest response to high frequencies, whereas cells in the apex are best tuned to low frequencies (Muniak *et al.*, 2013). This organization of hair cells along the length of the cochlear duct is preserved in cochlear ganglion cells and in the brain in the form of frequency-specific map, also called the tonotopic organization of neurons and brain connections (Rubel and Fritzsch, 2002).

The stereociliary bundles of both types of hair cells are organized in a 'W' formation with cilia of different heights (Lim, 1986). In the outer hair cells, the 'W' formation is sharp,

but changes along the cochlear length. In the basal turn, the angle of the 'W' formation is wider and in apical turn it is narrower. The inner hair cell stereocilia are larger in diameter than those of the outer hair cells and the 'W' formation is wide.

The outer and inner hair cells of the mammalian cochlea function in different ways (Zheng *et al.*, 2000). The function of inner hair cells is to detect the sound demonstrated by the vibration of the basilar membrane and to transduce the mechanical vibrations into electric signal further transmitted by spiral ganglion neurons. The outer hair cells produce amplification of vibrations in the cochlea. They do so by rapid changes in their length and stiffness, which is caused by changes in membrane potential and by the motor protein called prestin.

1.3.2. Mechanotransduction

Mechanotransduction is the process of transduction of the mechanical vibrations into electric signal performed by hair cells in the vestibular organs and in the organ of Corti (Fettiplace, 2017; Torres and Giráldez, 1998). Hair cells detect sound or movement via deflections of their hair bundles containing the mechanoelectrical transducer (MET) channels (Fettiplace, 2017). Stereocilia are interconnected by various extracellular filaments, most importantly tip links (Figure 9). The shearing force produced by the displacement of otoconia in the vestibular organs causes the deflection of stereocilia on vestibular hair cells (Najrana and Sanchez-Esteban, 2016). Sound-driven deflections of the basilar membrane in the organ of Corti are translated into displacements of the auditory hair bundles embedded in the tectorial membrane (Fettiplace, 2017). The tip links, extending from the tip of one stereocilium to the side wall of its taller neighbour, cause positive or negative deflections of the bundle towards its taller or shorter edge, respectively. Positive deflection is excitatory and causes MET channels to open, whereas negative deflection causes MET channels to close. During channel opening, mainly potassium cations flow across the apical stereociliary membrane of the hair cell causing depolarizing receptor potential. Change of the membrane potential opens voltage gated ion channels located on the basolateral membrane of the hair cells (Králíček, 2004; Fettiplace, 2017). This causes influx of calcium ions, neurotransmitter release and

activation of spiral or vestibular ganglion neurons. These bipolar neurons convey an excitation of the hair cell to the central nervous system.

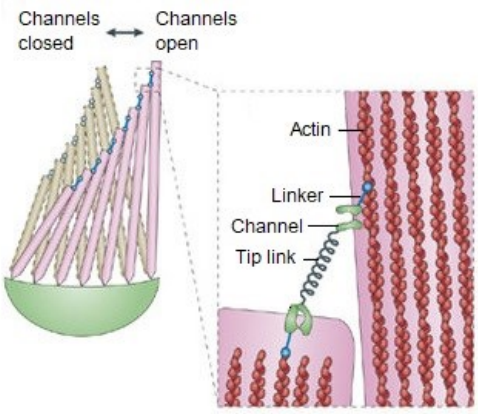

Figure 9: Connection of hair cell's stereocilia (modified from (Jaalouk and Lammerding, 2009))

1.3.3. Auditory neurons

The cochlear hair cells are innervated by two types of afferent neurons from the spiral ganglion. Type I and type II neurons differ in their number, morphology and form of innervation (Fuchs and Glowatzki, 2015). Type I afferent neurons are predominant and constitute 90-95 % of spiral ganglion neurons. Type I afferents are larger in diameter, myelinated, unbranched and are connected to a single inner hair cell (Liu, Glowatzki and Fuchs, 2015) (Figure 10). Each inner hair cell is innervated by 10–20 type I afferent neurons. In contrast, the remaining thinner, unmyelinated type II afferent neurons innervate ten or more outer hair cells.

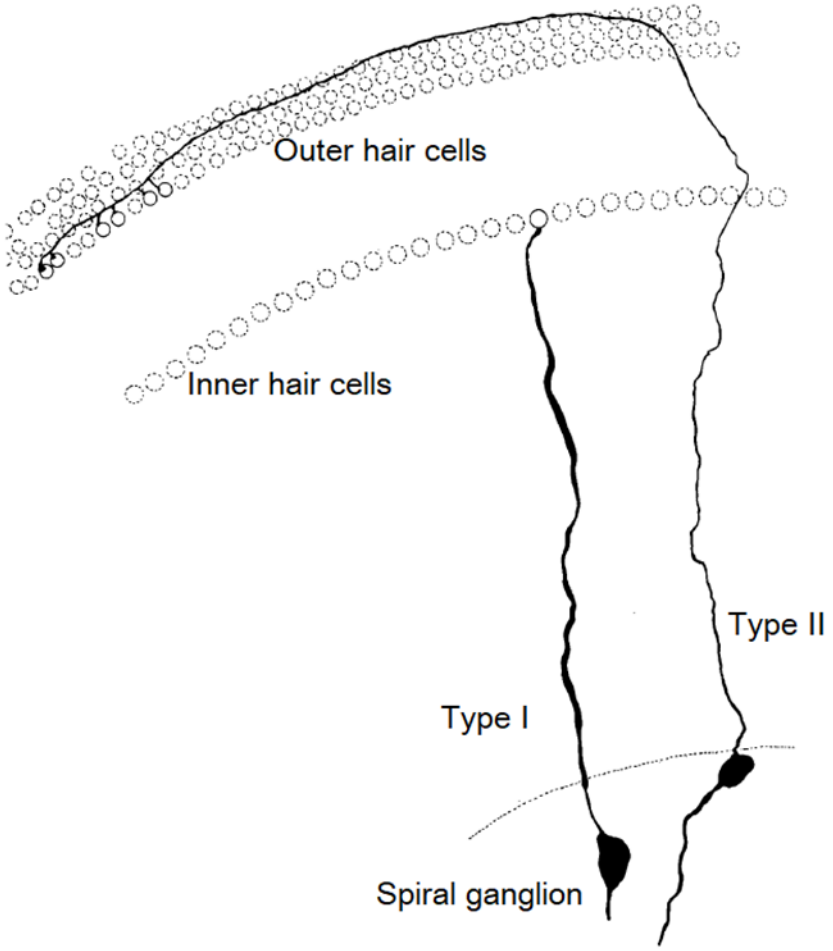

Figure 10: Afferent innervation of inner and outer hair cells (modified from (Berglund and Ryugo, 1987))

Transmission from hair cells to type II afferents is extremely weak in comparison to that in type I afferents (Fuchs and Glowatzki, 2015). The function of type I afferents in encoding the information content of sound is well established. However, the function of type II afferents remains unresolved. One hypothesis is that type II afferents are stimulated during acoustic trauma due to their sensitivity to a noxious stimulant adenosine triphosphate (ATP), which is released by supporting cells upon hair cell damage.

1.4. The development of sensory systems

1.4.1. Sensory placodes

Sensory organs of the vertebrate head develop from the specialized regions of the head ectoderm, the cranial placodes (Schlosser, 2006). The cranial placodes develop from the non-neural ectoderm of the embryo (Pieper *et al.*, 2012). The separation of the head surface ectoderm into neural and non-neural domains occurs at around the time of gastrulation. The head mesoderm was identified to be necessary and sufficient to induce the preplacodal region (PPR) by producing the PPR inducing signals (Litsiou, Hanson and Streit, 2005). Cells within the PPR are able to form any placode until late developmental stages. PPR character induction in naïve ectodermal cells is enabled by the signalling mechanism including the Wingless/Integrated (WNT) and Bone morphogenic protein (BMP) antagonists and the activation of the Fibroblast growth factor (FGF) pathway.

The cranial placodes include the adenohypophyseal, olfactory, lens, trigeminal, otic and other placodes (Schlosser, 2006). Several non-epidermal cell types including neurons, glia and secretory cells develop from cranial placodes. Placodes develop from the population of ectodermal cells located near the border of the neural plate, forming first thickened ectodermal patches and later invaginate into the underlying mesenchyme. Placodes are regions with abundant cell proliferation compared to the epidermis. Placodal derivatives undergo shape changes and morphogenetic movements during their development. Except from the adenohypophyseal and lens placodes, all other placodes are neurogenic. It is disputed whether all cranial placodes arise from a common panplacodal primordium or whether they form as distinct thickenings. However, there is an increasing evidence for a common developmental origin of all placodes. The common primordium is defined by the expression of Sineoculis homeobox (*Six*) and Eyes absent (*Eya*) transcription factor families. Later, multiple signalling pathways are involved in the induction and development of different placodes.

1.4.2. Cranial sensory nervous system

“The sensory nervous system of the vertebrate head comprises the three paired sense organs (the eye, ear and olfactory epithelium) and the cranial sensory ganglia” (Streit, 2008). Whilst some sensory placodes generate a large variety of cell types and contribute to sense organs (the olfactory, lens and otic placodes), others are simple neurogenic centers that generate neuroblasts (the trigeminal and epibranchial placodes).

The trigeminal placode produces the distal parts of the trigeminal (V^{th}) cranial ganglion (D'Amico-Martel and Noden, 1983). The epibranchial placodes produce the geniculate (VII^{th}), petrosal (IX^{th}) and nodose (X^{th}) cranial ganglia (Figure 11). Cranial nerves are numbered sequentially according to their position in the brain, starting from the front. The sensory fibers of the cranial nerves emerged from the cranial sensory ganglia. The vestibular and acoustic ganglia are associated with $VIII^{th}$ cranial nerve. The trigeminal ganglion contains the cell bodies of the trigeminal nerve (V). The geniculate ganglion contains neuronal bodies of the facial nerve (VII). The petrosal ganglion is sometimes named as superior (detached portion) and inferior (main part) ganglia of the glossopharyngeal nerve (IX) and the nodose ganglion is a sensory ganglion for the vagus nerve (X). Intermediate nerve is the part of the facial nerve (VII) that contains sensory and parasympathetic fibers of the facial nerve.

The trigeminal nerve relays head somatosensory information (Streit, 2008). The epibranchial placode-derived neurons are responsible for sensing taste in the oral cavity and transmitting sensory information from the heart and other visceral organs.

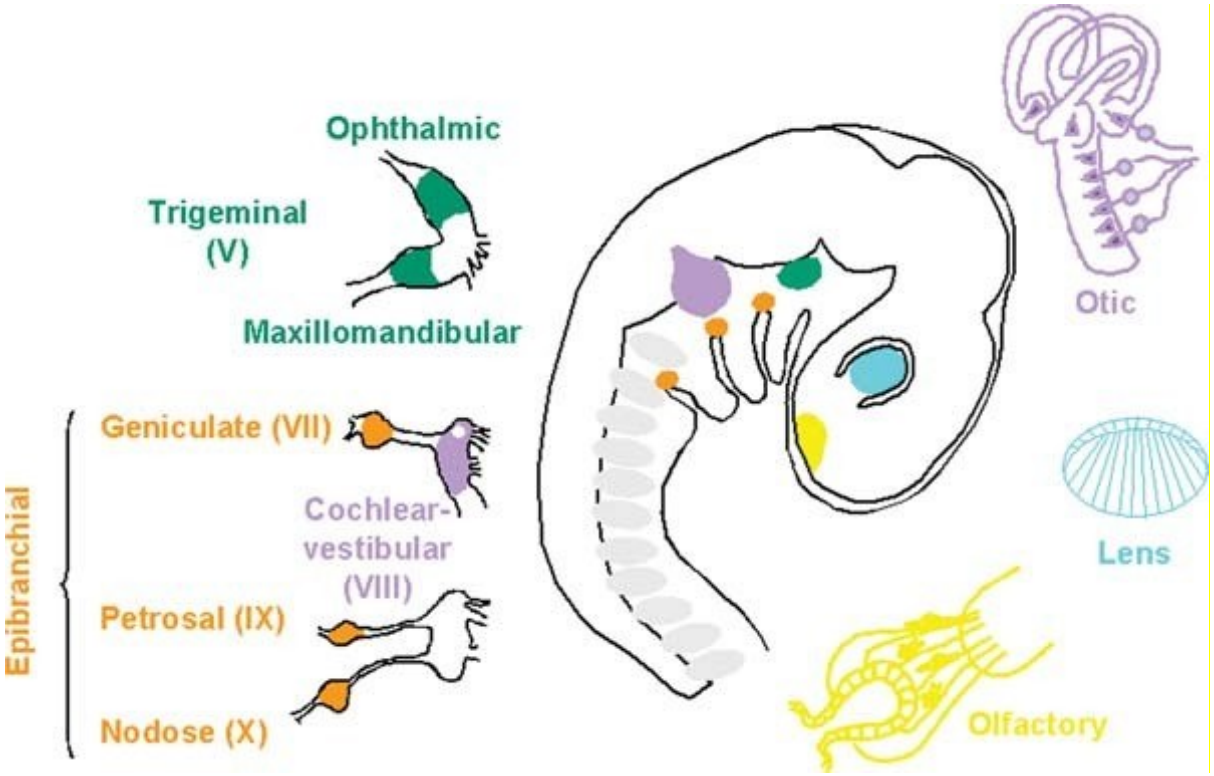

Figure 11: Sensory placodes and their derivatives – embryonic location of cranial placodes (Streit, 2008)

Cranial nerve VIII contains two components: auditory (cochlear) and vestibular (Streit, 2008; Torres and Giráldez, 1998). Both components begin in the inner ear and travel to the brainstem. The central projection of the auditory component conducts the information from the auditory system via the spiral ganglion neurons and projects to the cochlear nuclei. The central vestibular pathway begins in the vestibular ganglion of the inner ear and projects to the vestibular nuclei.

1.4.3. Eye development

"The neural ectoderm, the surface ectoderm and the periocular mesenchyme contribute to the formation of the mammalian eye" (Heavner and Pevny, 2012). From surface ectoderm, the lens and cornea are formed. Neural retina and retinal pigment epithelium are of neuroepithelial origin (Kanakubo *et al.*, 2006). All other tissues in the eye are derived from the periocular mesenchyme.

Shortly after gastrulation, the anterior neural plate undergoes specification events resulting in formation of progenitors of all neural-derived eye structures (Heavner and Pevny, 2012). Two bilaterally symmetric eyes arise from a single retina field in the anterior neural plate of vertebrate embryos (Li *et al.*, 1997). In mice, the first noticeable signal of eye field establishment is the formation of optic pits at embryonic day E8.0 (Heavner and Pevny, 2012). The vertebrate eye develops by invagination of the optic vesicle that forms the optic cup (Goldsmith, 1990). At E8.5–E9.0 of mouse development, the optic vesicles which consist of the retinal stem cells evaginate and contact the surface ectoderm, where the lens placode is formed (Heavner and Pevny, 2012) (Figure 12). Expression of *Bmp*s and *Fgf*s in the optic cup is required for lens induction (Schlosser, 2006). Possibly, expression of *Bmp*s in the lens placode itself is important for subsequent stages of lens development (Faber *et al.*, 2002). The lens placode arises from the PPR, an ectoderm-derived structure that forms the discrete thickened placode (Heavner and Pevny, 2012). The lens placode invaginates together with the optic vesicle to form the lens cup, which eventually separates from the surface ectoderm and creates the lens vesicle. Once lens vesicle detached from the surface ectoderm, the surface ectoderm proliferates giving rise to the corneal epithelium (Kanakubo *et al.*, 2006). The optic vesicle folds into itself creating two nested cups (Heavner and Pevny, 2012). The inner layer of optic cup becomes the presumptive neural retina, whereas the outer layer of the optic cup becomes the presumptive retinal pigmented epithelium (Goldsmith, 1990).

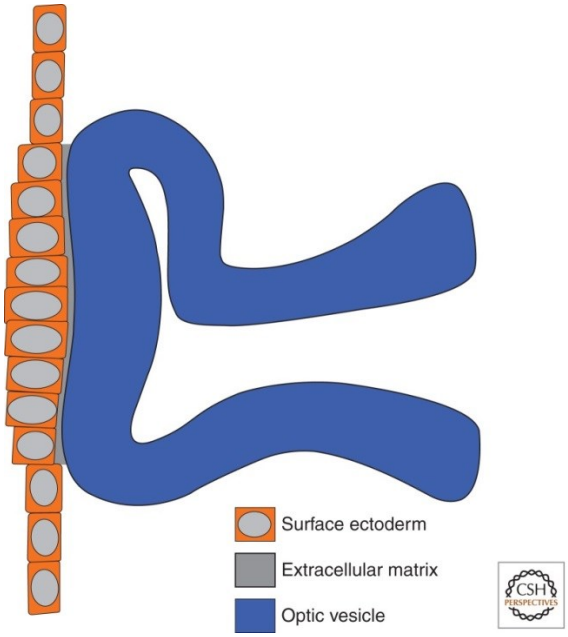

Figure 12: Mechanics of lens placode formation (Heavner and Pevny, 2012)

The retina is a highly conserved part of the central nervous system, with cell types and gene activities comparable from Drosophila to humans (Zaghloul, Yan and Moody, 2005). The specification of embryonic cells to produce retina is a multi-step process with gradual restriction of cell fate potentials. From a subset of embryonic cells, which become competent to form the retina, the definitive retinal stem cells are specified during gastrulation by interactions with underlying mesoderm. During the rearrangement of the eye field into the optic vesicle, retinal progenitor cells generate different parts of the retina, the optic stalk, retinal pigmented epithelium and neural retina. Cell-cell interactions then lead to further differentiation of retinal cell types. The optic stalk elongates and eventually gives rise to the optic nerve (Heavner and Pevny, 2012).

1.4.4. Olfactory development

Olfactory epithelium development depends on retinoic acid, FGFs and BMPs from the adjacent frontonasal mesenchyme and on the olfactory ectoderm itself (Schlosser, 2006). The olfactory placode invaginates to create the epithelia of the olfactory and vomeronasal organs. The olfactory placode gives rise to several various cell types including supporting cells, primary sensory cells and glia. The olfactory neuroepithelium is also the origin site

of secretory cells, which migrate along the olfactory nerve towards the brain and have no apparent role in the sense of smell *per se* (Fornaro *et al.*, 2001). Secretory gonadotropin releasing hormone (GnRH) neurons of the central nervous system grow in the medial olfactory placode and migrate over the nasal septum to the brain during prenatal development (Schwanzel-Fukuda and Pfaff, 1989). Gonadotropic hormones are responsible for reproductive behavior. Subsets of migratory GnRH neurons, olfactory epithelial cells and cells of the vomeronasal organ are of neural crest origin (Forni *et al.*, 2011). The neural crest is an embryonic cell type originating between the neural tube and epidermis of vertebrates. During early developmental stages pluripotent neural crest cells (NCCs) migrate to several locations in the organism, where they give rise to neurons and glia of the peripheral nervous system. The GnRH cells and vomeronasal and olfactory sensory epithelia derive, therefore, from two different lineages, with the majority cells originating from the ectoderm and with some cells of neural crest origin.

The olfactory placode is the only one, which retains stem cells and therefore can restore various differentiated cell types throughout life (Schlosser, 2006).

The formation of the nasal epithelium involves complex morphogenesis with generation of distinct domains of olfactory sensory epithelium and the respiratory epithelium (Croucher and Tickle, 1989). Both the olfactory sensory epithelium and the respiratory epithelium derive mainly from the olfactory placode (Maier *et al.*, 2010). The lining of the nose exhibits two distinctly different epithelial domains, with the sensory olfactory epithelium in the deeper regions and the nonsensory respiratory epithelium located more distally (Croucher and Tickle, 1989). FGF signalling promotes generation of sensory epithelial cells, whereas BMP activity stimulates respiratory epithelial character (Maier *et al.*, 2010). FGF functions to suppress the ability of BMP signalling to induce respiratory cell fate in the nasal epithelium.

The olfactory placode first becomes visible at E9.5 in the mouse as an ectodermal thickening, which subsequently invaginates to form the olfactory pit (Maier *et al.*, 2010). With further development the nasal pits invaginate and form grooves (Croucher and Tickle, 1989). The definitive nasal cavities are covered by distinctly distributed olfactory and respiratory epithelia.

The sensory epithelium consists of several cell types including the olfactory sensory neurons which transduce odor signals (Maier *et al.*, 2010). The respiratory epithelium is responsible for removing particles from inhaled air and does not contain neurons.

Neurogenesis in the olfactory epithelium begins already at the placodal stage (Fornaro *et al.*, 2001). Cell migration from the olfactory neuroepithelium begins simultaneously with the early differentiation of the olfactory placode that occurs several hours before the ectodermal invagination of the olfactory pit.

Olfactory epithelium is one of few tissues that maintain adult neurogenesis (Kaplan and Hinds, 1977).

1.4.5. Otic placode and inner ear development

Different cell types of a complex structure of the inner ear are derived from the otic placode, a seemingly simple epithelial structure (Sai and Ladher, 2015). Multiple stages of ear development are controlled by different gradients of signalling molecules (Groves and Fekete, 2012). FGFs, WNTs, BMPs and Sonic hedgehog (SHH) are activated at different times to regulate inner ear differentiation. Induction of the otic placode depends on FGF signals from adjacent tissues acting on the PPR (Sai and Ladher, 2015; Schlosser, 2006). Further development of the otic vesicle requires WNT and SHH signalling from the adjacent notochord and neural tube (Schlosser, 2006). The development of the inner ear is an advancing process with a gradual restriction of cell fates: beginning as non-neural ectoderm, continuing to PPR and then to inner ear fate (Sai and Ladher, 2015).

Inner ear development includes otic placode invagination and the formation of otic vesicle (otocyst), which gives rise to the inner ear itself and to sensory neuron precursors of the vestibular and spiral ganglia (Schlosser, 2006). The otic placode undergoes a series of morphogenetic changes forming a closed vesicle in the cephalic mesoderm (Sai and Ladher, 2015). The placodal thickening, which occurs in 4–6-somite murine embryo, is thought to be necessary for the proliferation of cells in the inner ear. Cells within the inner ear divide by interkinetic nuclear migration, which is characterized by active apical migration of dividing cells and passive push back of daughter nuclei to the basal side. The invagination of the otic placode starts when the embryo has between 8 and 10 somites. From 16 to 22-somite stages, the otic placode is driven deeper into the mesenchyme and

is called the otic cup. Otic invagination comprises two phases: basal expansion and apical constriction. The otic cup is internalized, closed off as an otic vesicle and is ready to undergo further shape changes to form the final structure of the membranous labyrinth.

One of the initial markers activated during otic specification is the transcription factor Paired-box gene 2 (*Pax2*) or its homolog *Pax8* (Sai and Ladher, 2015). *Pax2* expression is located next to the caudal part of the future hindbrain. The refinement of the *Pax2*-expressing progenitor domain into otic and non-otic territories is regulated by graded WNT signals (Groves and Fekete, 2012). Cells that are determined to make the otic placode receive high levels of WNT signalling, whilst more lateral non-otic cells receive less or no WNT signals. Different processes are employed to transform the WNT gradient into otic and non-otic fates. First, the Notch signalling pathway further amplifies WNT signalling in future otic, but not in non-otic regions. This is enabled by high levels of WNT signalling that activate the components of the Notch pathway, whereas low levels of WNT signalling do not activate Notch. Therefore, a gentle gradient of WNT signalling is turned into a discontinuous pattern causing separation of otic and non-otic tissues. Second, the FGF signalling pathway is negatively regulated by the differentiating otic placode. This rapid attenuation of FGF signalling allows subsequent otic tissue differentiation, as active FGF signalling blocks the appearance of later otic markers.

At the stage of invagination, asymmetries in gene expression are already apparent in the otocyst (Groves and Fekete, 2012). Progressively, the three axes of the ear become established, each axis being specified by different signals. The exact timing and regulation of inner ear patterning is not clear, but the following scheme is conceivable (Bok, Chang and Wu, 2007). The otic placode first acquires medial character from WNTs and FGFs and then antero-posterior orientation is established by specifying the neurosensory domain. In mice, the antero-posterior identity is influenced by an extrinsic gradient of retinoid acid (Groves and Fekete, 2012). At the same time, dorso-ventral differences are generated by the exposure of ventral otic cells to SHH signalling, whereas dorsal development is regulated by WNT signalling (Bok, Chang and Wu, 2007; Groves and Fekete, 2012). However, the function of these signals differs in action. The neurosensory domain is restricted to the antero-ventral region of the otic cup (Bok, Chang and Wu, 2007). The lateral fate is formed by migrating cells that form the lateral wall of the otocyst. Semicircular canals and cochlear duct are formed from the lateral region of the otocyst.

The majority of inner ear organs consist of both sensory and nonsensory regions (Bok, Chang and Wu, 2007). The morphogenetic process of patterning of sensory and nonsensory organs in the developing inner ear is mediated by a number of different morphogens (Figure 13). For example, in the mouse developing cochlea at E11.5, SOX2 marks the sensory-competent region (Groves and Fekete, 2012). On a transverse section through cochlea at this age, asymmetric gene expression is observed with FGF on the neural (close to the forming spiral ganglion) and BMP on the abneural side. Other morphogens and signalling molecules define the individual cells of the organ of Corti, the greater epithelial ridge (GER) located medially and the outer sulcus laterally to the organ of Corti in the coiled cochlear duct. However, nonsensory cells in the GER, if induced, are still able to differentiate into either hair cells or spiral ganglion neurons at embryonic ages (Cheah and Xu, 2016). Some of the morphogens acting in cochlear development from E11.5 to E18.5 are depicted in Figure 13. Transcription factor PAX2 was shown to be important for proper cochlear outgrowth and coiling in the mouse inner ear by governing differential proliferation within the various regions of the cochlea (Burton *et al.*, 2004). Lack of PAX2 affects tissue specification within the cochlear duct and causes arrest of the cochlear outgrowth at an early stage.

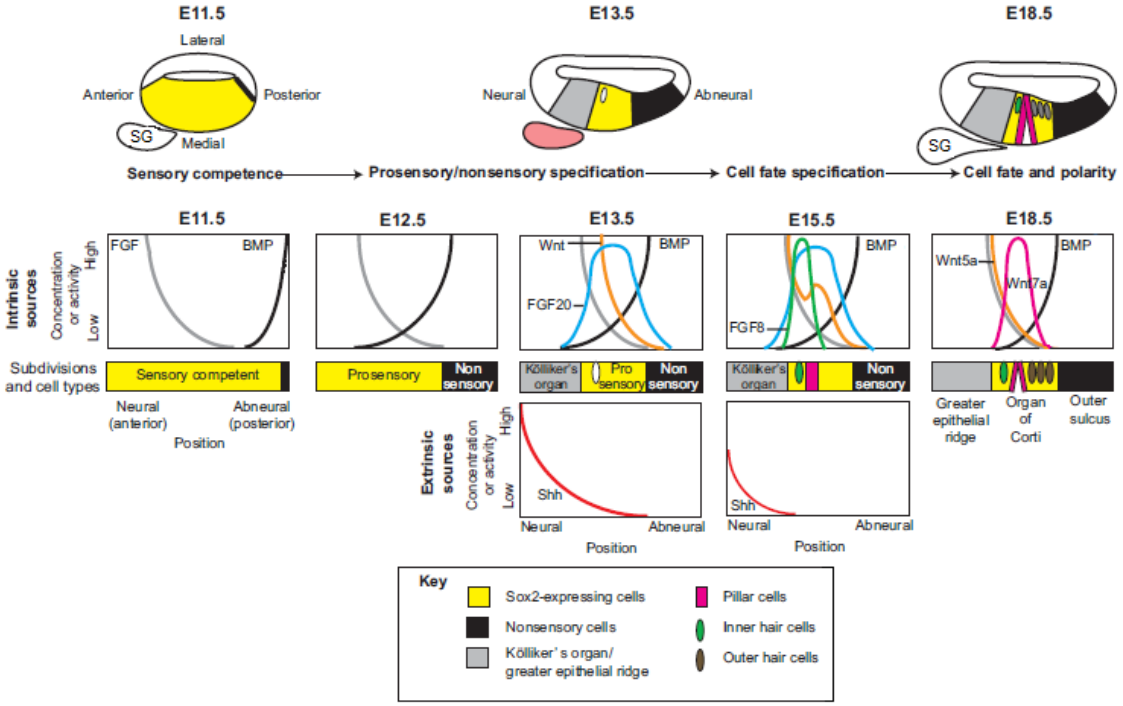

Figure 13: Cochlear patterning (modified from (Groves and Fekete, 2012)): sequential subdivision into sensory and nonsensory cells in the mouse cochlea under the influence of several morphogens. Cells in the prosensory domain, marked by *Sox2* expression, divide, differentiate and form the organ of Corti. The organ of Corti is flanked by two nonsensory regions: the GER and the outer sulcus. Some genes for several morphogens and signalling molecules are depicted in territories, where they are expressed. The predicted gradients are shown for the mid-base of the cochlea.

The molecular evidence that sensory organs control the development of related non-sensory tissues was found in the development of semicircular canals (Chang *et al.*, 2004). FGFs in the prospective cristae stimulate the growth of semicircular canals, probably by inducing *Bmp2* in the canal genesis zone. A canal genesis zone contributes to the majority of the canal outgrowth.

An important general feature of developmental systems is the ability of a small number of signalling pathways to be used in different contexts and provide patterning information (Groves and Fekete, 2012). This is possible by the temporal separation of the patterning actions and by variable transcriptional conditions of inner ear cells as inner ear development proceeds. Therefore, similar series of signals can be interpreted differently.

1.4.5.1. The development of sensory cells of the inner ear

The ventral portion of the otocyst begins to elongate around E10.5 and forms a rudimentary cochlear duct by E11.5 (Lee, Liu and Segil, 2006). The cochlear duct continues to grow and coil until E18.5 when it reaches a full 1.5 turn.

Vertebrate hair cells and sensory neurons evolved from a ciliated mechanosensory cells found in insects (Fritzsch and Beisel, 2004). This suggests a clonal relationship between hair cells and neurons and a common neurosensory precursor for hair cells and neurons.

In the inner ear, the canonical WNT/β-catenin signalling pathway has been shown to regulate the size of the otic region from which the cochlea will arise (Jacques *et al.*, 2012). WNT signalling is high in early hair- and supporting cell precursors and WNT activity becomes reduced as the development of the inner ear progresses. WNT/β-catenin signalling has two roles in cochlear development; it regulates proliferation and also hair cell differentiation.

The Notch pathway plays a critical role in the regulation of cell fates and differentiation of hair cells and supporting cells (Schimmang and Pirvola, 2013; Lanford *et al.*, 1999). This pathway is initially required for the specification of prosensory domains within the inner ear via lateral induction, but it is subsequently necessary for the establishment of hair cell- and supporting cell fates within the sensory domain via lateral inhibition.

Determination of cell fates in the cochlea occurs via lateral inhibition between adjacent progenitor cells such that developing hair cells suppress differentiation in their immediate neighbours (Lanford *et al.*, 1999) (Figure 14). A subset of cells, for which the hair cell phenotype represents the default fate, express Notch ligands Jagged2 (*Jag2*) and Delta-like protein 1 (*Dll1*) (Lanford *et al.*, 1999; Brooker, Hozumi and Lewis, 2006). Ligands then bind to Notch receptors in neighbouring cells preventing them from developing as hair cells, while ligand-expressing cells develop into hair cells.

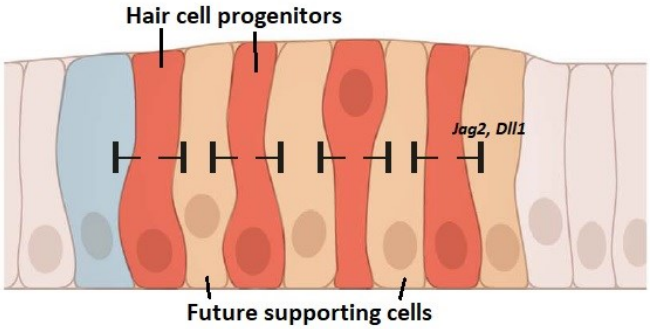

Figure 14: Lateral inhibition in the organ of Corti (modified from (Sjöqvist and Andersson, 2019)): *Jag2* and *Dll1* expression in progenitor cells (red) repress adjacent cells from adopting a hair cell fate via lateral inhibition. The repressed cells become different types of supporting cells.

The controlling of cell cycle length and timing of cell cycle exit of precursor cells are critical in the differentiation of sensory and nonsensory cells in the inner ear (Schimmang and Pirvola, 2013). The spatial-temporal gradients of terminal mitosis (the last division, which a cell undergoes) are opposite for hair cells and spiral ganglion neurons in the mouse cochlea (Ruben, 1967). Spiral ganglion neurons in the base are the first to become postmitotic; the cell cycle exit of neurons then proceeds to the apex and is followed by cell cycle exit of hair cells in the apex (Matei *et al.*, 2005). Cell cycle exit of hair cells then progresses to the base. Short overlap of cell cycle exit of both hair cells and sensory neurons occurs in the apex. In the base, hair cells exit the cell cycle up to three days after spiral sensory neurons. Hair cell cycle exit starts at E11.5 in the apex. Paradoxically, cochlear hair cell differentiation begins in the mid-basal turn at E14.5 and progresses to the apex in the opposite direction to the cell cycle exit (Chen *et al.*, 2002).

Hair cells of the vestibular system start to differentiate shortly after the first are born, around E13.5 but the process of proliferation and differentiation occurs over a much longer period compared to the cochlea (Burns *et al.*, 2012). More than thousand new utricular hair cells are produced postnatally during the first week. However, the most rapid postnatal hair cell production occurs until postnatal day 2 (P2). Cells near the striola exit the cell cycle and differentiate early, whereas those close to the periphery exit and differentiate later.

Following terminal mitoses and the onset of differentiation of progenitor cells, cochlear and vestibular hair cells do not re-enter the cell cycle (Schimmang and Pirvola, 2013). Unlike hair cells in nonmammalian vertebrates such as birds and fish, lost or damaged

hair cells in mammals cannot be replaced by transdifferentiating supporting cells (Cheah and Xu, 2016).

Hair cell differentiation begins when a subset of cells within the prosensory domain starts to express Atonal homolog 1 (*Atoh1*), a gene for transcription factor necessary for hair cell differentiation, and when *Sox2* is downregulated in sensory precursors (Dabdoub *et al.*, 2008). SOX2 is required for the specification of the sensory precursors of the inner ear, which develop from the ventral and lateral region of the otocyst. Although activation of *Atoh1* can induce hair cell fate, ATOH1 alone is not sufficient to promote hair cell differentiation, maintenance and function (Cheah and Xu, 2016).

1.4.5.2. The development of inner ear sensory neurons

All cochlear and vestibular ganglion neurons derive from several sites of the otocyst (Noden and Van de Water, 1992; Hemond and Morest, 1991; Rubel and Fritzsch, 2002). The delaminated neuroblasts form the primary neurons of the auditory and vestibular pathways linking the inner ear and the central nervous system (Rubel and Fritzsch, 2002). The way of ganglion cell precursor determination in the otocyst region is not yet known.

The vestibular ganglion neuroblasts delaminate from the ventromedial and ventrolateral epithelium of the otocyst (Hemond and Morest, 1991). The delaminated neurons migrate rostrally and accumulate to form the vestibular ganglion adjacent to the ventromedial border of the otocyst. The neuroblast lineage is specified immediately after the determination of the otic placodal field (Liu *et al.*, 2000). Formation of the vestibular ganglion starts around E9.5, when neuronal progenitors delaminate from the otic placode. Vestibular ganglion neurons innervate the *cristae ampullares* of the semicircular canals and the utricular and saccular maculae and project to the primary vestibular nuclei in the brainstem (Hemond and Morest, 1991).

The cochlear spiral ganglion neurons transmit acoustic information from the inner ear to the brain (Rubel and Fritzsch, 2002). Whilst existing results indicate that ganglion cells influence the differentiation of their hair cell targets only slightly, cochlear innervation is essential for the normal development of neurons in the cochlear nucleus in the brain. The maturation of the inner ear goes along with the delamination of ganglion neurons and differentiation of sensory cells.

The spiral ganglion neurons delaminate mainly from the growing cochlear duct but they do not delaminate uniformly (Yang *et al.*, 2011). Auditory neurons delaminate particularly from the region of the future *ductus reuniens* and the middle cochlear turn and later from the apex. However, whether neurons delaminating from the future *ductus reuniens* differentiate into spiral ganglion neurons or inferior vestibular ganglion neurons is unclear. Auditory bipolar neurons innervate the organ of Corti (type I neurons project to inner hair cells, type II neurons to outer hair cells) and also send axons to the cochlear nuclei in a tonotopic manner. Precursors of the future organ of Corti express neurotrophic factors that attract fibers of developing neurons already before the onset of hair cell differentiation (Fariñas *et al.*, 2001).

1.4.5.3. Dual origin of inner ear cells

It has long been thought that all inner ear epithelial cells and neurons of the auditory and vestibular ganglia originate in the otic placode ectoderm (Freyer, Aggarwal and Morrow, 2011). However, Freyer *et al*. demonstrated that cranial neuroepithelial cell (NEC) lineages, that include also NCCs, constitute a significant population of cells of the inner ear. Therefore, other tissues participating in the inner ear development include melanocytes derived from NCCs, which give rise to the cells of the *stria vascularis* and to the mesenchyme surrounding the non-sensory epithelia of vestibular organs. Also *Sox10*-expressing glial cells in the vestibular ganglion are of NCC origin. NCCs are specified in the dorsal neural tube and then migrate throughout the embryo.

NEC/NCC derivatives remain in the inner ear throughout development and assign to the spiral and vestibular ganglia and to sensory epithelia of the utricle, saccule and cochlea (Freyer, Aggarwal and Morrow, 2011). Some NEC derived cells express the neuroblast markers Neuronal differentiation 1 (NEUROD1) and Insulin gene enhancer protein ISL-1 (ISL1), other differentiate into hair cells or supporting cells and express their specific markers Myosin VIIA (MYO7A) or Low-affinity nerve growth factor receptor (P75), respectively. The arrangement of NEC derivatives differentiating into hair cells or supporting cells of the organ of Corti, utricle and saccule seems to be random.

Contribution of cells from neural tube to the inner ear occurs after otic placode formation and is completed around E10.5 in mice (Freyer, Aggarwal and Morrow, 2011). NEC

derivatives constitute approximately 20% of the total number of cells in the otic vesicle and 25% of the total number of cells in the vestibular ganglion at E10.5 (Figure 15). Some NEC-derived cells in the otic epithelium express *Neurod1* suggesting that at least some NEC-derived neuroblasts are specified from within the otic epithelium.

Taken together, these data show that both otic placode ectoderm and NECs contribute to the mammalian inner ear.

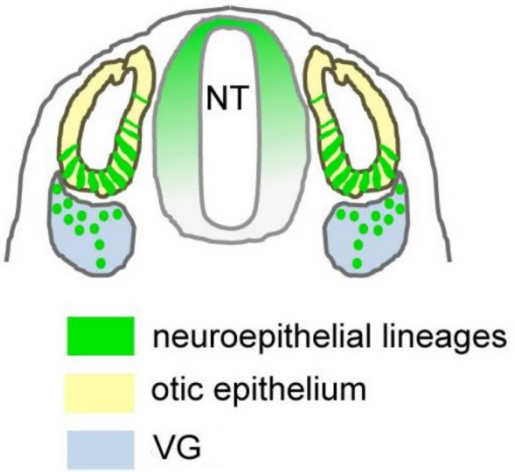

Figure 15: Distribution of neuroepithelial lineage derivatives in the otocyst and vestibular ganglion (modified from (Freyer, Aggarwal and Morrow, 2011)); VG vestibular ganglion

1.5. Regulatory factors involved in inner ear development

Cascades of transcription factors and signaling molecules control the neurosensory development of the inner ear. Some of the important factors are briefly mentioned in the above sections. This chapter describes in detail selected transcription factors and some other regulatory molecules, which are particularly important in our study.

1.5.1. LIM homeodomain transcription factor ISL1

Homeobox transcription factors play essential roles in development (Hobert and Westphal, 2000). LIM homeodomain proteins are important for tissue patterning and differentiation. These proteins are characterized by LIM domains which are two specialized zinc fingers and the homeodomain. The acronym LIM derives from the three homeodomain proteins first recognized as sharing this structural feature: **L**IN11, **I**SL1 and **M**EC-3 (Gill, 1995). LIM homeodomain interactions with cofactors depend mostly only on the LIM domains of the proteins, whereas the homeodomain structure is responsible for DNA binding (Hobert and Westphal, 2000). LIM homeodomain proteins are able to combinatorically interact with other transcriptional regulators and therefore, participate in a wide range of developmental events. Particularly important role of LIM homeodomain proteins is the determination of terminal differentiation features of a nervous system. For example, loss-of-function studies in the mouse have revealed crucial roles for ISL1 in the development of motor neurons, sensory neurons or pancreas (Pfaff *et al.*, 1996).

In the inner ear, ISL1 protein is expressed early in the otocyst in both the neuronal and the sensory lineages (Radde-Gallwitz *et al.*, 2004). First ISL1-expressing cells are found near the otic placode as early as E8.5 in mouse embryos. At E10.5, all delaminated vestibular ganglion neurons and some cells in the otic epithelium express ISL1 (Deng *et al.*, 2014). ISL1 expression is maintained in neurons but is temporary in the sensory lineage throughout inner ear development. ISL1 is found at relatively high concentrations in the sensory primordium of the cochlea but is downregulated as the cochlear epithelium starts to differentiate (Radde-Gallwitz *et al.*, 2004).

The expression of ISL1 in the inner ear reveals an early common step in the development of both sensory and neuronal lineages and raises the possibility that ISL1 plays a role in

specifying the inner ear neuronal and sensory competency together with basic helix-loop-helix (bHLH) proteins (Radde-Gallwitz *et al.*, 2004).

1.5.2. Forkhead box transcription factor FOXG1

"Forkhead box (FOX) proteins are transcription factors that are responsible for fine-tuning the spatial and temporal expression of a broad range of genes" (Lam *et al.*, 2013). FOX proteins regulate the cell cycle progression, cell proliferation and differentiation. They are also involved in regulating metabolism, senescence, survival and apoptosis. FOX proteins contain evolutionary conserved 'fork-head' or 'winged-helix' DNA-binding domain.

FOXG1 transcription factor was discovered in 1992 and its expression was localized into the telencephalon of the developing rat brain, namely into the cortex, olfactory bulb, hippocampus and caudate putamen (Tao and Lai, 1992). *Foxg1* expression is absent in the cerebellum and thalamus. The telencephalon-derived structures also express *Foxg1*. The diencephalic neuroepithelium, such as the optic stalk and optic cup, which will give rise to the retina were initially thought to be devoid of *Foxg1* expression. However, *Foxg1* is specifically expressed, from E8.5–E9.5, in the mouse ventral nasal retina and by E12.5 moves to the dorsal nasal retina (Mui *et al.*, 2002). Also some sites outside of the central nervous system, including the olfactory epithelium, otocyst and pharyngeal pouches, demonstrate *Foxg1* expression (Tao and Lai, 1992). It was suggested that FOXG1 plays a role in the regional differentiation of the neural tube and the formation of the telencephalon.

FOXG1 is essential for the normal growth and differentiation of the telencephalic neuroepithelium (Xuan *et al.*, 1995). In *Foxg1* mutant mice, the proliferation of the ventral telencephalic neuroepithelium is disrupted already at E9.5 and the dorsal telencephalic NECs are prematurely leaving the cell cycle to differentiate. This suggests that FOXG1 enhances cell proliferation by facilitating cell cycle progression and that FOXG1 is an important regulator of the progenitor-to-neuron transition in the mammalian telencephalon.

Foxg1 is expressed in the developing otocyst and persists to be expressed in most cell types of the inner ear of the adult mouse (Pauley, Lai and Fritzsch, 2006). At E18.5,

Foxg1 was expressed in all sensory regions of the inner ear and also in the spiral and vestibular ganglion neurons. *Foxg1* null mutant mice have severe defects of the inner ear: shortened cochlea with excessive rows of hair cells, reduction of canals and canal cristae and aberrations in cochlear and vestibular innervation. *Foxg1-cre* mice have been used for otic-specific recombination that occurs already at the 5-6-somite stage in the prospective otic ectoderm (Barrionuevo *et al.*, 2008).

1.5.3. Basic helix-loop-helix transcription factor NEUROD1

NEUROD1 is a bHLH transcription factor that is expressed during embryonic development in the mammalian pancreas, nervous system and intestine (Naya, Stellrecht and Tsai, 1995).

Neurod1 is expressed in both sensory ganglion neurons and sensory epithelia during the development of the cochlear and vestibular system in the inner ear (Liu *et al.*, 2000). The expression of *Neurod1* is regulated by Neurogenin 1 (NGN1) in inner ear sensory neurons and by ATOH1 in hair cells (Ma *et al.*, 1998; Jahan *et al.*, 2010). *Neurod1* expression is first detected within the otic vesicle wall in the neuroblast precursors at E8.75 (Liu *et al.*, 2000).

Neurod1 is expressed in both proliferating neural precursors and postmitiotic neurons (Liu *et al.*, 2000). Neuroblast precursors in mice with targeted disruption of *Neurod1* gene failed to initiate differentiation (Naya *et al.*, 1997; Liu *et al.*, 2000). Therefore, NEUROD1 does not play a primary role in the proliferation or specification of neuroblast precursors, instead, NEUROD1 is important for the delamination, differentiation and survival of neuroblast precursors (Kim *et al.*, 2001; Liu *et al.*, 2000). NEUROD1 suppresses ATOH1-mediated hair cell differentiation in neuronal precursors in sensory ganglia (Jahan *et al.*, 2010). In *Neurod1* null mice, some ganglion cells differentiate into hair cells due to lack of ATOH1 suppression by NEUROD1. NEUROD1 also suppresses *Ngn1* in differentiating neurons.

Loss of NEUROD1 also causes alterations in the mechanosensory hair cells of the inner ear (Liu *et al.*, 2000). *Neurod1* null mice have a shortened cochlea and alterations in the organization of hair cells in the cochlear apex (Jahan *et al.*, 2010). Therefore, NEUROD1 is important for the correct differentiation of neurosensory cells of the inner ear.

1.5.4. SRY related HMG box protein SOX2

HMG domain of SOX proteins has a twisted L-shape and consists of three alpha-helices; two of which interact with target DNA, exclusively in the minor groove (Werner *et al.*, 1995). SOX2 is involved in early developmental processes and organogenesis, particularly it regulates a wide spectrum of stem cells (Kondoh and Lovell-Badge, 2016; Takahashi and Yamanaka, 2006). Various stem cells express and require the activity of SOX2 (Bylund *et al.*, 2003). In embryonic stem cells, SOX2 is necessary for the maintenance of pluripotency by maintaining requisite level of *Pou5f1* expression (Masui *et al.*, 2007). SOX2 and POU5F1 form a heterodimer in embryonic stem cells activating *Sox2* and *Pou5f1* genes by formation of co-activation loops of these genes (Kondoh and Lovell-Badge, 2016). *Sox2* is expressed from the earliest developmental stages in embryonic nervous system (Pevny and Nicolis, 2010). *Sox2* is active predominantly in the proliferating, undifferentiated precursors, including neural stem cells.

SOX2 together with SOX1 and SOX3 belong to the SoxB1 group of proteins, which share not only the overall amino acid sequences but also the expression patterns in embryos (Wood and Episkopou, 1999; Kondoh and Lovell-Badge, 2016). This suggests that these proteins overlap in their functions in tissues, in which they are co-expressed. However, *Sox2* is the only *SoxB1* gene expressed before implantation and it is essential during early stages of embryogenesis as mutant embryos fail to survive shortly after implantation (Avilion *et al.*, 2003). It was found that SOX2 is essential for the inner cell mass and trophectoderm lineage development.

All SoxB1 transcription factors are critical determinants of neurogenesis (Bylund *et al.*, 2003). The generation of neurons from stem cells depend on the inhibition of *SoxB1* expression by proneural proteins. Therefore, SoxB1 factors are important for the maintenance of the neural stem cell state by inhibiting the bHLH-mediated neuronal differentiation.

SOX2 regulates the development of sensory primordia derived from the cephalic placodes, the lens and inner ear (Kondoh and Lovell-Badge, 2016).

1.5.4.1. Role of SOX2 during eye development

Regulation of *Sox2* expression is critical for correct eye development in vertebrates (Heavner, Andoniadou and Pevny, 2014). Deletion of *Sox2* in mouse optic cup progenitor cells caused loss of neural competence and changed the neural retina into a non-neurogenic fate. Upon deletion of *Sox2*, response to WNT signalling is expanded, which correlates with loss of neural competence. This observation suggests that SOX2 negatively regulates the WNT pathway to maintain the neurogenic fate in the developing retina.

Heterozygous mutations of *Sox2* in humans are mostly resulting in anophthalmia (absence of eye) (Heavner and Pevny, 2012). However, in some cases *Sox2* mutation causes microphthalmia (small eye). In these cases, the retina is functional.

1.5.4.2. Role of SOX2 during the olfactory system development

Sox2 is expressed in the neuroectoderm from the onset of somitogenesis (Wood and Episkopou, 1999). In the developing olfactory placode, *Sox2* was detected at E8.5 in mice. At postnatal stages, *Sox2* is expressed in neural stem cells within the olfactory epithelium, namely in basal cells (Guo *et al.*, 2010).

The olfactory epithelium maintains adult neurogenesis (Kaplan and Hinds, 1977). SOX2 is essential for the establishment, maintenance and expansion of the neuronal progenitor pool in the nasal epithelium by suppressing *Bmp4* and upregulating *Hes5* expression (Panaliappan *et al.*, 2018). SOX2 activity therefore promotes the formation of the neurogenic sensory domain and restricts the respiratory domain in the nasal epithelium.

1.5.4.3. Role of SOX2 during inner ear development

SOX2 marks the neurosensory progenitors within the otic epithelium as one of the earliest factors (Cheah and Xu, 2016). *Sox2* is first detected in the ventral half of the otic placode at E8.5 in mouse embryo (Wood and Episkopou, 1999). Based on the expression pattern, it was postulated that *Sox2* is important for the early development of sensory neurons and

prosensory organs and for the later development, the specification and differentiation of hair cells and supporting cells (Cheah and Xu, 2016).

The otic vesicle closes at E9.5 (Cheah and Xu, 2016). At this time, SOX2 is expressed in the ventral and lateral region of the otocyst, the proneural region, from which neuroblasts delaminate and form the vestibular ganglion (Mak *et al.*, 2009). This expression pattern continues in the otocyst at E10.5 with the addition of delaminating neuroblasts expressing SOX2. At E12.5, SOX2 marks the sensory precursors of the cristae, maculae and cochlear duct and later is expressed in both developing hair cells and supporting cells in the mouse inner ear. In addition, SOX2 is expressed in cells of the GER located medially of the developing cochlear sensory epithelium (Dabdoub *et al.*, 2008). As the inner ear matures, the expression of SOX2 is restricted to the supporting cells in both the vestibular system and auditory system and to a subset of type II hair cells in the vestibular system (Hume, Bratt and Oesterle, 2007). During the differentiation of chick sensory epithelia, *Sox2* is expressed only in supporting cells (Neves *et al.*, 2007). SOX2 expression in mice is maintained in high levels in supporting cells and GER cells at postnatal stages (Cheah and Xu, 2016).

1.5.4.3.1. Impact of *Sox2* mutations on inner ear development

Analyses of two allelic mouse mutants with balance and hearing impairment showed the essential role of SOX2 in the establishment of a prosensory domain of the inner ear (Kiernan *et al.*, 2005). *Yellow submarine* (*Ysb/Ysb*) recessive mutation arises from the insertion of a transgene and *Light coat and circling* (*Lcc/Lcc*) mutation is caused by X-irradiation (Dong *et al.*, 2002). Both mutations involve chromosome 3 and cause absence (*Lcc/Lcc*) or reduced expression (*Ysb/Ysb*) of transcription factor SOX2 in the developing inner ear (Kiernan *et al.*, 2005; Dong *et al.*, 2002). The *Sox2* gene itself is intact in these mutants (Kiernan *et al.*, 2005). *Lcc/Lcc* and *Ysb/Ysb* mutations are caused by inactivation of regulatory elements controlling the expression of *Sox2* in the inner ear.

Mice with both mutations fail standard balance tests (Dong *et al.*, 2002). Moreover, *Lcc/Lcc* mice are completely deaf, whereas *Ysb/Ysb* mutation causes severe hearing impairment.

Both mutations cause abnormal development with aberrant inner ear morphology (Kiernan *et al.*, 2005). The most severely affected regions are those that contain sensory regions (Figure 16). In *Lcc/Lcc* mice, all three ampullae are missing and the semicircular canals show only rudimentary development. The most prominent structure of the mutant inner ear is cochlea, but it is not properly coiled; the saccule and utricle are extremely small. *Ysb/Ysb* mice have missing anterior and lateral ampullae and the corresponding semicircular canals are truncated.

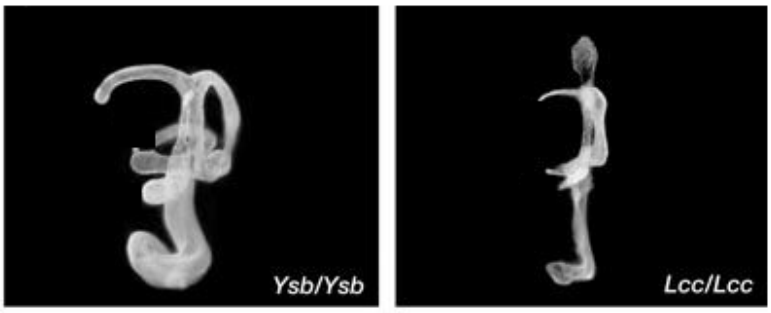

Figure 16: Inner ear malformations in *Ysb* and *Lcc* mice (modified from (Kiernan *et al.*, 2005)); paintfilled inner ears at E16.5

Lcc/Lcc mice fail to develop any hair cells or supporting cells, but some sensory formation is found in *Ysb/Ysb* mice (Kiernan *et al.*, 2005). The base of the cochlea contains patches of hair cells and continuous but irregular rows of hair cells develop in the apex. The utricle contains almost no hair cells.

"The molecular controls regulating specification, delamination and proliferation of otic neuroblasts and their differentiation and maturation are only partially understood" (Cheah and Xu, 2016). The fact that SOX2 expression was detected in the spiral ganglion neurons in P0 cochleae and that spiral ganglion neurons are absent in cochleae from *Lcc/Lcc* mice indicate that SOX2 is required for neuronal formation in the cochlea (Puligilla *et al.*, 2010). Additionally, ectopic expression of SOX2 in nonsensory regions of the cochlea induced neuronal fate, which suggests that SOX2 is sufficient for the induction of neurogenesis in the inner ear.

1.5.4.3.2. SOX2 and its interactions

Sox2 is expressed in response to JAG1-mediated activation of the Notch cascade within prosensory cells of the cochlea (Dabdoub *et al.*, 2008). High levels of SOX2 antagonize activity of ATOH1, a transcription factor necessary for hair cell development, and ATOH1 in turn leads to downregulation of *Sox2*. Therefore the role of SOX2 in sensory development is complex. SOX2 expression is required for specification of prosensory cells and subsequent downregulation of SOX2 is required for differentiation of prosensory cells into hair cells.

SOX2 was shown to bind not only to *Atoh1*, but also to particular *Atoh1* antagonists, such as *Ngn1* and *Neurod1* (Cheah and Xu, 2016).

A subpopulation of epithelial cells at the otic cup stage begins to express *Ngn1* and continues expressing *Neurod1*, until the early stages of otocyst development (Evsen *et al.*, 2013). This subpopulation of neuroblasts soon exits from the otocyst epithelium and coalesces to form neurons of the vestibular ganglion. SOX2 may confer neural competency by promoting *Ngn1* expression and then negative feedback inhibition of *Sox2* by NGN1 would be essential for the progression of neurogenesis to form nascent neurons. Using a transient gain-of-function approach, Evsen *et al*. showed that overexpression of *Sox2* can induce *Ngn1* expression in the otocyst but *Neurod1* expression and delamination of neuroblasts from the otic epithelium are inhibited.

Regulated transcription of Cyclin-dependent kinase inhibitor 1B ($p27^{Kip1}$) is necessary to guide the accurate pattern of cell cycle exit that is essential for normal development (Lee, Liu and Segil, 2006). In the prosensory phase of cochlear development, prosensory progenitors proliferate and then exit the cell cycle following the expression of cell cycle inhibitor $P27^{Kip1}$. It was shown that SOX2 directly activates $p27^{Kip1}$ in postmitotic inner pillar cells (IPCs) and therefore, regulates cell cycle of IPCs by mediating expression of $p27^{Kip1}$ (Liu *et al.*, 2012). Deletion of *Sox2* in IPCs at different postnatal ages causes a loss of $p27^{Kip1}$ expression and IPC proliferation. Hence, SOX2 also promotes proliferation and cell fate determination. These data show that SOX2 is an upstream regulator of $p27^{Kip1}$ and that its function is to keep the quiescent state of postmitotic IPCs.

During inner ear hair cell specification, transcription factors EYA1 and SIX1 have been identified as binding partners of SOX2 (Ahmed *et al.*, 2012; Zou *et al.*, 2008). Hair cell

differentiation requires activation of ATOH1 function, whereas *Eya1*, *Six1* and *Sox2* are co-expressed in sensory progenitors (Ahmed *et al.*, 2012). EYA1/SIX1 cooperatively act with SOX2 to induce the hair cell fate in cochlear nonsensory epithelium by activating *Atoh1* transcription via direct binding to the *Atoh1* enhancers.

The binding of SOX2 protein alone to DNA does not elicit a regulatory function but it is necessary for the formation of transcriptional complexes (Kamachi and Kondoh, 2013). Thus, the function of SOX2 protein is dependent on the characteristics of its binding or cooperating factors and DNA binding sites.

SOX2 is a crucial factor regulating neurosensory development in the inner ear (Kamachi and Kondoh, 2013). However, its precise function is not clear. Particularly, investigation of the downstream targets of SOX2 and the full range of SOX2 partners and their interactions leading to the regulation of specification, proliferation, differentiation and maintenance of inner ear cells is an important task (Cheah and Xu, 2016). For example, we do not understand why SOX2-positive supporting cells in mammals do not respond to damage by inducing re-expression of developmental regulatory genes and to regenerate hair cells as it does in nonmammalian vertebrates (Corwin and Cotanche, 1988; Raphael, 1992; Corwin and Oberholtzer, 1997). Similarly, the role of SOX2 in the specification of otic neuronal precursors and neuronal development is not solved.

1.5.5. Other important genes in the inner ear development

In mice, the formation of ganglion neuronal precursors that express *Ngn1* is an early event in ear development (Ma *et al.*, 1998). NGN1 is required for the activation of downstream genes encoding bHLH factors, such as *Neurod1*, a differentiation-regulating transcription factor. *Ngn1* is expressed in delaminating ganglion neuronal precursors in the mouse otocyst as early as E9, followed by *Neurod1* expression in the otocyst and in the delaminating ganglion neurons.

Gata3 is expressed in the developing and adult inner ear efferent neurons, which extend from the rhombomere 4 and innervate both vestibular and auditory system (Karis *et al.*, 2001). In addition, *Gata3* is expressed in all sensory epithelia of the ear (except for the saccule) and in delaminating cochlear afferent neurons. Vestibular afferent neurons do not

express *Gata3*. GATA3 also plays a pivotal role in prosensory domain specification in the cochlea (Luo *et al.*, 2013).

Otic sensory neurons require Brain-derived neurotrophic factor (BDNF) and Neurotrophin 3 (NTF3) proteins for their correct outgrowth and survival (Fariñas *et al.*, 2001). *Bdnf* and *Ntf3* neurotrophins are expressed in inner ear sensory epithelia, whereas sensory neurons express their receptors Tyrosine receptor kinase B (*TrkB*) (for BDNF) and *TrkC* (for NTF3). During embryonic development, all cochlear neurons express both *TrkB* and *TrkC* and, consequently, can respond to both neurotrophins, whose distribution in cochlear epithelium is different. Interestingly, delaminating sensory neurons also transiently express *Ntf3* and *Bdnf* at the time or soon after delamination from the sensory epithelium. Differentiated otic sensory neurons do not express neurotrophins but grow neurites toward the sensory epithelium over the region of neurotrophin-expressing cells.

2. AIMS OF WORK

Understanding the molecular interactions necessary for the early neurosensory development of the inner ear is an essential basis for implementation of new therapeutic strategies of hearing loss. *Sox2* is one of early genes expressed in both neuronal and sensory precursors of the developing inner ear suggesting its importance in the specification of both these lineages.

The aim of this study was to gain an insight into the role of SOX2 transcription factor during inner ear development. To determine the requirements of SOX2, we generated different conditional deletions of *Sox2* gene using *cre-loxP* strategy. Specifically, we used *Isl1-cre*, *Foxg1-cre* and *Neurod1-cre* drivers to eliminate $Sox2^{flox/flox}$ (details see below). In these different $Sox2^{-/-}$ mutant mice, we evaluated morphological changes of the inner ear structure, the formation of sensory epithelia, innervation pattern, number of developing sensory cells and neurons and hearing functions.

Additionally, we showed changes in the development of the olfactory and lens placodes in the absence of SOX2.

2.1. *Isl1-cre* conditional *Sox2* knockout (*Isl1-cre, Sox2 CKO*)

Isl1-expressing cells give rise to both sensory epithelia and neurons of the inner ear (Radde-Gallwitz *et al.*, 2004). Therefore, we have expected that *Isl1-cre* driver will eliminate *Sox2* in neuronal and sensory precursors in the otocyst and we will be able to evaluate the effects of *Sox2* conditional deletion on the development of inner ear sensory epithelia and neurons.

2.2. *Foxg1-cre* conditional *Sox2* knockout (*Foxg1-cre, Sox2 CKO*)

Foxg1 gene is strongly expressed at placodal stages of embryonic development. Thus, we selected *Foxg1-cre* driver to delete *Sox2* at the very beginning of inner ear development, at the otic placodal stage. Since *Foxg1-cre* is also expressed early in the development of olfactory and lens placodes (Pandit, Jidigam and Gunhaga, 2011), we additionally have planned to compare the requirements for SOX2 in the inner ear, eye and olfactory sensory systems.

2.3. *Neurod1-cre* conditional *Sox2* knockout (*Neurod1-cre, Sox2 CKO*)

Neurod1 is expressed during neurosensory differentiation in both sensory ganglion neurons and sensory epithelia (Jahan *et al.*, 2010). *Neurod1* is expressed both in proliferating neural precursors and in postmitiotic neurons. In differentiating neuronal cells, NEUROD1 suppresses ATOH1-mediated hair cell fate. Therefore, we have expected that *Neurod1-cre* will eliminate *Sox2* in neuroblasts and differentiating neurons and thus, we will be able to establish the requirements for SOX2 in neuronal precursors.

3. MATERIALS AND METHODS

3.1. Mouse models

All methods were performed in accordance with the Guide for the Care and Use of Laboratory Animals (National Research Council. Washington, DC. The National Academies Press, 1996). The experimental outline was approved by the Animal Care and Use Ethics Committee of the Institute of Molecular Genetics, Czech Academy of Sciences. The experimental mice were housed in a controlled environment (12-h light, 12-h dark cycles) with free access to food and water. Mice were kept under standard experimental conditions with a constant temperature (23–24°C). The females were housed individually during the gestation period and the litter size was recorded.

The experiments were performed with the littermates cross-bred from following transgenic mouse lines obtained from The Jackson Laboratory: *Sox2*^{flox} (*Sox2*$^{tm1.1Lan}$/J, stock #013093) with either *Isl1-cre* (*Isl1*$^{tm1(cre)Sev}$/J, stock #024242), *Foxg1-cre* (*Foxg1*$^{tm1(cre)Skm}$/J, stock #004337) or *Neurod1-cre* [Tg(Neurod1-cre)1Able/J, stock #028364] (Shaham *et al.*, 2009; Yang *et al.*, 2006; Hebert and McConnell, 2000; Li *et al.*, 2012). Breeding pairs contain a mouse with two floxed *Sox2* alleles (*Sox2*$^{f/f}$) and a mouse with one floxed *Sox2* allele together with one *cre* allele of either type. To determine the efficiency of cre-mediated recombination, we used reporter Ai9 mice (RCL-tdTomato, stock #007909, The Jackson Laboratory) (Madisen *et al.*, 2010). The noon of the day the vaginal plug was found was determined as E0.5.

Heterozygous mice *Sox2*$^{+/f}$, *cre*$^{+/-}$ were comparable to the control mice with genotype *Sox2*$^{f/f}$ or *Sox2*$^{+/f}$ without any detectable morphological or functional differences and were therefore used as controls if needed.

3.1.1. DNA isolation and genotyping

Genotyping was performed by polymerase chain reaction (PCR) on DNA extracted from murine tail tip.

The DNA was precipitated by isopropanol from the aqueous solution. The tails were incubated overnight at 55°C with lysis buffer (1M Tris; 0.5M EDTA; 5M NaCl; 10% SDS; pH 8) and proteinase K (Sigma-Aldrich) to lyse the tissue. The lysate was

centrifuged and the supernatant was transferred to a clean vial before adding isopropanol. The precipitated DNA was centrifuged, dehydrated in ethanol and air dried. Finally, the DNA was dissolved in water prior to measuring concentration on spectrophotometer (NanoDrop 1000).

1 µl DNA was used for PCR in total volume of 20 µl. 5x HOT FIREPol® Blend Master Mix Ready to Load (Solis BioDyne) together with primers and DNA were all reagents used for the reaction. The primers used for genotyping were the following:

Sox2 forward (F) (5′-TGG AAT CAG GCT GCC GAG AAT CC-3′), *Sox2* reverse (R) wild type (5′-TCG TTC TGG CAA CAA GTG CTA AAG C-3′) and *Sox2* R mutant (5′-CTG CCA TAG CCA CTC GAG AAG-3′) with 427 base pair (bp) product for wild type allele or with 546 bp product for floxed allele;

Isl1-cre F (5′-GCC TGC ATT ACC GGT CGA TGC AAC GA-3′) and *Isl1-cre* R (5′-GTG GCA GAT GGC GCG GCA ACA CCA TT-3′) with 700 bp product;

Foxg1-cre F (5'-GCG GTC TGG CAG TAA AAA CTA TC-3') and *Foxg1-cre* R (5'-GTG AAA CAG CAT TGC TGT CAC TT-3') with 100 bp product;

Neurod1-cre F (5′-CCA TTT TGC AGT GGA CTC CT-3′) and *Neurod1-cre* R (5′-ACG GAC AGA AGC ATT TTC CA-3′) with 320 bp product.

PCR products were evaluated by 2% agarose gel electrophoresis and detected by adding ethidium bromide to the gel.

3.2. Immunohistochemistry

For whole-mounts, dissected tissues (inner ears, heads or all embryos) were fixed in 4% paraformaldehyde (PFA) in Phosphate buffered saline (PBS) or stepwise methanol series (up to 100%). For vibratome sections, fixed samples were embedded in 4% agarose gel and sectioned at 80 µm on a Leica VT1000S vibratome.

Samples fixed in PFA were defatted in 70% ethanol and then rehydrated prior to immunostaining. Vibratome sections, whole inner ears or whole embryos were blocked with serum (2.5% serum; 0.5% Tween; 0.1% Triton in PBS). Samples were then incubated with primary antibodies diluted in blocking solution at 4ºC for 72 hours.

The primary antibodies used were:

anti-acetylated α-TUBULIN (Sigma-Aldrich T6793, 1:400),

anti-cleaved CASPASE 3 (Cell Signaling Technology 9661, 1:100),

anti-CRE (BioLegend 908001, 1:500),

anti-GATA3 (R&D Systems AF2605, 1:20),

anti-ISL1 (Developmental Studies Hybridoma Bank (DSHB) 39.3F7, 1:130) and anti-ISL1/2 (DSHB 39.4D5, 1:200); 39.3F7 was deposited to the DSHB by Jessell, T.M./Brenner-Morton, S.

anti-KI67 (Cell Signaling Technology 9129, 1:400),

anti-MYO7A (Proteus BioSciences 25-6790, 1:500),

anti-Neuronal nuclei (NeuN) (Abcam ab177487, 1:500),

anti-NEUROD1 (Santa Cruz Biotechnology sc-1084, 1:100),

anti-Neurofilament 200 (NF200) (Sigma-Aldrich N4142, 1:200)

anti-P75 (Sigma-Aldrich N3908, 1:1000)

anti-PAX2 (Covance PRB-276P, 1:500)

anti-SOX2 (Millipore AB5603, 1:500) and anti-SOX2 (Santa Cruz Biotechnology sc-17320, 1:250),

anti-SOX10 (Abcam ab155279, 1:250),

anti-TRKC (R&D Systems AF1404, 1:100).

After several PBS washes and blocking with serum, secondary antibodies diluted in blocking solution were added and incubated at 4°C for 24 hours.

Following secondary antibodies were used in dilution 1:400:

Alexa Fluor® 488 AffiniPure Goat Anti-Mouse Immunoglobulin G (IgG) (Jackson ImmunoResearch Laboratories 115-545-146),

Alexa Fluor® 594 AffiniPure Goat Anti-Rabbit IgG (Jackson ImmunoResearch Laboratories 111-585-144),

DyLight 488-conjugated AffiniPure Mouse Anti-Goat IgG (Jackson ImmunoResearch Laboratories 205-485-108),

DyLight 594-conjugated AffiniPure Mouse Anti-Goat IgG (Jackson ImmunoResearch Laboratories 205-515-108),

Alexa Fluor® 488 AffiniPure Donkey Anti-Goat IgG (Jackson ImmunoResearch Laboratories 705-545-003),

Alexa Fluor® 594 AffiniPure Donkey Anti-Goat IgG (Jackson ImmunoResearch Laboratories 705-585-003).

Nuclei were stained by Hoechst 33258 (Sigma-Aldrich 861405, 1:2000). Samples were mounted on slides in Aqua-Poly/Mount (Polysciences 18606) or in prepared Antifade medium (21.2 mg *n*-propyl gallate; 200 µl 1M Tris pH 8; 800 µl glycerol) and images were taken on Zeiss LSM 5 DUO, Zeiss LSM 880 or Leica SPE confocal microscopes. Images were processed in ImageJ and ZEN software.

3.2.1. BrdU, EdU staining

Pregnant mice were intraperitoneally injected with 10 µg/g 5-ethynyl-2'-deoxyuridine (EdU) in PBS at E9.5 and with 50 µg/g 5-bromo-2'-deoxyuridine (BrdU) in PBS one day later, at E10.5. Embryos from injected mothers were collected at E11.5 and fixed in 4% PFA for one hour. 80 µm transverse sections of whole embryos were prepared on vibratome. Proliferating cells were stained using Click-iT EdU Alexa Fluor 647 Imaging Kit (C10340, ThermoFisher) and mouse anti-BrdU antibody (Sigma-Aldrich B2531, 1:1000).

3.2.2. Cells quantification

Cells quantification was made on whole-mounted immunostained samples or on vibratome sections using LAS AF Lite draw counter or ImageJ Cell Counter.

The total number of hair cells was counted in the entire utricle and saccule and in the entire cochlea of *Isl1-cre, Sox2 CKO* mice. The number of hair cells in the control cochlea was counted in the 1.5 mm long segment of the base.

CASPASE 3-positive cells were quantified in the vestibular ganglion at E11.5–E13.5 and in the superior vestibular ganglion at E14.5–E15.5 in both control and *Isl1-cre, Sox2 CKO* mice after the whole-mount immunostaining.

CASPASE 3-positive areas in the vestibular ganglia of controls and *Foxg1-cre, Sox2 CKO* mutants were assessed using the thresholding tool in ImageJ. The Mann-Whitney U test (GraphPad Prism) was used for statistical analysis.

The difference of vestibular ganglion size and number of neurons between *Foxg1-cre, Sox2 CKO* mice and their littermate controls was quantified on vibratome sections from embryos at E10.5 after immunohistochemistry.

The statistically significant differences between controls and mutants were analyzed by GraphPad Prism multiple Student's *t*-test with the Holm-Sidak method. At least three specimens of each group were included to increase the significance of the test.

The length of the immunostained and mounted cochlear duct along the basilar membrane was measured by ImageJ.

3.3. Haematoxylin-eosin staining

Embryonic heads were dehydrated in graded methanol series and transferred into 70% ethanol. Subsequent transfer into xylene and saturation with paraffin was done in Leica ASP200 Vacuum tissue processor. Samples were embedded into paraffin blocks on Leica EG1150 Tissue Embedding System. Paraffin blocks were sectioned on Leica RM2255 microtome into 7 µm thick sections.

Paraffin was removed from the sections of embryonic heads by xylene. Samples were rehydrated in decreasing ethanol series. Sections were then stained with haematoxylin-eosin by following scheme: haematoxylin (40 seconds), washing in tap water (5 minutes), washing in acid alcohol to remove color from the surrounding tissue, tap water (5 minutes), eosin (5 seconds) and washing in distilled water (5 minutes). After staining, samples were dehydrated in ethanol series, transferred into xylene and mounted with DPX Mountant for histology (Sigma-Aldrich). Images of embryonic eyes were taken on Nikon ECLIPSE 50i microscope.

3.4. Skeletal staining

Heads of E17.5 mouse embryos were left in a water-filled vial for 2 hours at room temperature. Then the vials were placed in a thermoblock with 65°C for one minute to allow the skinning of the samples. Skinning and subsequent evisceration was done on a Petri dish. Heads were then dehydrated in 100% ethanol and cartilages were stained with Alcian Blue 8GX (Sigma) in 80% ethanol and 20% acetic acid for one day. Samples were rinsed in 100% ethanol overnight and cleared in 2% potassium hydroxide for 6 hours before staining the bones with Alizarin red S (Sigma) in 2% potassium hydroxide for 3 hours. Final clearing was done by 2% potassium hydroxide for one day and then transferred stepwise into 100% glycerol. The skulls were photographed with a Nikon stereomicroscope.

3.5. *In situ* hybridization

In situ hybridization was performed using a RNA probe labelled with digoxigenin (Jahan *et al.*, 2010). Plasmids containing complementary DNAs (cDNAs) were used to generate the RNA probe by *in vitro* transcription. Plasmids were gifts from H. Zoghbi (*Atoh1*), D. Wu (*Bmp4*), K. Cheah (*Sox2*) and D. Ornitz (*Fgf10*).

Mice were transcardially perfused with 4% PFA. The ears were dissected in 0.4% PFA and dehydrated and rehydrated in graded methanol series. Samples were washed in RNase-free PBS and then digested with 20 µg/ml of Proteinase K (Ambion, Austin, TX, USA) for 15–20 minutes. The digestion was stopped by brief washing in 4% PFA. Then the samples were hybridized overnight at 60°C to the riboprobe in hybridization solution containing 50% formamide, 50% 2X Saline sodium citrate (SSC) (Roche) and 6% dextran sulphate. The unbound probe was washed off and the samples were incubated overnight with an anti-digoxigenin antibody conjugated with alkaline phosphatase (Roche Diagnostics GmbH, Mannheim, Germany). After a series of washes, the samples were reacted with nitroblue phosphate/5-bromo, 4-chloro, 3-indolyl phosphate (BM purple substrate) (Roche Diagnostics, Germany). The ears were mounted flat in glycerol and viewed in a Nikon Eclipse 800 microscope using differential interference contrast. Finally, images were captured with Metamorph software.

3.6. Electron microscopy

All of the excessing structures and membranes were removed from PFA fixed inner ears. Samples in porous specimen pots were then dehydrated in ethanol series followed by absolute acetone. Tissues were critical point dried in liquid carbon dioxide in a K850 Critical Point Dryer (Quorum Technologies Ltd, Ringmer, UK). The dried samples were mounted onto carbon conductive double-sided adhesive discs with sensory epithelia facing upwards and sputter-coated with 20 nm of gold in a Polaron Sputter-Coater E5100 (Quorum Technologies Ltd, Ringmer, UK). Samples were examined in FEI Nova NanoSem 450 scanning electron microscope (FEI Czech Republic s.r.o.) at 5 kV using a secondary electron detector.

3.7. 3D reconstruction

3D reconstruction was performed on mouse inner ears at E12.5 and E14.5 (Kopecky *et al.*, 2012b). Inner ears were dehydrated in ethanol or methanol series and stained with 0.5 μg/ml Rhodamine B isothiocyanate in 100% ethanol for two days. Samples were then cleared by MSBB solution (5:3 methyl salicylate and benzyl benzoate) overnight, rinsed with fresh MSBB and mounted onto a glass slide with chamber made with vacuum grease. Images of whole inner ears were taken by confocal microscopes (Zeiss LSM 5 DUO, Zeiss LSM 880 or Leica SPE) and processed in ImageJ (Preibisch, Saalfeld and Tomancak, 2009). 3D structures of inner ears were reconstructed from confocal stacks in 3D Slicer or Amira 3D software (Thermo Fisher Scientific) by manually segmenting areas of interest.

3.8. Lipophilic dye tracing

The pattern of peripheral and central innervation was evaluated in whole or dissected ears and brains using lipophilic dye tracing (Fritzsch *et al.*, 2016). The samples (whole embryos or embryonic heads) were fixed overnight in 10% PFA with 0.3M sucrose and then transferred into 0.4% PFA with 0.3M sucrose prior to labelling.

Heads were split along the midline to enable insertion of filter strips loaded with differently colored lipophilic dyes. We inserted filter strips into the specific areas in the

brain or in the ear. The dyes were inserted into the trigeminal ganglion to label the trigeminal nerve, into the jugular foramen of IX/X (glossopharyngeal/vagus nerve) to label IX–XI nerves, into the cochlear and vestibular nuclei of the brainstem around rhombomere 5 to label inner ear afferents, into the alar plate of rhombomere 5/6 to label intermediate nerve fibers and vestibular and cochlear afferents, into the basal plate of rhombomere 4 to label vestibular afferents and inner ear efferents, into rhombomere 4 near the midline to label the facial nerve and inner ear efferents, into the cochlear duct to label cochlear afferents and into vestibular end organs to label vestibular afferents, as described in (Maklad *et al.*, 2010).

After diffusion of the lipophilic dye from insertion to the target, we prepared the ears or brains as whole-mounts, mounted with glycerol on a glass slide. Appropriate spacers were used to avoid distortion. Images were taken by Leica SP5 or Leica SP8 confocal microscope. Selected ears were then dissected to allow imaging of the detailed innervation of the flat mounted sensory epithelia. Image stacks were collected and single images or sets of stacks were recorded to provide detailed information about the ear innervation. Images were compiled into plates using Corel Draw.

3.9. Hearing function evaluation

To define the auditory function of the experimental animals recording of auditory brainstem response (ABR) and distortion product otoacoustic emission (DPOAE) was performed (Chumak *et al.*, 2016). All tests were carried out on mice, anesthetized with ketamine and xylazine and maintained in a sound-attenuating and anechoic chamber.

For ABR recording, needle electrodes were placed subcutaneously on the cranial vertex (active electrode) and in the neck muscles (ground and reference electrodes). Acoustic stimuli were generated with a TDT System 3 (Tucker Davis Technologies). Hearing thresholds were determined at 2, 4, 8, 16, 32 and 40 kHz. The response threshold to each frequency was determined as the minimal tone intensity that still evoked a noticeable potential peak in the expected time window of the recorded signal.

DPOAEs were recorded at individual frequencies over the frequency range from 4 to 38 kHz with a low-noise microphone system ER-10B+ probe (Etymotic Research). Acoustic stimuli were presented to the ear canal with two custom-made piezoelectric

stimulators connected to the probe. The signal from the microphone was analyzed by the TDT System 3.

4. RESULTS

Results collected during my PhD study and summarized in this thesis were published in two first-authored publications:

- Incomplete and delayed Sox2 deletion defines residual ear neurosensory development and maintenance (Dvorakova *et al.*, 2016)
- Early ear neuronal development, but not olfactory or lens development, can proceed without SOX2 (Dvorakova *et al.*, 2019)

4.1. The effect of delayed and incomplete *Sox2* deletion on inner ear development

Isl1-cre, Sox2 CKO mice were used to study the effect of *Sox2* deletion in both the inner ear sensory and neuronal lineages. *Isl1-cre, Sox2 CKO* mice died immediately after birth, although they did not manifest any external morphological defects except for a reduced and malformed eye.

First, we confirmed that ISL1 and SOX2 expression partially overlapped in the otic neurosensory epithelium at E9.5 (Figure 17).

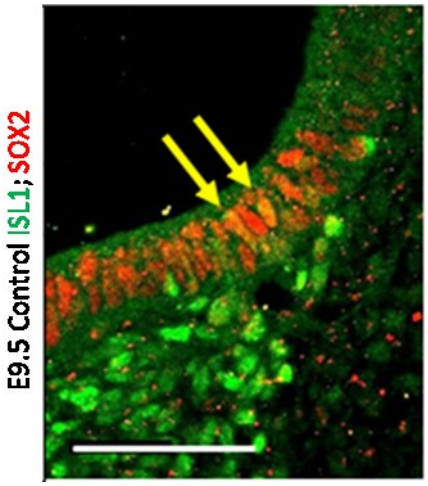

Figure 17: ISL1 (green) was co-expressed with SOX2 (red) in the otic neuroepithelium at E9.5 (arrows) (Dvorakova *et al.*, 2016). Scale bar: 100 µm

Isl1-cre mediated deletion of *Sox2* resulted in considerably altered inner ear morphology as revealed by 3D reconstruction of inner ears at E12.5 and E14.5 (Figure 18). The *Isl1-cre, Sox2 CKO* inner ears had no ampullae of the semicircular canals and only rudiments of the posterior and anterior semicircular canals. The horizontal canal was the only canal ever forming. The utricle and saccule were smaller and the cochlear duct was 20% shorter than the control cochlea at E14.5. This phenotype was similar to previous observations on the *Lcc* mutant (Kiernan *et al.*, 2005).

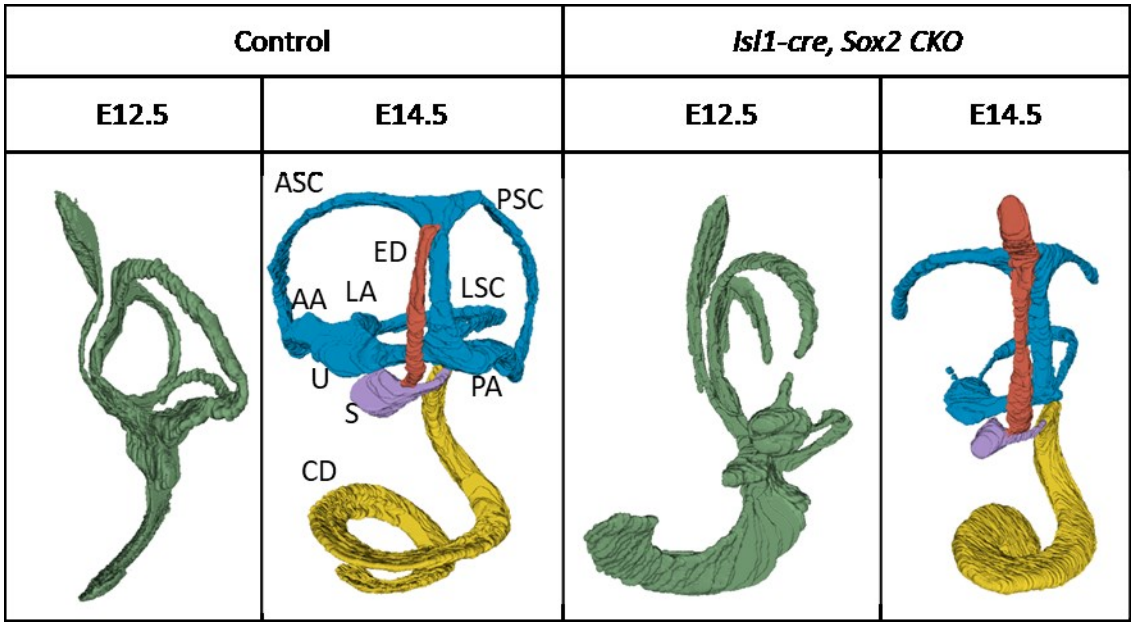

Figure 18: 3D reconstruction of the *Isl1-cre, Sox2 CKO* inner ears revealed severe changes at E12.5 and E14.5 (Dvorakova *et al.*, 2016): no semicircular canal ampullae and only rudiments of the posterior and anterior semicircular canals, smaller utricle and saccule and shorter cochlear duct. AA anterior ampulla; ASC anterior semicircular canal; CD cochlear duct; ED endolymphatic duct; LA lateral ampulla; LSC lateral semicircular canal; PA posterior ampulla; PSC posterior semicircular canal; S saccule; U utricle

Scanning electron microscopy showed that only individual hair cells or small clusters of hair cells formed in the base of the cochlea (Figure 19 B, B'). Mutant hair cells differed in their size, orientation and bundle organization. There was no sign of hair cell differentiation in the cochlear apex. Differentiated hair cells in the utricle of *Isl1-cre, Sox2 CKO* were of normal size and stereocilia formation was comparable to controls, although the number of differentiated hair cells was significantly reduced in the mutant utricle (Figure 19 C, D).

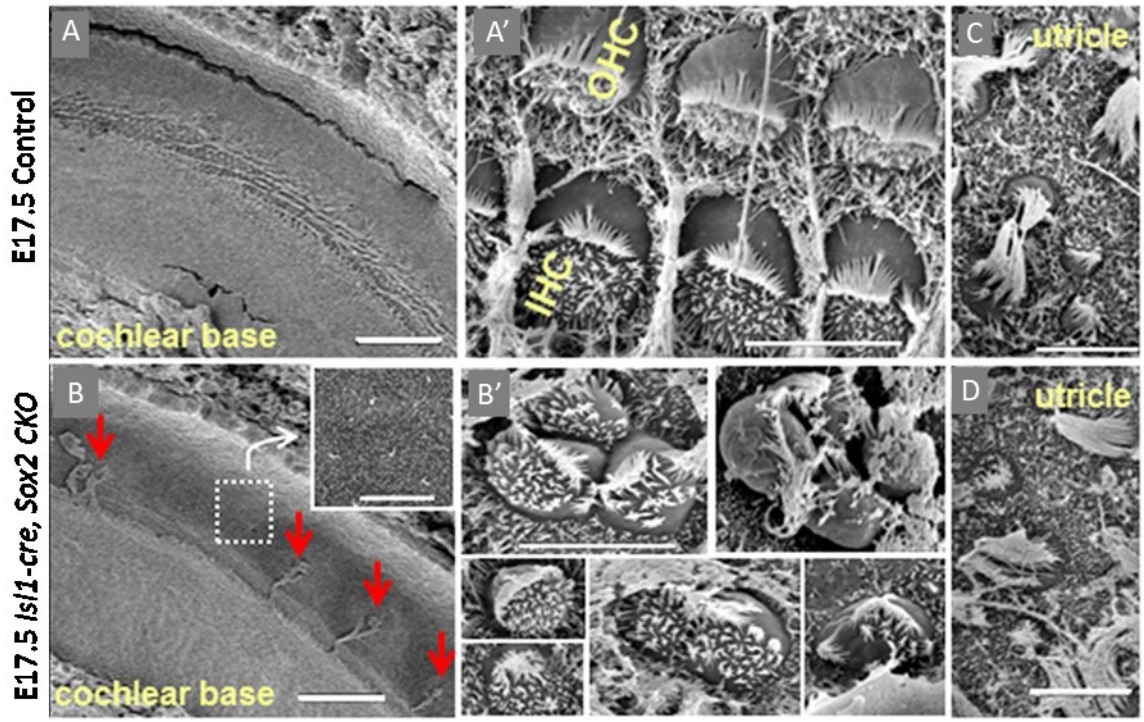

Figure 19: Scanning electron microscopy of cochlear and utricular sensory organ (Dvorakova *et al.*, 2016): Few individual cells and small clusters of cells with hair cell-like phenotype were detected in the base of the *Isl1-cre, Sox2 CKO* cochlea (red arrows in B). The rest of the organ of Corti was missing as shown by the overview of the whole cochlear duct width and by magnification of the sensory epithelium area (B). Hair cells varied in size, orientation and bundle organization (B'). The cellular phenotype of differentiated hair cells in the *Isl1-cre, Sox2 CKO* utricle was comparable to controls (C, D). IHC inner hair cells; OHC outer hair cells; scale bars: 50 µm (A, B), 5 µm (A', B', C, D)

Immunolabelling of SOX2 protein showed that *Isl1-cre* effectively recombined *Sox2*$^{f/f}$ in some areas but not so in others. As *Sox2* is expressed before *Isl1*, this suggests delayed *Isl1-cre*-mediated recombination. The first loss of SOX2-positive cells in the neurosensory epithelium was visible at E10.5 (Figure 20 A, B). At E13.5 in the *Isl1-cre, Sox2 CKO* cochlea, SOX2 was detected only in the base, whereas in controls, SOX2 was expressed throughout the entire length of the cochlea (Figure 20 C, D). Similar data were observed for *Sox2* mRNA. At E13.5, there was a very limited expression of *Sox2* mRNA only in the base of the cochlea and weak expression in the utricle and saccule (Figure 20 E, F).

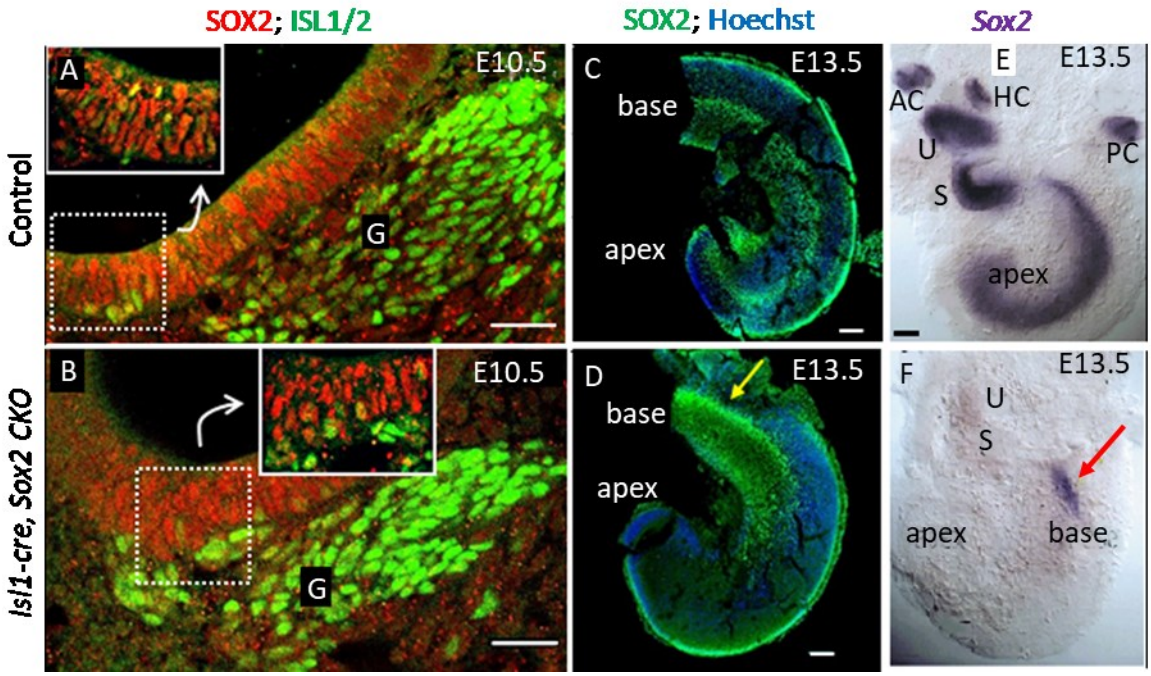

Figure 20: SOX2 expression was altered in *Isl1-cre, Sox2 CKO* mutants (Dvorakova *et al.*, 2016): Reduced overlap of ISL1 and SOX2 immunostaining was apparent in *Isl1-cre, Sox2 CKO* ears at E10.5 (A, B). Vestibular neurons (green) delaminate from the otocyst epithelium (A, B). At E13.5, SOX2 (green) was expressed only in the base of the mutant cochlea, whereas in the controls, the expression of SOX2 occured throughout the entire length of the cochlea (C, D). At E13.5, there was only a weak expression of *Sox2* mRNA in the base of the cochlea compared to controls (E, F). AC anterior crista; G ganglion; HC horizontal crista; PC posterior crista; U utricle; S saccule; scale bars: 50 µm (A, B) and 100 µm (C–F)

Biphasic loss of neurons occurred in the inner ear of *Isl1-cre, Sox2 CKO*. The early delamination of neuroblasts was unaffected by *Isl1-cre* mediated *Sox2* elimination. The formation of delaminated vestibular neurons was comparable between mutants and controls at E10.5 (Figure 20 A, B). Additionally, the expression of NEUROD1, an early neuronal differentiation marker, was comparable at E11.5, which suggests normal neuronal differentiation (Figure 21).

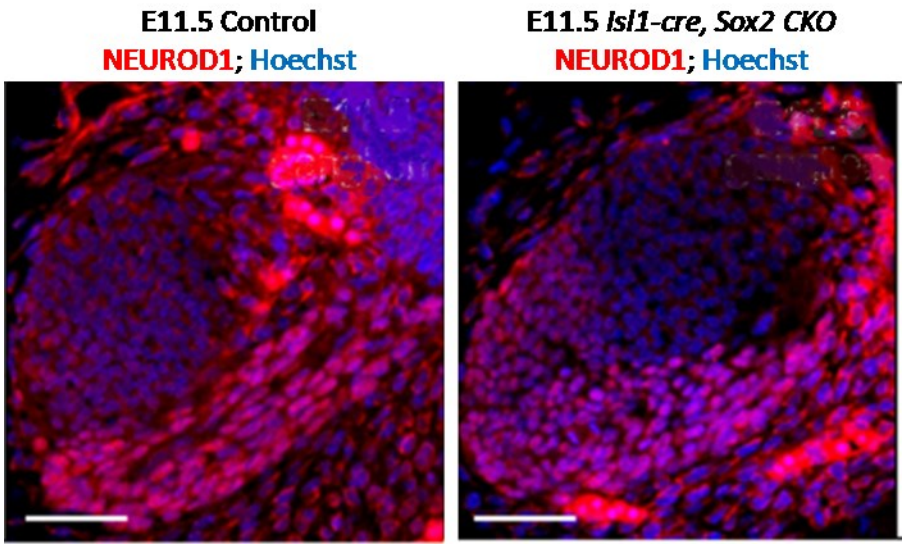

Figure 21: NEUROD1 expression in the otocyst-derived ganglion neurons was comparable between *Isl1-cre, Sox2 CKO* and controls at E11.5 (Dvorakova *et al.*, 2016). Scale bar: 100 µm

Immunohistochemistry of neuronal fibers showed similar growth of fibers toward the utricle, saccule and posterior crista between controls and mutants at E11.5 (Figure 22 A, B). Fibers of the posterior crista remained until E14.5, when they started to regress in *Isl1-cre, Sox2 CKO* (Figure 22 D, F). Only variably reduced innervation of the mutant utricle and saccule remained at E18.5 (Figure 23 F). Our results suggest that many vestibular neurons form and project but are later eliminated after delayed excision of *Sox2* using *Isl1-cre*. In line with the progressive loss of vestibular fibers, we found increased CASPASE 3 staining in the mutant vestibular ganglion neurons at E15.5 (Figure 23 A, B). This indicates strong apoptosis of most vestibular neurons, probably due to the lack of neurotrophins and hair cells.

Based on the innervation pattern, spiral ganglion neurons were formed only near the base but never in the apex of the mutant (Figure 22, Figure 23). Fewer basal spiral ganglion neurons were present after E15.5 and by E18.5 only a few neurons were left projecting toward the base (Figure 23 C–F). We also found CASPASE 3 immunostaining in the base of the cochlea at E15.5, showing a loss of initially formed spiral ganglion neurons due to missing sensory epithelium in *Isl1-cre, Sox2 CKO* (Figure 23 A, B).

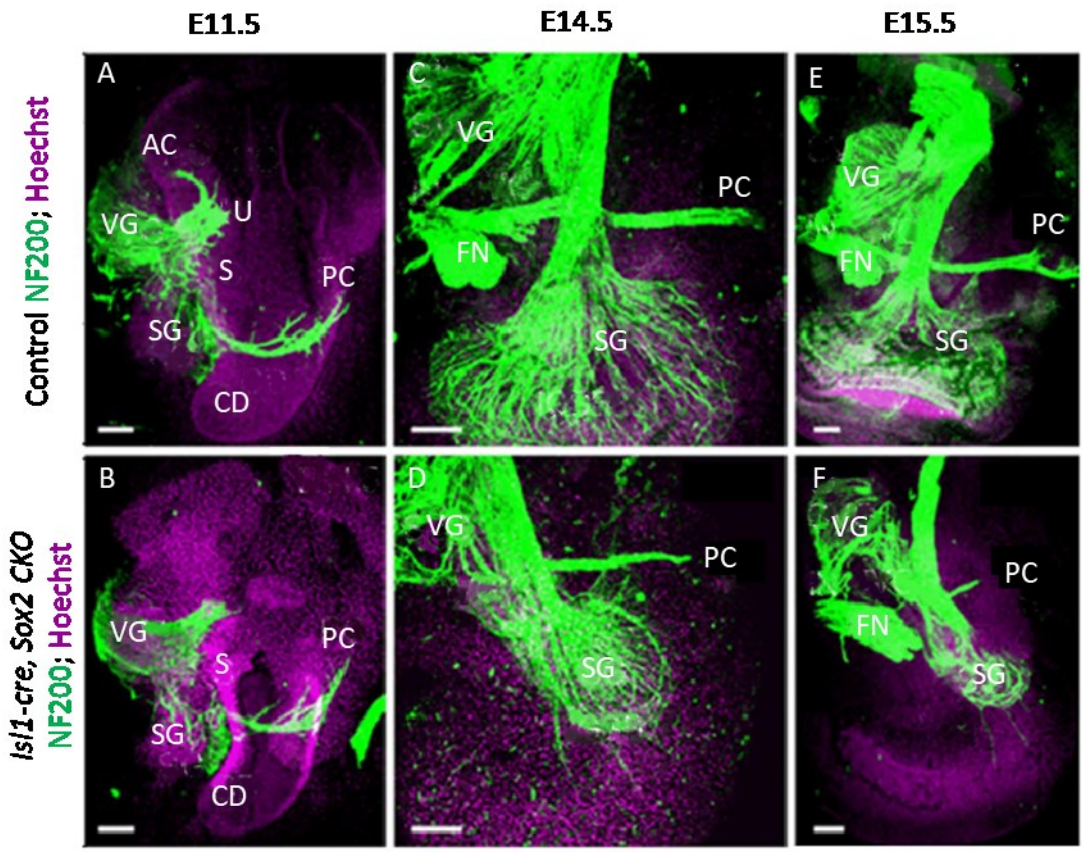

Figure 22: Formation of neurons in the inner ear was changed in *Isl1-cre, Sox2 CKO* mutants (Dvorakova *et al.*, 2016): Formation of vestibular neurons was comparable to controls at E11.5 (A, B). Fibers projecting toward the posterior crista started to retract at E14.5 in the absence of target hair cells (C–F). Only a few radial fibers of the spiral ganglion were formed near the base of the mutant cochlea (D, F). AC anterior crista; CD cochlear duct; FN facial nerve; PC posterior crista; S saccule; SG spiral ganglion; U utricle; VG vestibular ganglion; scale bar 100 µm

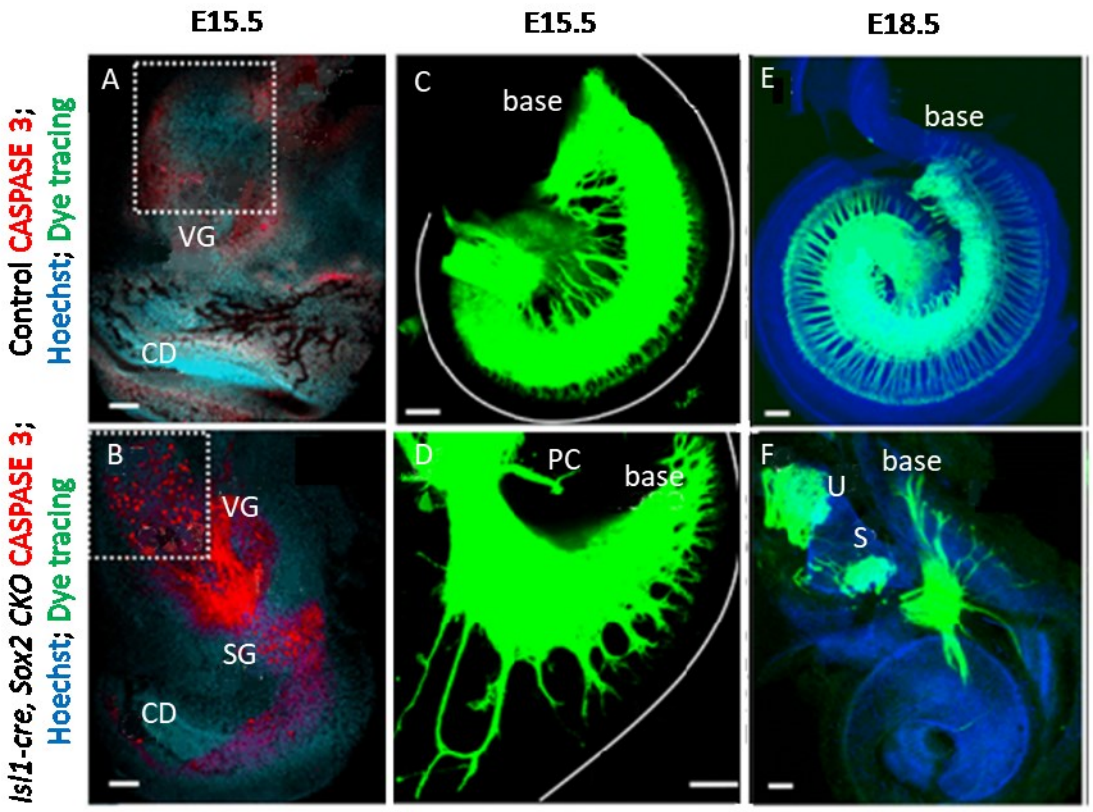

Figure 23: Neuronal degeneration and changes in the pattern of innervation in the absence of SOX2 (Dvorakova *et al.*, 2016): Immunofluorescence of activated CASPASE 3-mediated cell death showed massive activity in vestibular ganglion and spiral ganglion of mutants at E15.5 compared to no caspase-positive cells in the control littermates (A, B). The pattern of innervation differed dramatically between control and mutant littermates at E15.5 and E18.5 (C–F). Spiral ganglion neurons were present only in the basal turn in mutants (D, F). Due to further reduction of spiral ganglion by apoptosis, only a small population remained near the base of the cochlea in the mutant and only limited innervation remained to the saccule and utricle (F). CD cochlear duct; PC posterior crista; S saccule; SG spiral ganglion; U utricle; VG vestibular ganglion; scale bar 100 µm

Delayed deletion of *Sox2* allowed limited sensory cell differentiation in some inner ear epithelia. The utricular, saccular and cochlear sensory epithelium of *Isl1-cre, Sox2 CKO* was smaller with a reduced domain of SOX2-positive hair- and supporting precursor cells when compared to controls (Figure 24). SOX2 protein was detected only in the base and never in the cochlear apex (Figure 24 A, B). However, the expression domain was altered also in the base. The domain of strong SOX2 expression was shifted medially toward the GER, whereas only scattered cells with limited SOX2 expression were detected in the organ of Corti (Figure 24 B, dotted area). Similarly, MYO7A-positive hair cells were detected only in epithelia with SOX2 positivity, namely in the utricle, saccule and basal

turn of the cochlea (Figure 24, Figure 25). However, a significant reduction of hair cells, in most cases down to around 10% of the control littermates, was detected in all sensory organs (Table 1, Figure 26). A complete deletion of SOX2 in *crista ampullares* and cochlear apex led to a complete loss of all hair cell differentiation in these organs.

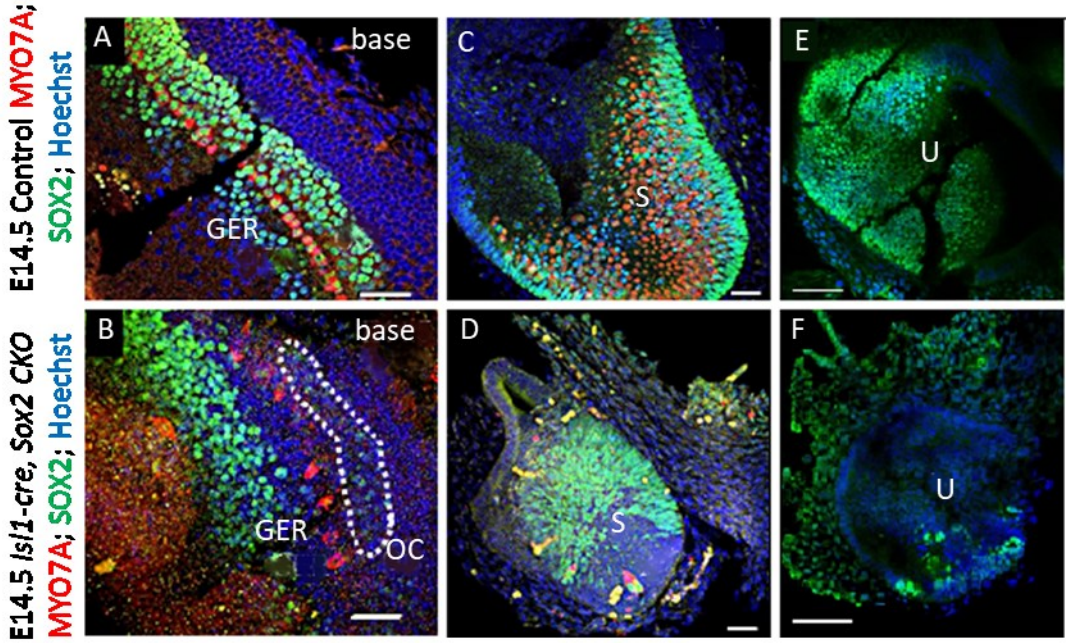

Figure 24: Differentiation of some hair- and supporting cell precursors in the cochlear base and in the vestibular organs of *Isl1-cre, Sox2 CKO* (Dvorakova *et al.*, 2016): SOX2-positive cells were detected only in the basal turn of *Isl1-cre, Sox2 CKO* cochlea at E14.5 and disappeared later in development. The strong SOX2 expression domain was shifted toward the GER in the mutant. Likewise, MYO7A-positive cells did not differentiate in the proper area of organ of Corti. Some weak SOX2 expression remained in the area of organ of Corti of the mutant (dotted area) (A, B). Variable numbers of hair cells and supporting cells developed in the mutant vestibular system (C-F). GER greater epithelial ridge; OC organ of Corti; S saccule; U utricle; scale bars 50 µm (A–D), 100 µm (E, F)

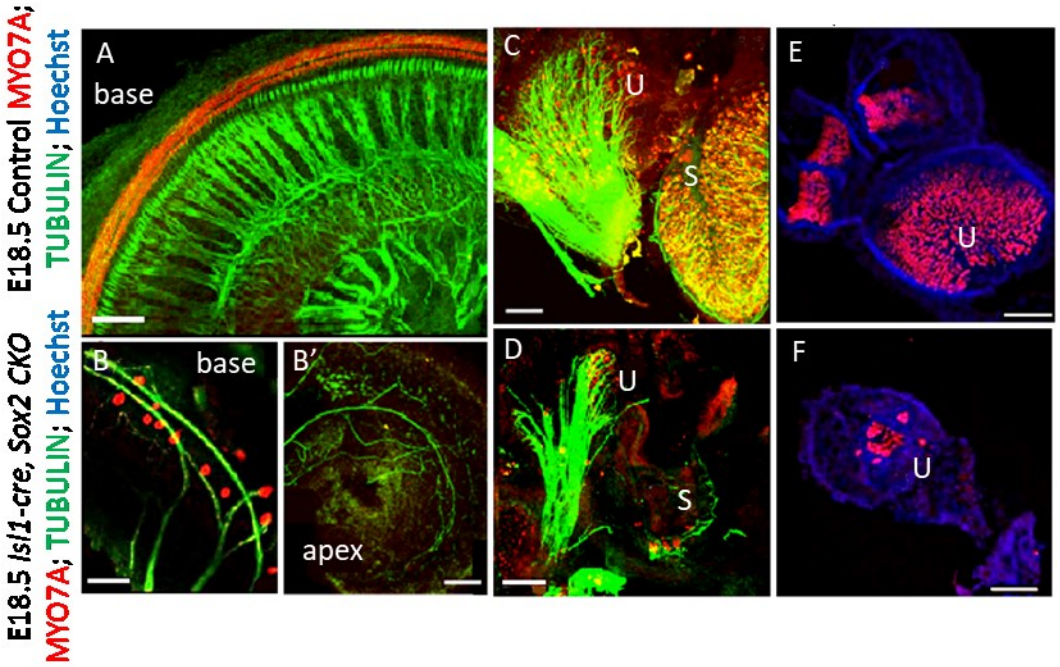

Figure 25: Residual hair cells and unusual pattern of innervation in *Isl1-cre, Sox2 CKO* inner ears (Dvorakova *et al.*, 2016): Some differentiated hair cells were present in the utricle, saccule and basal turn of the cochlea of the *Isl1-cre, Sox2 CKO* at E18.5 (A–F). The innervation of mutant cochlea, saccule and utricle was significantly reduced and showed an abnormal pattern compared to controls (A–D). Fibers showed mostly directional growth toward remaining hair cells (B, D) but also transient expansion into hair cell-free regions (B'). S saccule; U utricle; scale bars 50 µm (B, E, F), 100 µm (A, B'–D)

Quantification of hair cells

	Control utricle	Mutant utricle	Control saccule	Mutant saccule	Control cochlea	Mutant cochlea
	1031	132	880	15	908	21
	1068	247	910	59	774	42
	978	112	1190	28	719	31
	1005	197	817	12	871	22
		88		94	774	36
		334		95	717	28
					809	
Average	1021	185	949	51	796	30
SD	38	94	165	38	72	8

Table 1: Quantification of MYO7A-positive hair cells in control and mutant (*Isl1-cre, Sox2 CKO*) inner ears at E18.5 (Dvorakova *et al.*, 2016): The total number of hair cells in the entire utricle and saccule, in the entire *Isl1-cre, Sox2 CKO* cochlea and in the 1.5 mm long segment of the base in the control cochlea was determined.

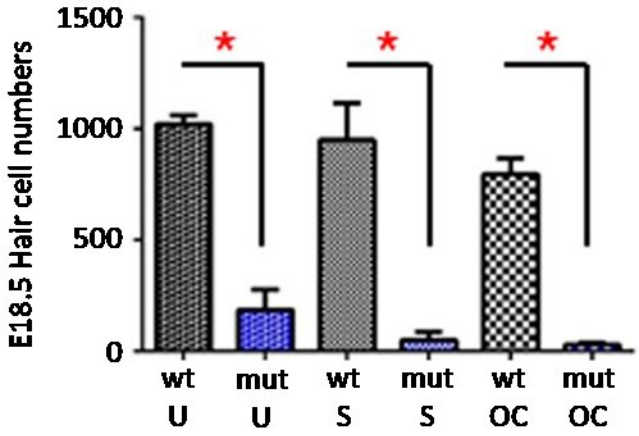

Figure 26: Quantification of hair cells in control and *Isl1-cre, Sox2 CKO* inner ears (Dvorakova *et al.*, 2016): Quantification of immunolabelled MYO7A-positive hair cells showed a considerable reduction of hair cells in the *Isl1-cre, Sox2 CKO* inner ears compared to littermate controls. The values represent means ± standard deviation (SD) (N = 4–7 individuals/group). *P < 0.0001, *t*-test. mut mutant (*Isl1-cre, Sox2 CKO*); OC organ of Corti (cochlea); S saccule; U utricle; wt wild type (control)

The patterning of the inner ear innervation depends on a multitude of molecules that guide nerve fibers to sensory epithelia and organize the fibers to the distinct cell types within the epithelia (Rubel and Fritzsch, 2002). Only some of the factors are known. The loss of SOX2 seemed to have no effect on the initial growth of fibers. However, since only scattered hair cells remained, the pattern of innervation developed aberrantly with fibers showing directional growth toward remaining hair cells (Figure 25 B). Additionally, also transient expansion of fibers into hair cell-free territories occurred, like those in the apex or in the posterior crista (Figure 22, Figure 25 B'). These findings suggest that the remaining hair cells were the target of residual innervation but fibers could overshoot and extend into hair cell-free territory. The variability in the distribution of hair cells together with the transient viability of neurons in hair cell-free areas determined the variability in the pattern of residual innervation in individual specimen.

The inner ear epithelia were found to have unusual features. Hair cells can differentiate with a complete absence of innervation (Ma, Anderson and Fritzsch, 2000). Hair cells in *Isl1-cre, Sox2 CKO* mice had a variable degree of differentiation in terms of stereocilia development, cell size and distribution (Figure 19). Stereocilia bundles of cochlear hair cells are very different from those in the vestibular organs. However, SOX2 seemed to play a minor role in the general stereocilia bundle organization, as many differentiating

hair cells in the *Isl1-cre, Sox2 CKO* had the sensory-epithelium-specific polarity and bundle organization. Yet, some hair cells showed mixed features of vestibular and cochlear stereocilia, suggesting an incomplete segregation of vestibular and cochlear hair cell types after transient expression of *Sox2*.

Moreover, huge variability in numbers of hair cells occurred in mutants. This variability was probably caused by two facts: the reduced formation of viable hair cells and the loss of some unviable hair cells.

Normal differentiation of hair cells is regulated by both level and duration of *Atoh1* expression (Pan *et al.*, 2012). On that account we studied the expression of *Atoh1* using *in situ* hybridization. We only found restricted expression of *Atoh1* in the base of the cochlea, consistent with the expression of SOX2 in the base of *Isl1-cre, Sox2 CKO* (Figure 27 B, B'). These results confirmed that *Atoh1* expression depends on SOX2. Similarly, the hair cell marker MYO7A showed clusters of differentiated hair cells only in the basal turn of the cochlea (Figure 24 B, Figure 25 B). This phenotype confirmed that hair cell differentiation requires SOX2, because *Atoh1* expression and differentiated hair cells were found only in the cochlear base, where SOX2 was originally expressed. However, the atypical features of differentiated hair cells suggest that the hair cell differentiation requires a specific level and duration of SOX2 expression.

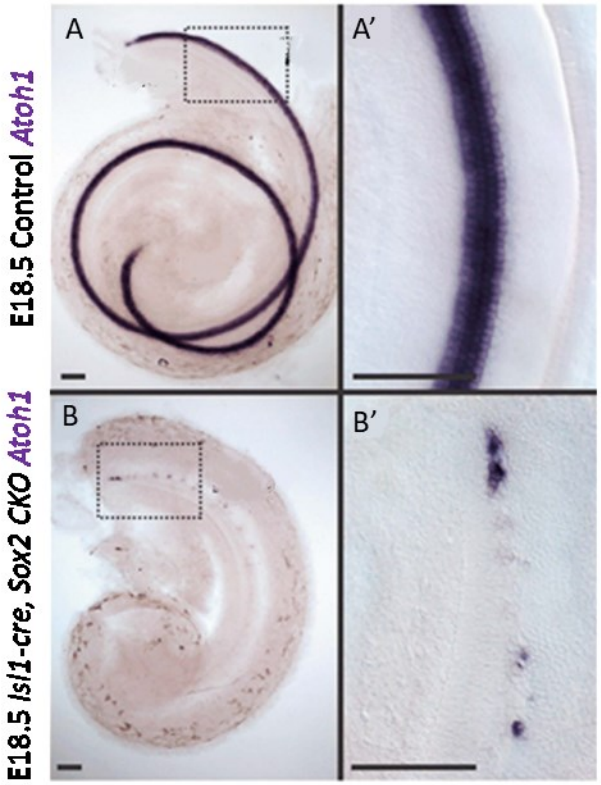

Figure 27: Loss of SOX2 affected expression of downstream gene *Atoh1* in the organ of Corti (Dvorakova *et al.*, 2016). Scale bar 100 µm

Inner ear hair cells are generally negative for TUBULIN, which is used as a neuronal marker. In *Isl1-cre, Sox2 CKO*, however, we found several hair cells positive for TUBULIN staining (Figure 28). This suggests that SOX2 may also be important during the segregation of neuronal and hair cell phenotype and that this segregation was incomplete in our *Isl1-cre* conditional mutant.

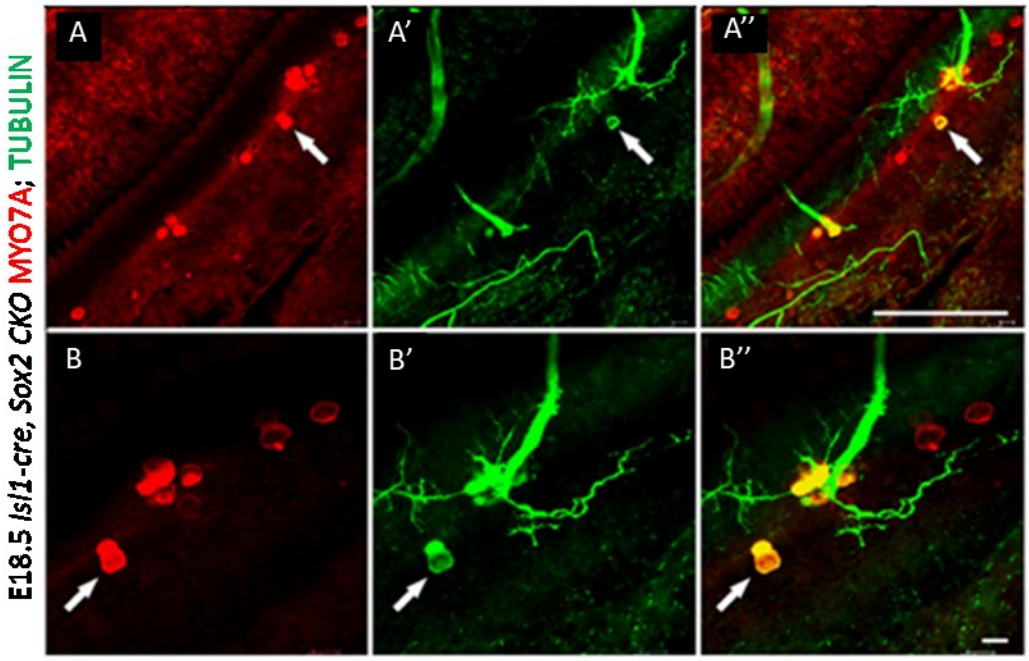

Figure 28: Some hair cells positive for both MYO7A and TUBULIN (Dvorakova *et al.*, 2016): Some MYO7A-positive cells of *Isl1-cre, Sox2 CKO* mice were also positive for antibody against TUBULIN, normally a widely used and reliable neuronal marker in the ear. Scale bars 100 µm (A–A''), 10 µm (B–B'')

Due to the deletion of *Sox2* in our mutant, SOX2 could not be used as a general marker of supporting cells. Given that, we could use only very early markers of supporting cells in order to examine the possible dependency of supporting cell differentiation on the expression of *Sox2*.

One of the earliest markers of supporting cells is a low-affinity nerve growth factor receptor P75 expressed in IPCs. P75 protein was found in the organ of Corti, but closer inspection of the morphology of possible IPCs showed unusually shaped cells with no resemblance to IPCs and also unusual distribution of these cells (Figure 29 A, B). The remaining basal spiral ganglion neurons in mutants showed no *p75* expression compared to the strong *p75* signal in the spiral ganglion neurons of controls (Figure 29 C, D).

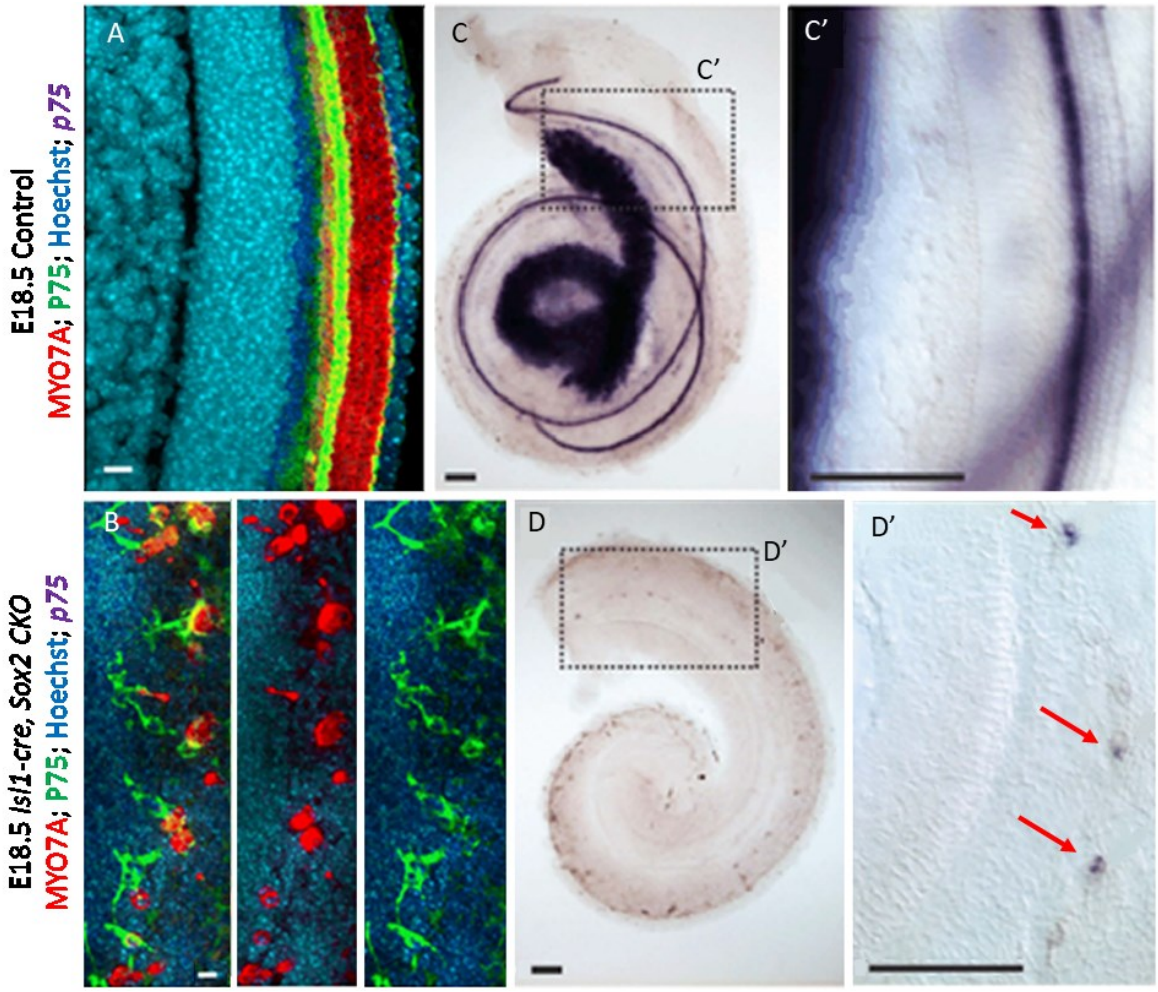

Figure 29: Abnormal pillar cells in the *Isl1-cre, Sox2 CKO* (Dvorakova *et al.*, 2016): The double immunolabelling of P75 and MYO7A showed an abnormal morphology and distribution of P75-positive cells near the remaining MYO7A-positive hair cells in mutant inner ear at E18.5 (B). Normally, a single row of P75-positive IPCs is formed in controls (A). *P75* expression (arrows) was discontinuous in the base and absent in the apex compared to strong labelling in the IPCs and the spiral ganglion neurons in controls (C-D'). Scale bars 10 µm (A, B), 100 µm (C–D')

Next, we inquired to the expression pattern of markers that define the boundaries of the organ of Corti: *Fgf10* expression in GER (medial to OC) and *Bmp4* expression in Claudius cells (immediately lateral to OC). Previous work has shown that *Fgf10* expression depends on some not yet known signals from the organ of Corti (Pan *et al.*, 2012). Correspondingly, we found no *Fgf10* expression in the cochlea at E13.5 (Figure 30 A, B). In contrast, cochlear *Bmp4* expression was near-normal in the absence of the proper organ of Corti (Figure 30 C, D). However, *Bmp4* expression was not lateral to the organ of Corti but rather adjacent to GER, forming rings around remaining, more lateral

hair cells (Figure 30 C'-D''). Together, these data suggest that SOX2 may play a direct role in differentiation of supporting cells beside its simple expression in these cells.

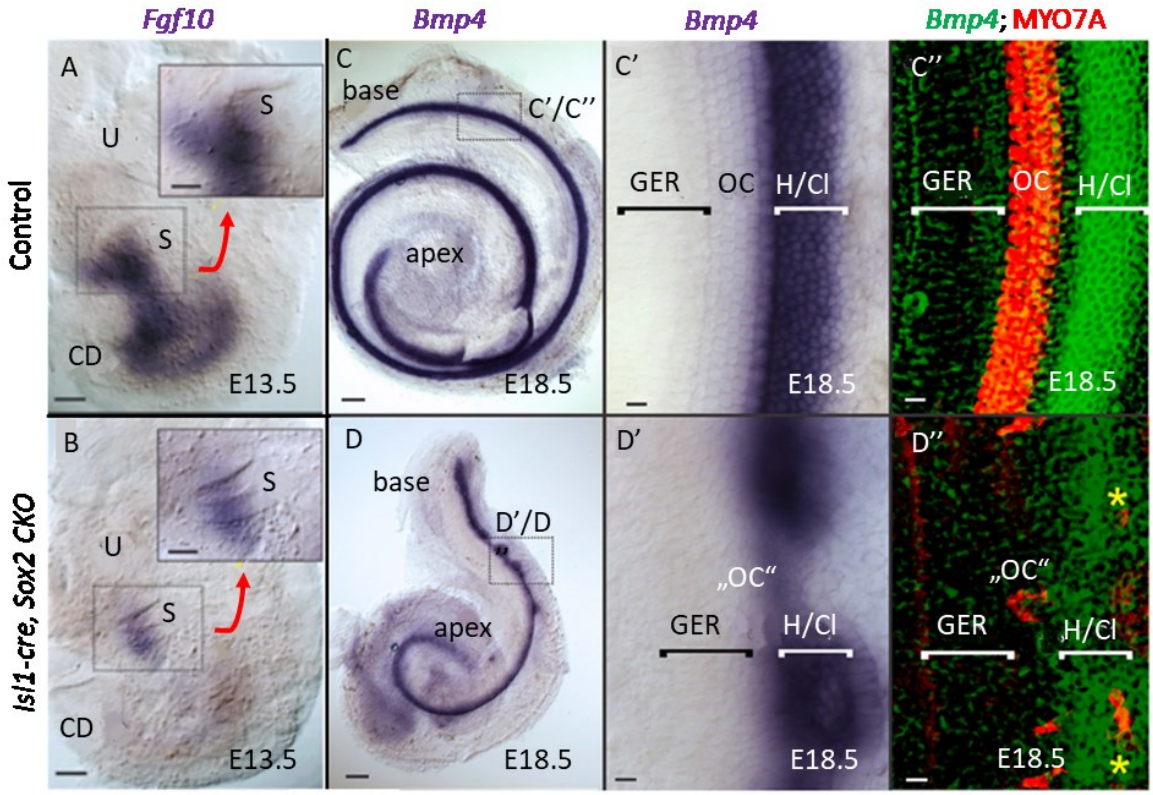

Figure 30: The cellular boundaries of the organ of Corti were changed in the *Isl1-cre, Sox2 CKO* (Dvorakova *et al.*, 2016): No *Fgf10* mRNA was detected in the cochlear duct of the *Isl1-cre, Sox2 CKO* at E13.5 and only limited *Fgf10* mRNA labelling was in saccular neurons (A, B). Loss of SOX2 resulted in aberration of *Bmp4* expression. In controls, the *Bmp*4 expression in supporting Hensen/Claudius cells was always lateral to the organ of Corti (C', C''). In mutants, instead of being separated by the organ of Corti from the GER, *Bmp4* expression was adjacent to the GER (C–D''). Only the base showed rings of lateral *Bmp4* expression and MYO7A-positive hair cells were both in the center of these rings (D'', yellow asterisks) as well as at the boundary between GER and *Bmp4* domain (C–D''). CD cochlear duct; GER greater epithelial ridge; H/Cl Hensen/Claudius cells; OC organ of Corti; „OC" atypical organ of Corti in the mutant ;U utricle; S saccule; scale bars 100 µm (A–D), 10 µm (C'–D'')

4.2. Effects of early deletion of Sox2 on inner ear, olfactory and lens development

Foxg1-cre, Sox2 CKO mice were used to study the effect of *Sox2* deletion at the level of the otic placode on inner ear development and to study the distinct differences for SOX2 requirements in placodal sensory organs, particularly olfactory, lens and ear placode development.

The *Sox2*-deficient embryos in this study (*Foxg1-cre, Sox2 CKO*) were generated by crossing $Sox2^{f/f}$ to *Foxg1-cre*. The decreased gene dose in heterozygous animals ($Sox2^{+/f}$, *Foxg1-cre*) did not affect normal development. Heterozygous mice were indistinguishable from controls ($Sox2^{+/+}$ or $Sox2^{+/f}$) (Figure 31). However, homozygous *Sox2* deletion ($Sox2^{f/f}$, *Foxg1-cre*) was lethal at birth with significant changes in the gross external morphology of *Foxg1-cre, Sox2 CKO* embryos, including an abnormal eye phenotype, a shortened nose without olfactory pits and a flattened forehead (Figure 31).

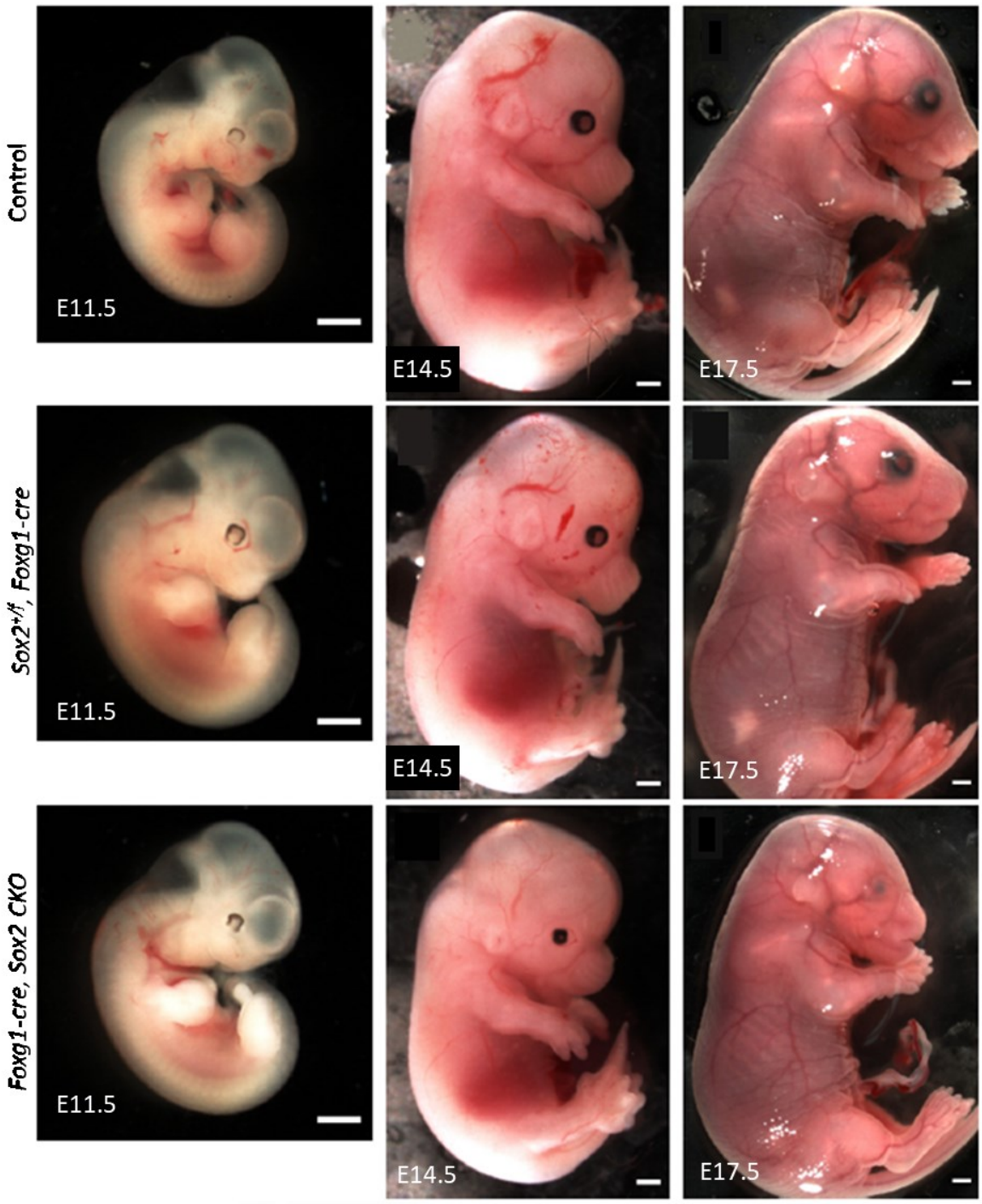

Figure 31: External phenotype of embryos (Dvorakova *et al.*, 2019): Comparison of lateral views of control, heterozygote (*Sox2*$^{+/f}$*; Foxg1-cre*) and mutant (*Foxg1-cre, Sox2 CKO*) embryos at E11.5, E14.5 and E17.5 showed eye defects, a shortened nose and slightly reduced body size in mutants. Scale bar 1 mm

To establish the onset of *Sox2* deletion in *Foxg1-cre, Sox2 CKO* embryos, we studied the presence of SOX2 protein at preplacodal lens stages, in the eye vesicle and in the ear placode at the 11-somite stage at E8.5 (Figure 32). We detected CRE protein but no

detectable SOX2 protein was found in the invaginating ear placode and in the presumptive lens ectoderm of *Foxg1-cre, Sox2 CKO* mutant mice compared to *Sox2*$^{+/f}$, *Foxg1-cre* heterozygotes. In contrast, SOX2 was eliminated only from some cells of the eye vesicle in *Foxg1-cre, Sox2 CKO* (Figure 32 F).

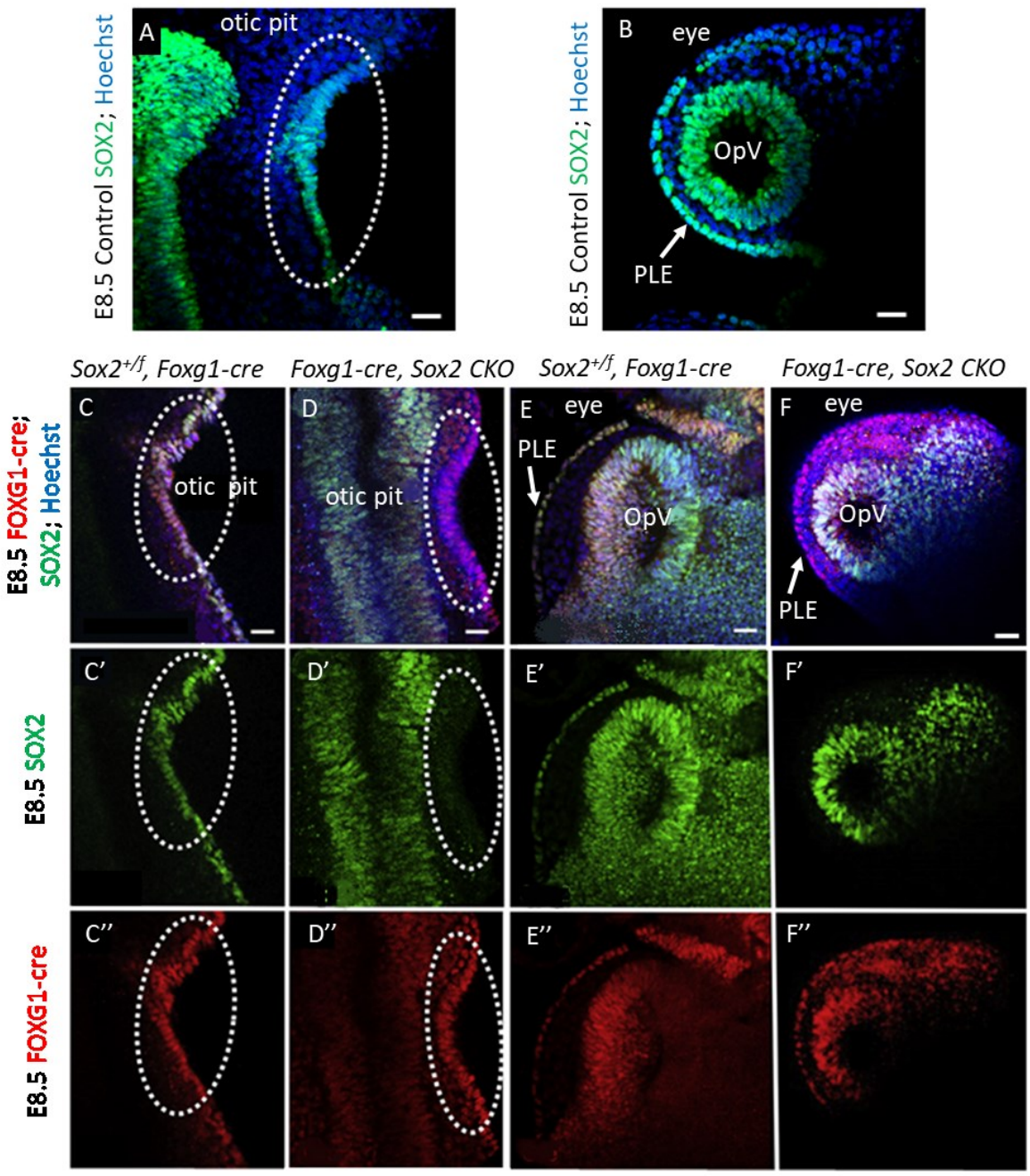

Figure 32: SOX2 was eliminated in the ear and pre-lens placodes in early *Foxg1-cre, Sox2 CKO* embryos (Dvorakova *et al.*, 2019): Analysis of whole-mount embryos at 11-somite stage at E8.5 (control, heterozygote *Sox*$^{+/f}$, *Foxg1-cre* and mutant *Foxg1-cre, Sox2 CKO*) showed SOX2 loss in the mutant invaginating otic placode when compared to control and heterozygote (A, C–D''). The dotted oval indicates

the area of the otic pit (A, C-D''). In the developing eye, SOX2 was eliminated in the presumptive lens ectoderm and some cells of the optic vesicle in mutant embryos (F–F''). In contrast, SOX2 expression in control and heterozygote was comparable (B, E–E''). FOXG1-cre was present in the surface ectoderm in the area of the presumptive lens ectoderm in both mutants and heterozygotes (E, E'', F, F''). OpV optic vesicle; PLE presumptive lens ectoderm; scale bar 50 µm

At E9.0, SOX2 was eliminated from all regions with CRE expression in *Foxg1-cre, Sox2 CKO* embryos, as visualized by tdTomato reporter expression (reflecting the pattern of FOXG1-cre activity) (Figure 33). SOX2 was expressed in the temporal region of the eye vesicle but was absent in the otocyst, the olfactory and pre-lens placodes and the nasal domain of the eye vesicle in *Foxg1-cre, Sox2 CKO*. These results indicate that FOXG1-cre effectively recombined $Sox2^{f/f}$ during the early stages of olfactory, lens (eye) and ear development.

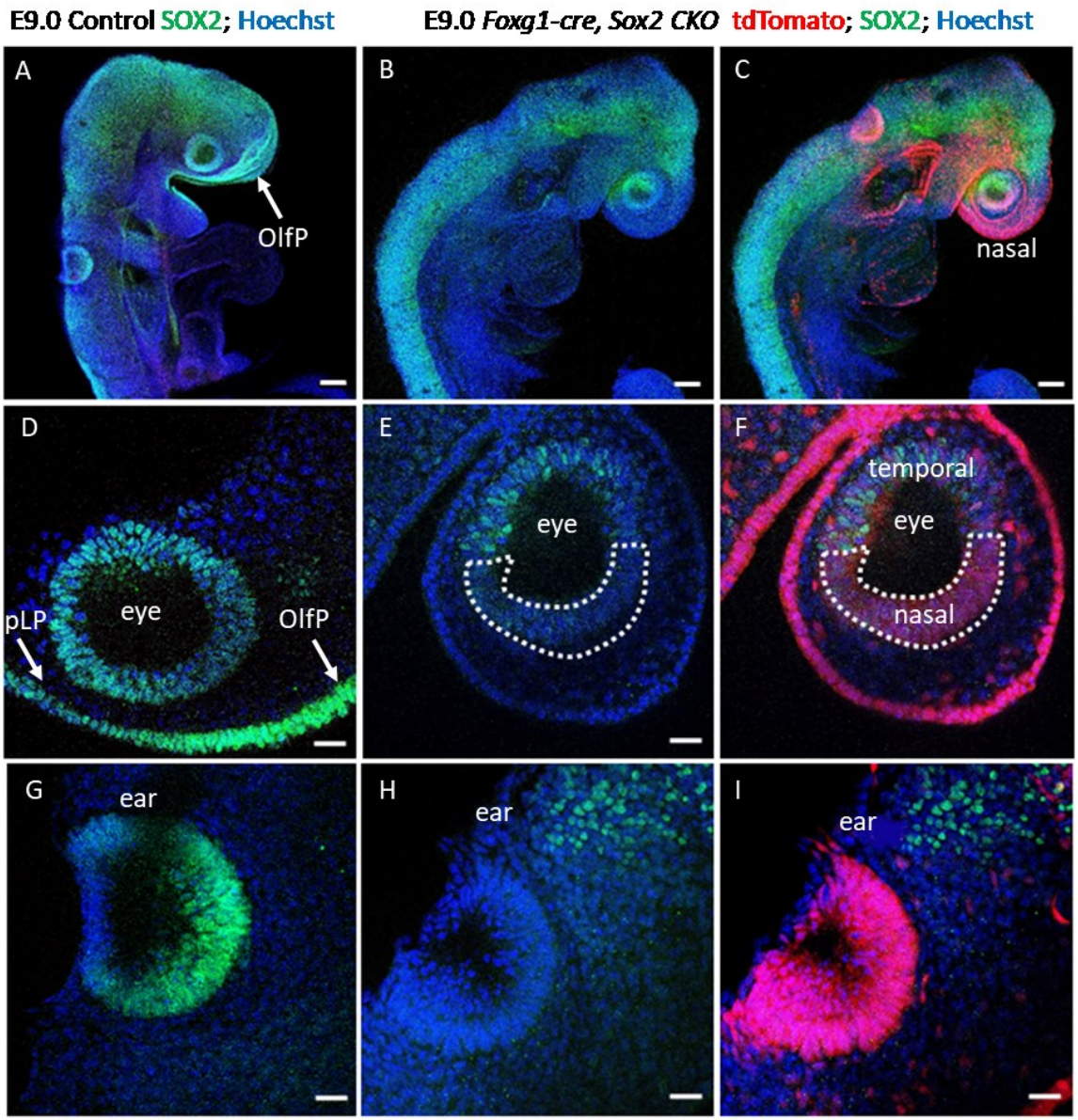

Figure 33: Complete SOX2 deletion in the otocyst, pre-lens and olfactory placodes and in the nasal half of the eye vesicle at E9.0 (18 somite-stage) in *Foxg1-cre, Sox2 CKO* embryos (Dvorakova *et al.*, 2019): SOX2 was expressed in neural tube, olfactory placode, eye vesicle and pre-lens placode and ear vesicle in control embryo (A, D, G). In *Foxg1-cre, Sox2 CKO*, SOX2 protein was detected in neural tube and in the temporal region of the eye vesicle (dotted area indicates the nasal part of the eye vesicle) (B, E). SOX2 was absent in the epithelium of the olfactory placode, pre-lens placode and the ear vesicle (B, E, H). TdTomato reporter, reflecting FOXG1-cre activity, indicated that FOXG1-cre expression matched the SOX2 deletion pattern (C, F, I). OlfP olfactory placode; pLP pre-lens placode; scale bars 200 µm (A–C), 50 µm (D–I)

The early loss of SOX2 affected olfactory development such that the entire neuronal lineage as well as olfactory placode invagination was abolished in *Foxg1-cre, Sox2 CKO* (Figure 34). Thus, mutant mice showed no morphological structure of the olfactory

epithelium formation or olfactory pit development. Abnormal olfactory development resulted in a shortened nose, flattened forehead and absence of nasal bones (Figure 34, Figure 35).

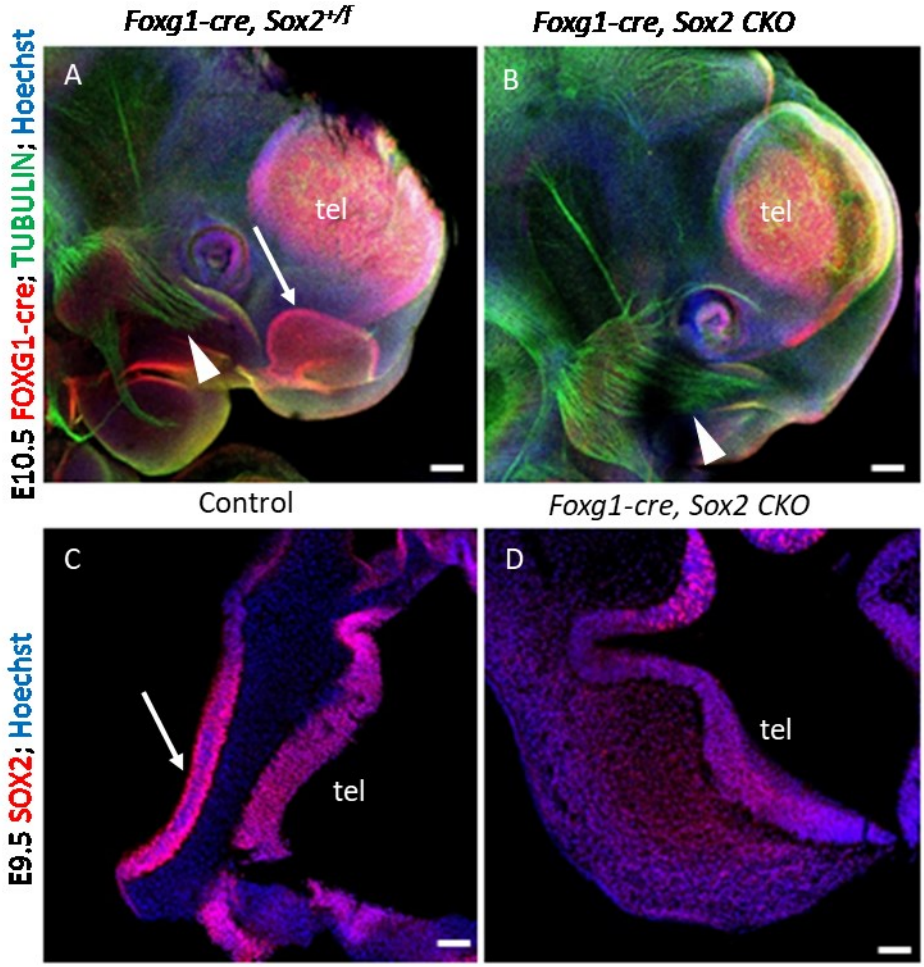

Figure 34: Failure of invagination of olfactory placode in *Foxg1-cre, Sox2 CKO* (Dvorakova *et al.*, 2019): The olfactory epithelium (arrow in A) was missing in *Foxg1-cre, Sox2 CKO* as shown by FOXG1-cre expression in whole-mounted embryos at E10.5 (A, B). TUBULIN staining showed innervation from the trigeminal ganglion to the presumptive olfactory area (arrowhead) in *Foxg1-cre, Sox2 CKO* similar to control. Developing olfactory placode expressed SOX2 in control at E9.5, as shown in cross section (arrow in C), in mutant, no SOX2 expression was detected in the area of presumptive olfactory epithelium (C, D). Consistent with the expression of FOXG1-cre in telencephalon, the expression of SOX2 in the telencephalon of *Foxg1-cre, Sox2 CKO* was reduced (B, D). tel telencephalon; scale bars 200 µm (A, B), 100 µm (C, D)

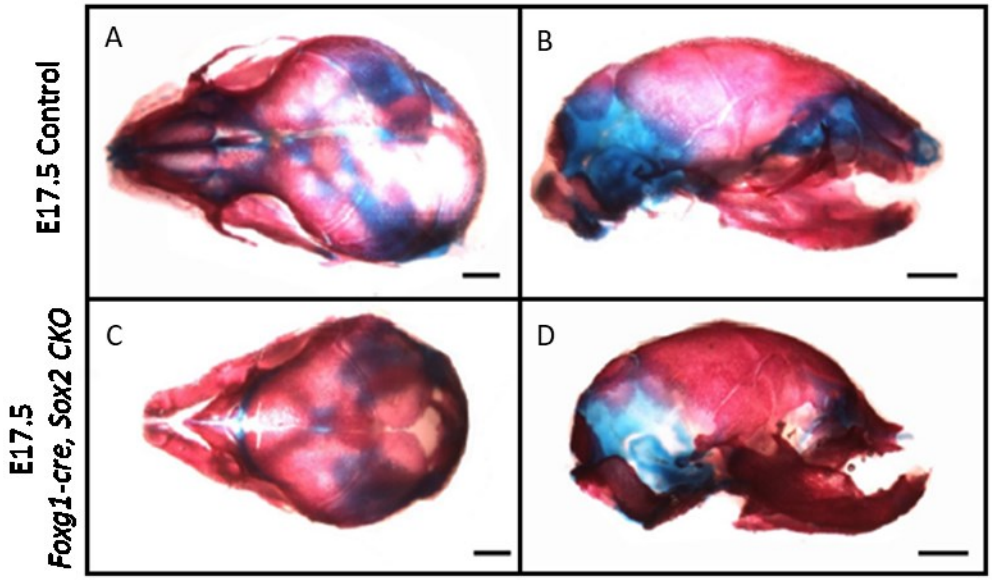

Figure 35: Dorsal and side views of the craniofacial skeleton of E17.5 embryos with missing nasal bones in mutants (C, D) (Dvorakova *et al.*, 2019); scale bar 1 mm

Sox2 deletion in the lens placode arrested lens formation and changed eye development, in part owing to a loss of SOX2 in the nasal domain of the optic cup (Figure 33 E, F). Failure of lens placode invagination and abnormalities in the formation of the optic cup were found as early as E9.5 (Figure 36). Likewise, at E9.5, no SOX2 was detected in the retina and SOX2 was considerably reduced in the telencephalon of *Foxg1-cre, Sox2 CKO* compared to controls (Figure 36).

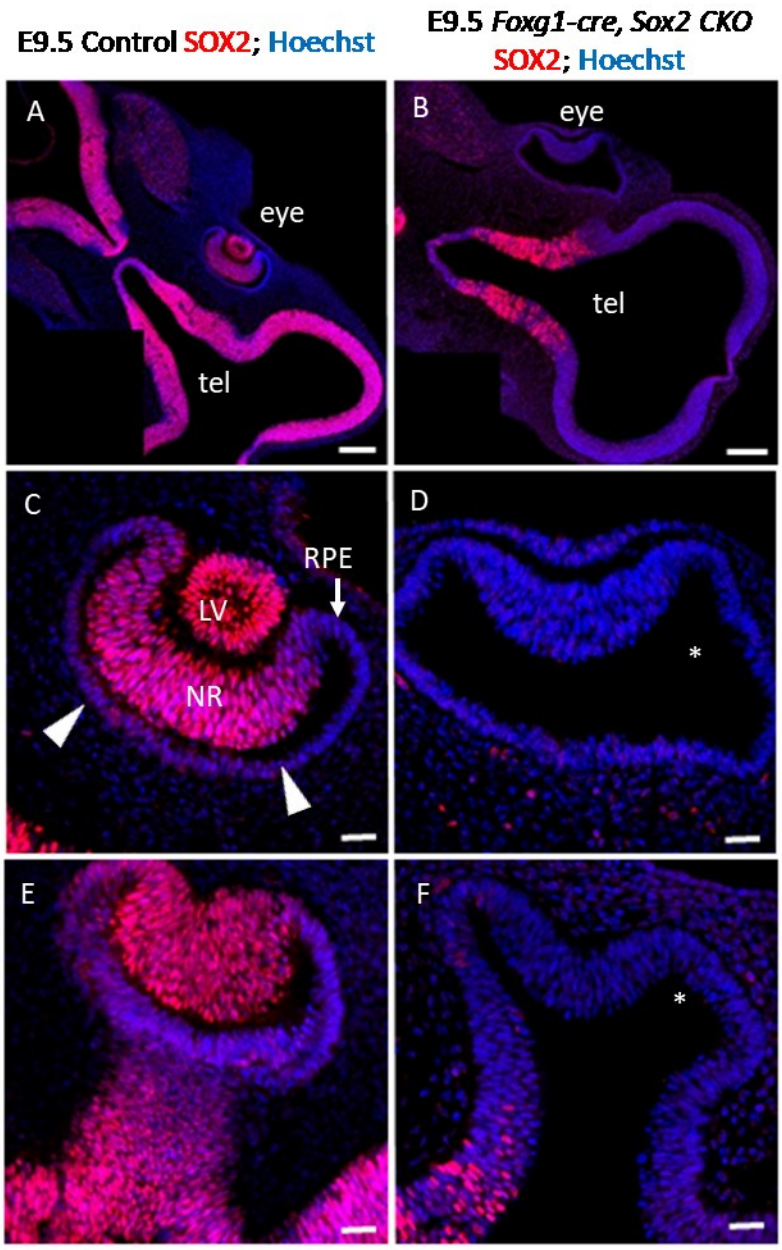

Figure 36: Failure of invagination of the lens placode in *Foxg1-cre, Sox2 CKO* (Dvorakova *et al.*, 2019): Cross-sections of embryonic head at E9.5 showed that SOX2 was undetectable in the developing eye in *Foxg1-cre, Sox2 CKO* when compared to control (A, B). Higher magnification images showed SOX2 expression in the neural retina, lens vesicle and in the ventral part of the eye cup (arrowheads in C) in control embryos, whereas in the mutant, no SOX2 expression was detectable in the eye (C–F). Images showed the failure of invagination of the lens placode and formation of the lens vesicle in *Foxg1-cre, Sox2 CKO*, the decreased number of neural retina cells and the gap between the neural retina and the retinal pigment epithelium (asterisk in D, F). LV lens vesicle; NR neural retina; RPE retinal pigment epithelium; scale bars 100 µm (A, B), 50 µm (C–F)

By E11.5, eye development of *Foxg1-cre, Sox2 CKO* was significantly altered with a missing lens, reduced retina and overall smaller ocular size compared to controls (Figure 37 A–C). Similarly, analyses at E14.5 and E17.5 revealed profound malformities including extremely reduced eye size (Figure 37 D–I). Interestingly, eye muscles were present in *Foxg1-cre, Sox2 CKO* mutant at E14.5 (Figure 37 F). In contrast, eye development of heterozygous embryos (*Sox2*$^{+/f}$*, Foxg1-cre*) was comparable to controls.

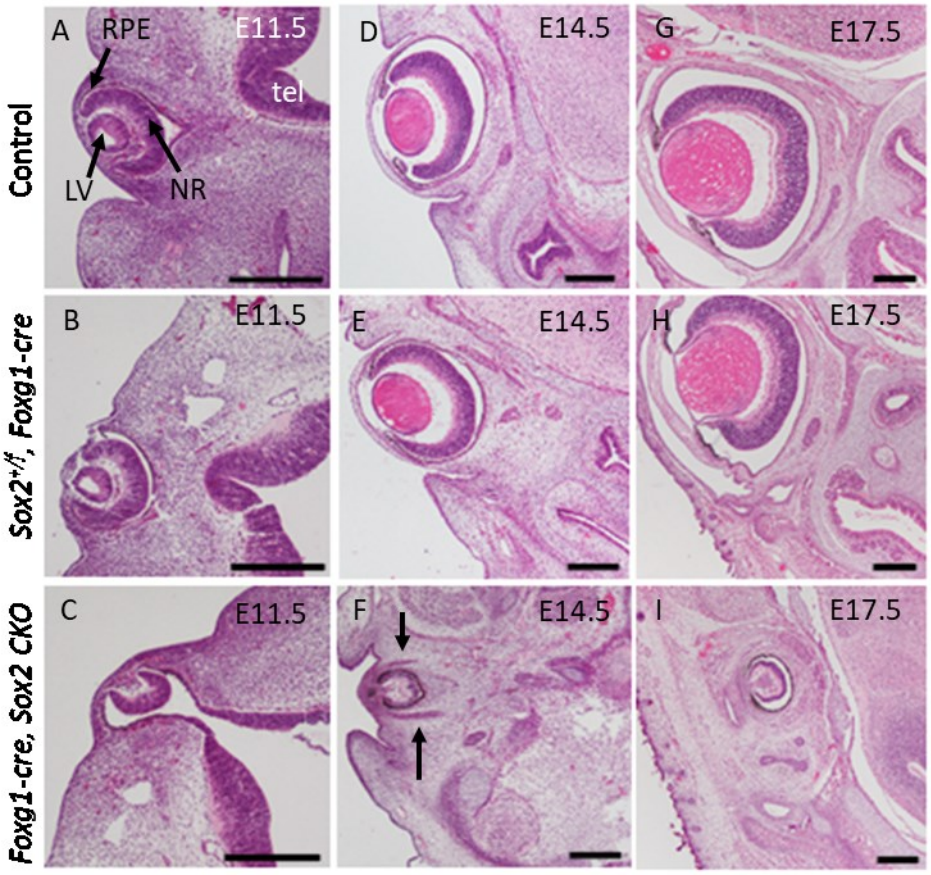

Figure 37: Total loss of lens formation and abnormal eye development after *Sox2* deletion (Dvorakova *et al.*, 2019): Controls and heterozygotes formed normal eye with the lens vesicle and two-layered optic cup with the layer of retinal pigment epithelium and the layer of the neural retina at E11.5 (A, B). *Foxg1-cre, Sox2 CKO* developing eye was smaller, had no detectable lens vesicle and showed a reduced size of neural retina domain (C). At E14.5 and E 17.5, the optic cup had severely reduced size and was missing the optic lens in the mutant compared to the control and heterozygote (D–I). The retinal pigment epithelium and neural retina were present, although significantly reduced in *Foxg1-cre, Sox2 CKO*. Interestingly, the extraocular muscles were present in the mutant at E14.5 (arrows in F). LV lens vesicle; NR neural retina; RPE retinal pigment epithelium; tel telencephalon; scale bars 200 µm (A–C), 100 µm (D–I)

Surprisingly, deletion of SOX2 from the developing ear placode (Figure 32 D) did not affect otic vesicle formation, neuroblast delamination from the otocyst epithelium and nor formation of the vestibular ganglion at E9.5 (Figure 38). In contrast to controls, SOX2 in mutants was not expressed in ISL1-positive vestibular neurons. All SOX2-positive cells detected in E10.5 *Foxg1-cre, Sox2 CKO* co-expressed SOX10, which matches with molecular characteristics of glial cells (Figure 38). These results confirmed elimination of SOX2 in the developing inner ear of *Foxg1-cre, Sox2 CKO.*

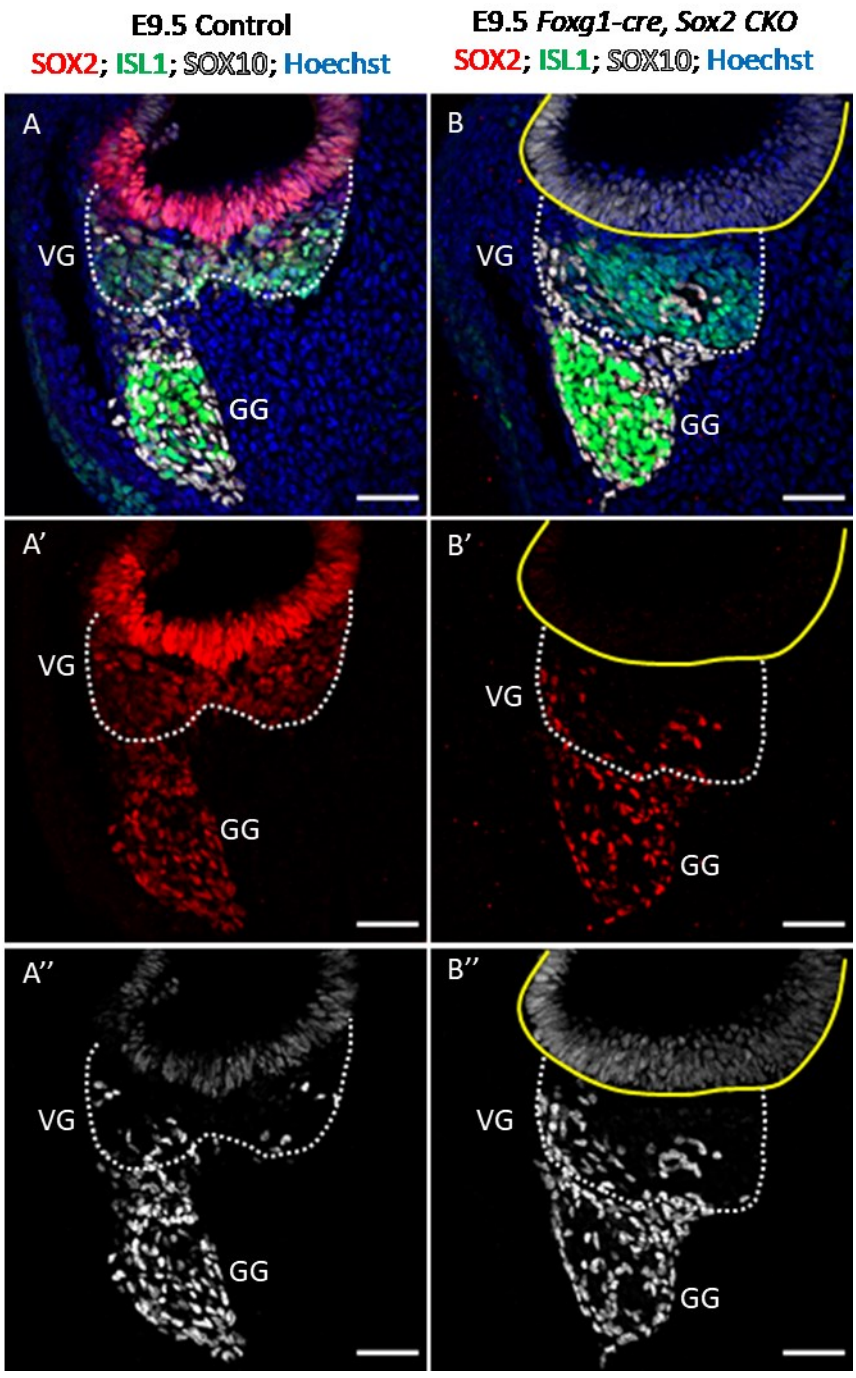

Figure 38: Formation of the vestibular ganglion in *Foxg1-cre, Sox2 CKO* was comparable to control embryos (Dvorakova *et al.*, 2019): SOX2 was expressed in the otocyst and in developing neurons of the vestibular ganglion in control embryos at E9.5, whereas SOX2 was not detectable in the otocyst epithelium or neurons in *Foxg1-cre, Sox2 CKO* (A, B). Dotted lines indicate the boundaries of the vestibular ganglion, yellow lines delineate boundaries of the ear vesicle in the mutant. Split channel images show SOX2 (A', B') and SOX10 immunolabelling (A'', B''). Note, SOX2 was not expressed in ISL1-positive neurons of the vestibular ganglion in the mutant and all SOX2-positive cells in the vestibular ganglion of the mutant co-expressed SOX10, consistent with glial cell molecular characteristics. GG geniculate ganglion; VG vestibular ganglion; scale bar 50 µm

Delaminating NEUROD1-positive neuroblasts (indistinguishable from controls) were detected in the ear epithelium of *Foxg1-cre, Sox2 CKO* at E9.5 (Figure 39). Additionally, at E10.5, the number of ISL1-positive neurons in the vestibular ganglion was comparable between controls and mutants (Figure 39). These results suggest that the early neurogenesis in the inner ear was not affected by early deletion of *Sox2* in the ear placode. Nevertheless, slight reduction in the neurite outgrowth towards the ear epithelium was observed in *Foxg1-cre, Sox2 CKO* embryos compared to control littermates at E10.5, indicating aberrations in inner ear development (Figure 39 F, G).

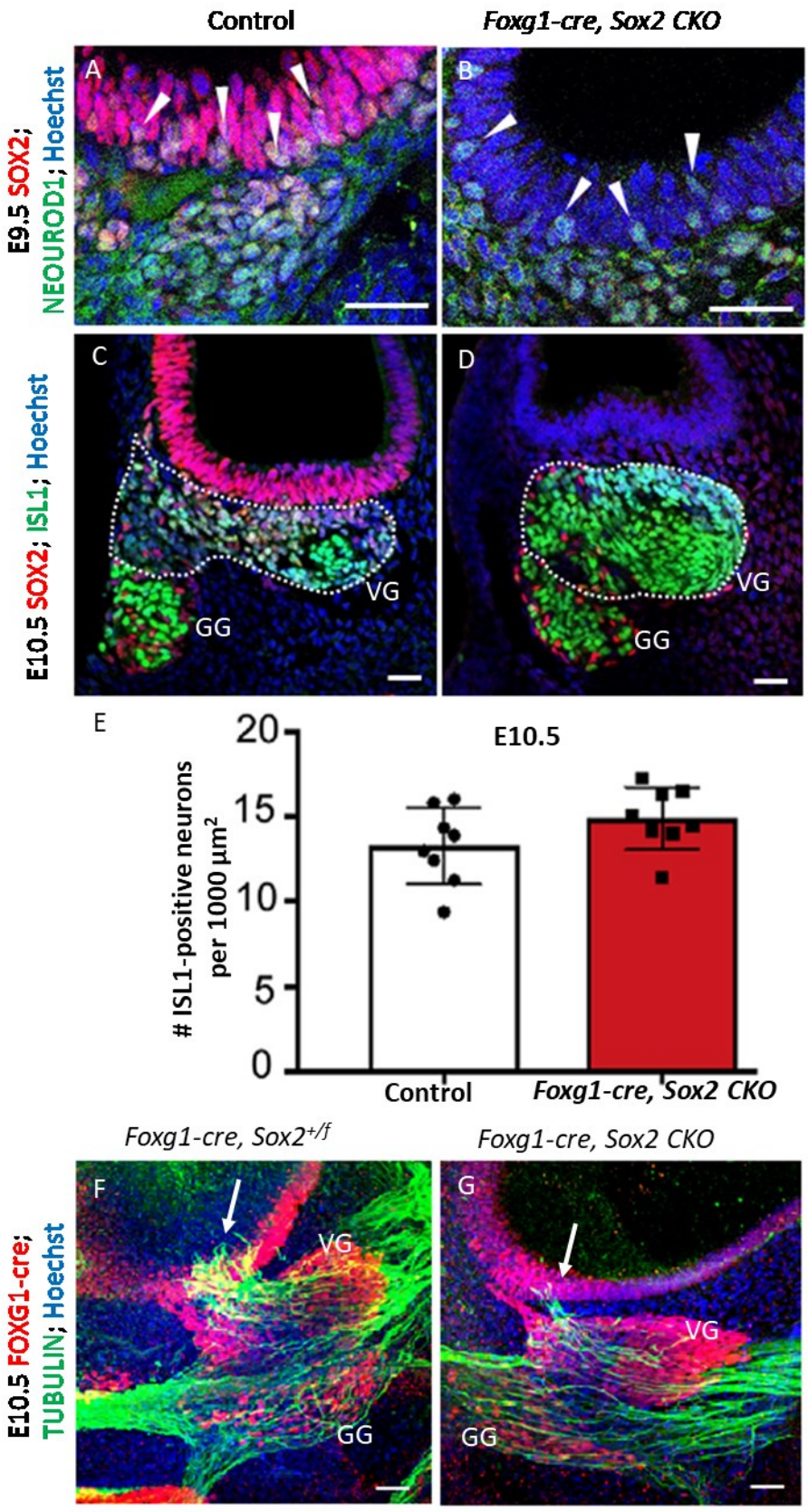

Figure 39: Delamination of NEUROD1-positive neuroblasts and quantification of the vestibular ganglion neurons (Dvorakova *et al.*, 2019): NEUROD1-positive neuroblasts delaminated from the SOX2-positive otic epithelium as well as from the SOX2-negative epithelium at E9.5 (arrowheads in A, B). The

quantification of neurons in the area of the vestibular ganglion showed no significant differences between control and mutant embryos at E10.5 (C–E). Dotted lines indicate the boundaries of the vestibular ganglion (C, D). The values represent ISL1-positive neurons per 1000 μm^2, mean ± SD (N = 4 embryos/genotype, 2 ganglia per embryo), multiple *t*-test with the Holm-Sidak method, P = not significant (E). Immunostaining of whole embryos at E10.5 showed clearly reduced innervation of the ear epithelium in *Foxg1-cre, Sox2 CKO* compared to control heterozygotes, indicating abnormalities in inner ear development (arrows in F, G). GG geniculate ganglion; VG vestibular ganglion; scale bar 50 μm

Changes in proliferation were assessed by examining the proliferation marker KI67 and BrdU and EdU incorporation in S phase of the cell cycle. Protein KI67 was present in proliferating cells and its expression in vestibular neurons was unaffected in *Foxg1-cre, Sox2 CKO* at E9.5 (Figure 40 A, B). Consistently, the pattern of incorporated EdU (injected at E9.5) and BrdU (injected at E10.5) in the vestibular ganglion was similar between control and *Foxg1-cre, Sox2 CKO* littermates, suggesting that mitotic activity was maintained in vestibular neurons. However, the number of BrdU-labelled cells in the vestibular ganglion was decreased in the mutant at E11.5, suggesting decreased incorporation of BrdU and thus, reduced number of actively proliferating cells at E10.5 (Figure 40 C, D).

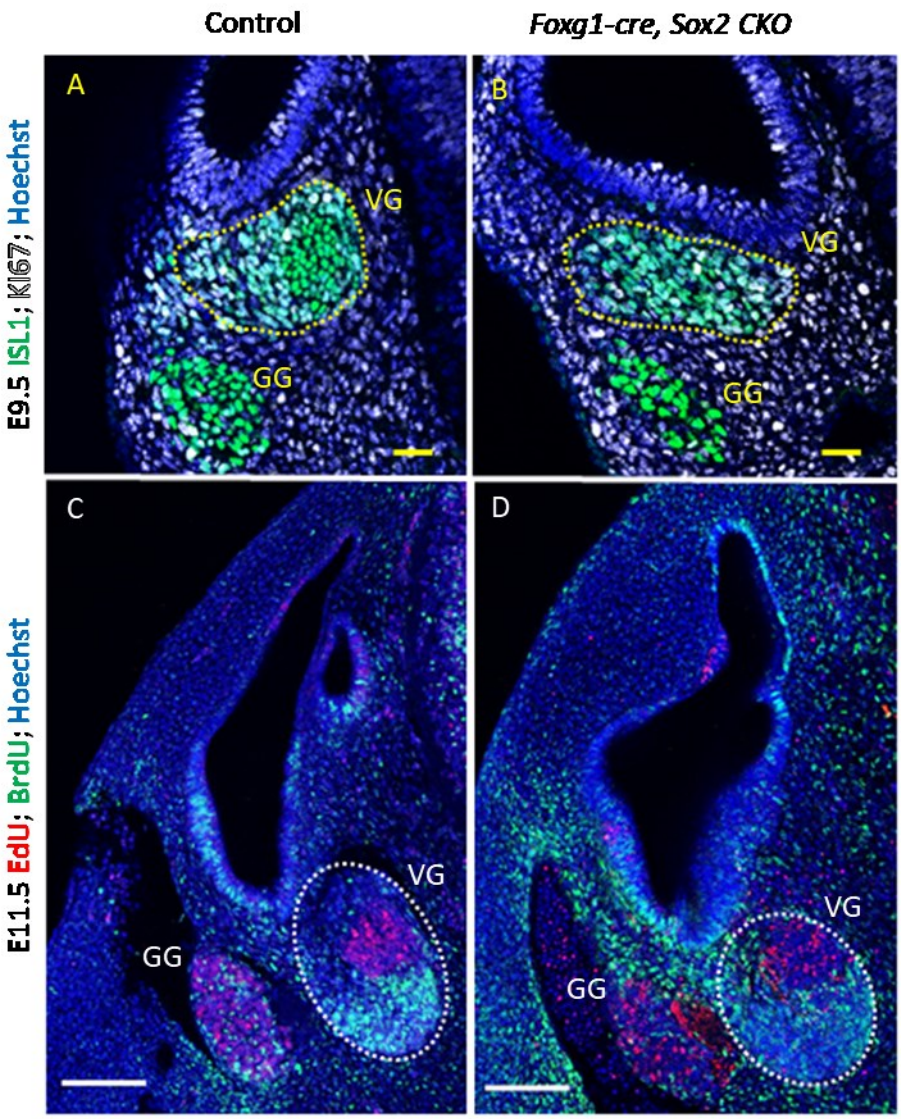

Figure 40: Proliferation in the vestibular ganglion of SOX2-deficient embryos (Dvorakova *et al.*, 2019): Immunolabelling of the proliferating marker KI67 showed proliferating ISL1-positive neurons in the vestibular ganglion of *Foxg1-cre, Sox2 CKO* and control embryos at E9.5 (A, B). The proliferation pattern defined by incorporation of EdU (injected at E9.5) and BrdU (injected at E10.5) showed a generally similar proliferation pattern in the vestibular ganglia of control and mutant littermates at E11.5, although decreased BrdU labelling in *Foxg1-cre, Sox2 CKO* was apparent in the vestibular ganglion (C, D). GG geniculate ganglion; VG vestibular ganglion; scale bars: 50 µm (A, B), 100 µm (C, D)

Inner ear neuronal development was disrupted by apoptosis in *Foxg1-cre, Sox2 CKO* as revealed by immunostaining of cleaved CASPASE 3. Apoptosis was significantly increased in the vestibular ganglion of *Foxg1-cre, Sox2 CKO* at E11.5 (Figure 41 A–C).

Increased apoptosis probably resulted in a rapid reduction of the size of the vestibular ganglion in mutant compared to control mice at E12.5 (Figure 41 D, E).

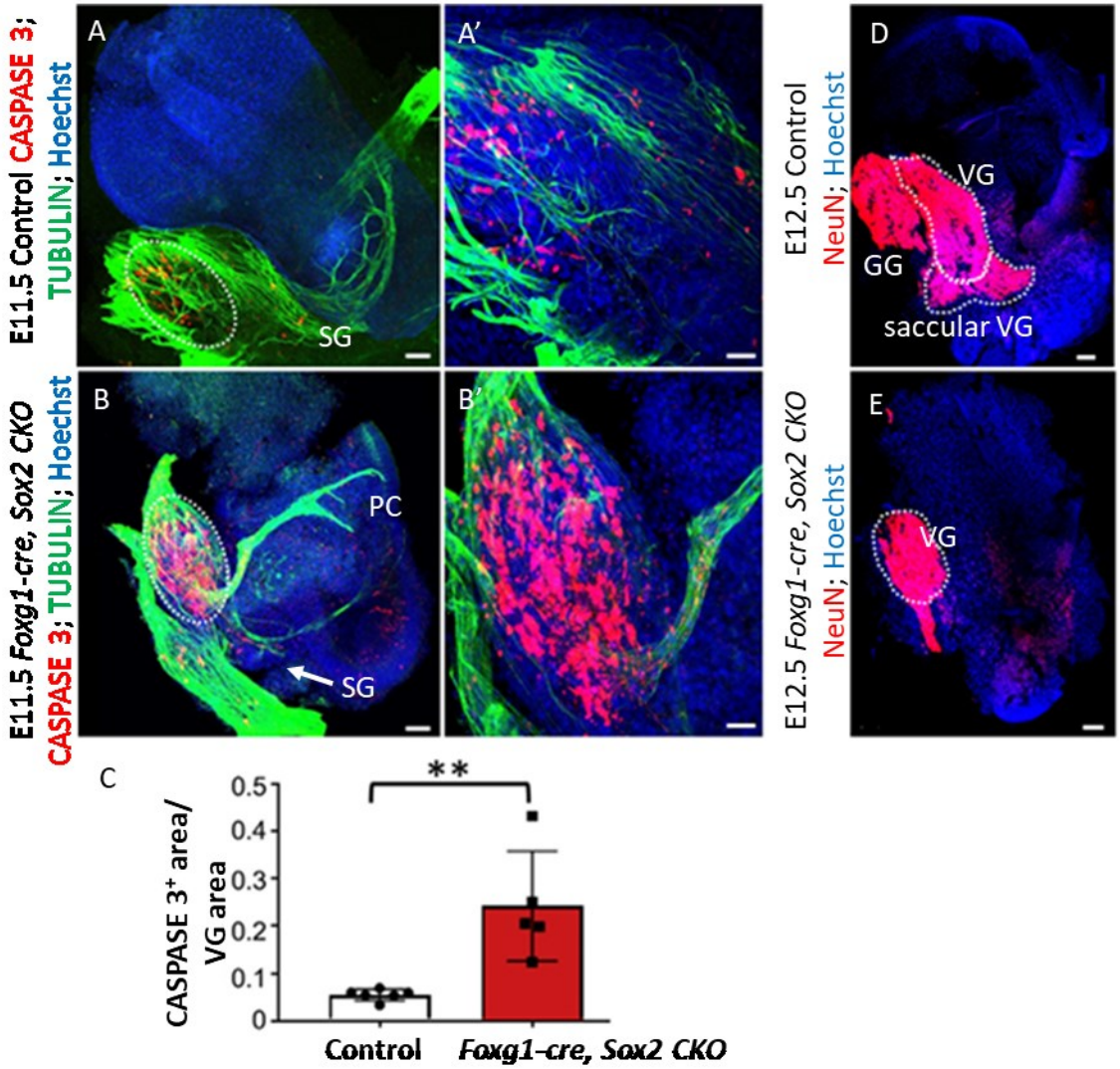

Figure 41: Neuronal development was eliminated by apoptosis in *Foxg1-cre, Sox2 CKO* vestibular ganglion at E11.5 (Dvorakova *et al.*, 2019): Immunostaining of whole inner ears at E11.5 showed significantly increased apoptosis in the mutant vestibular ganglion compared to controls (A, B). The innervation of the spiral ganglion in *Foxg1-cre, Sox2 CKO* was drastically reduced compared to control (arrow in B). Higher magnification images showed details of the CASPASE 3-stained vestibular ganglions (A', B'). Cleaved CASPASE 3 immunostaining was quantified using ImageJ, Mann-Whitney U test, mean ± SD, **P = 0.0043 (C). Whole inner ears with anti-NeuN, a marker for differentiated neurons, showed a diminished domain of the vestibular ganglion at E12.5 in the mutant (D, E). Vestibular ganglion area is demarcated by the dotted line. GG geniculate ganglion; PC posterior crista; SG spiral ganglion; VG vestibular ganglion; scale bars 100 µm (A, B, D, E), 50 µm (A', B')

In contrast to the early development of the vestibular ganglion, the spiral ganglion of *Foxg1-cre, Sox2 CKO* mice constituted only a few neurons expressing transcription factor GATA3 and TRKC, tyrosine kinase receptor for the nerve growth factor NTF3 (Figure 42). GATA3 is expressed in the prosensory domain of the cochlea and in the spiral ganglion (Luo *et al.*, 2013). GATA3 staining revealed abnormalities in the establishment of the prosensory epithelium in the cochlea of *Foxg1-cre, Sox2 CKO*, as shown by a broader expression of GATA3 in the cochlear duct when compared to controls (Figure 42 A–D).

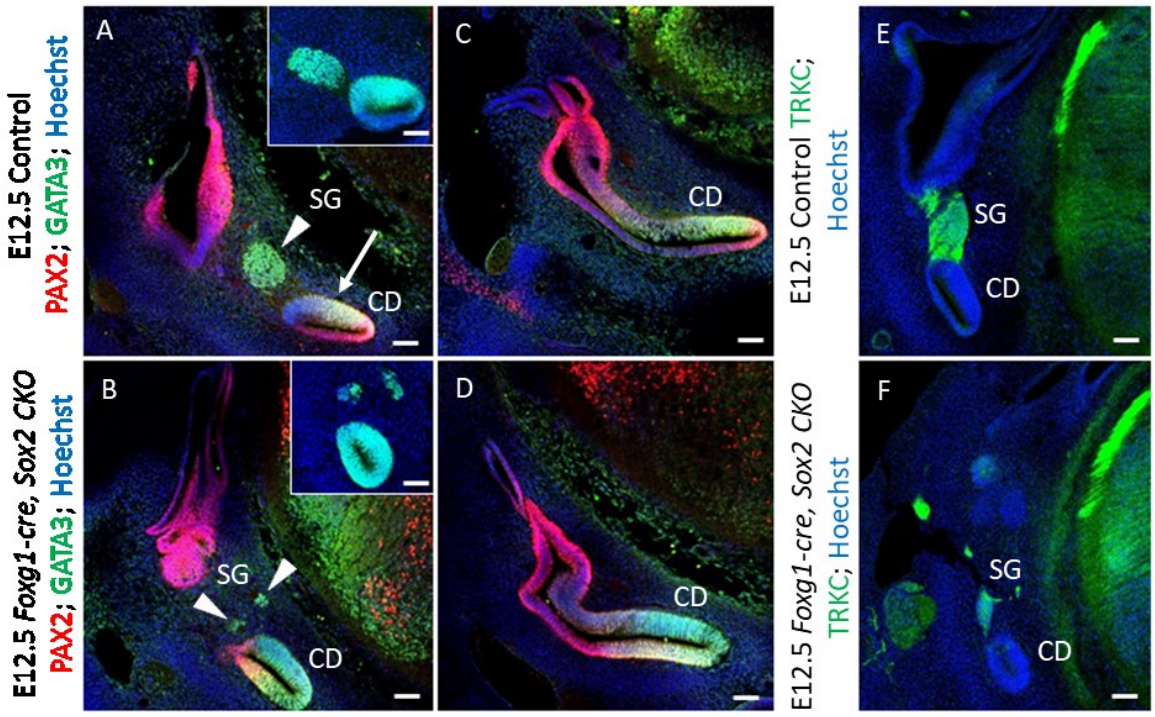

Figure 42: Abnormal specification of the cochlear sensory epithelium and spiral ganglion formation in *Foxg1-cre, Sox2 CKO* (Dvorakova *et al.*, 2019): Formation of cochlear sensory epithelium was abnormal with broader expression of GATA3 transcription factor and a lack of clearly established prosensory region in the cochlear duct of *Foxg1-cre, Sox2 CKO* inner ear (A–D). The prosensory domain was marked by co-expression of PAX2 and GATA3 in the control cochlea (arrow in A). Only residual spiral ganglion neurons were present in the mutant when compared to the control (arrowheads in A, B). The inserts show GATA3 expression. Spiral ganglion neurons in both control and mutant expressed TRKC, tyrosine receptor kinase (E, F). CD cochlear duct; SG spiral ganglion; scale bar 100 µm

Conditional deletion of *Sox2* by *Foxg1-cre* caused morphological changes in the inner ear structure. 3D reconstruction revealed profound differences between controls and mutants at E14.5 (Figure 43). Mutant inner ears developed a prolonged structure with agenetic cochlear duct and a small protrusion, presumably a rudimental saccule. No other structures were discernible.

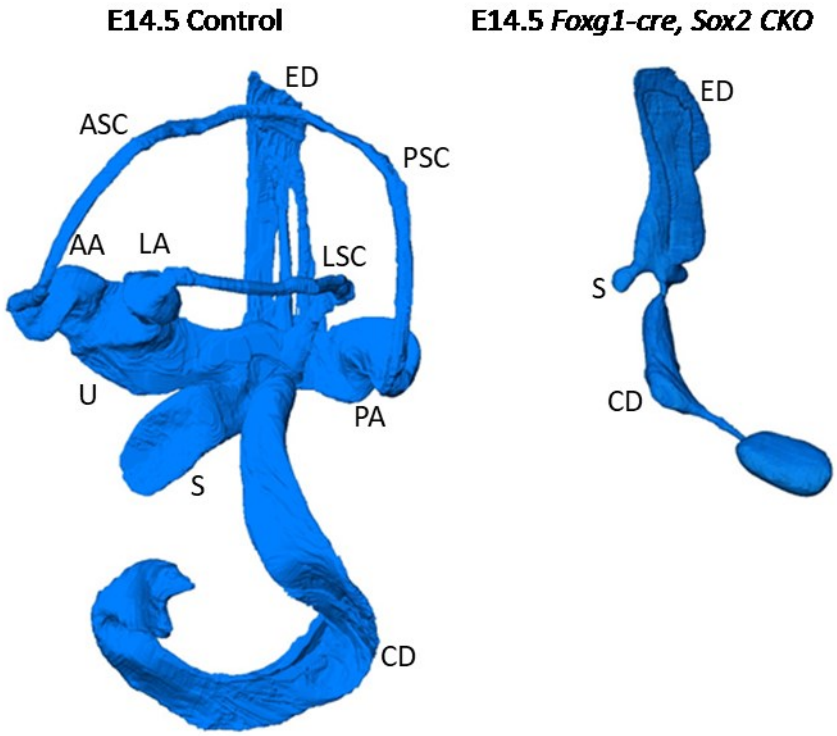

Figure 43: 3D reconstruction of the *Foxg1-cre, Sox2 CKO* inner ears revealed structural malformations at E14.5 (Dvorakova *et al.*, 2019): The inner ear of *Foxg1-cre, Sox2 CKO* showed rudimental cochlear duct and saccule but all other structures were missing or undiscernible compared to the control inner ear. AA anterior ampulla; ASC anterior semicircular canal; CD cochlear duct; ED endolymphatic duct; LA lateral ampulla; LSC lateral semicircular canal; PA posterior ampulla; PSC posterior semicircular canal; S saccule; U utricle

Next, we wanted to comprehend how the loss of SOX2 in all delaminating neurons affected their central projections and neurite navigation to the place of their origin. Using lipophilic dye tracing, we compared the innervation of the inner ear and formation of central projections in *Foxg1-cre, Sox2 CKO* and littermate controls.

At E11.5, inner ear vestibular afferents of *Foxg1-cre, Sox2 CKO* were comparable to controls, extending fibers to the cerebellum but the overall tract size was reduced compared to controls (Figure 44 A, B). Vestibular afferent and efferent fibers in the inner ear reached the area of the posterior crista in both control and mutant mice at E11.5 despite the fact that no posterior crista sensory epithelium ever formed in the mutant (Figure 44 C, D). These data showed that, interestingly, the initial development of the inner ear sensory neurons from E8.5 to E11.5 was near-normal, with proper peripheral and central projections despite the lack of SOX2.

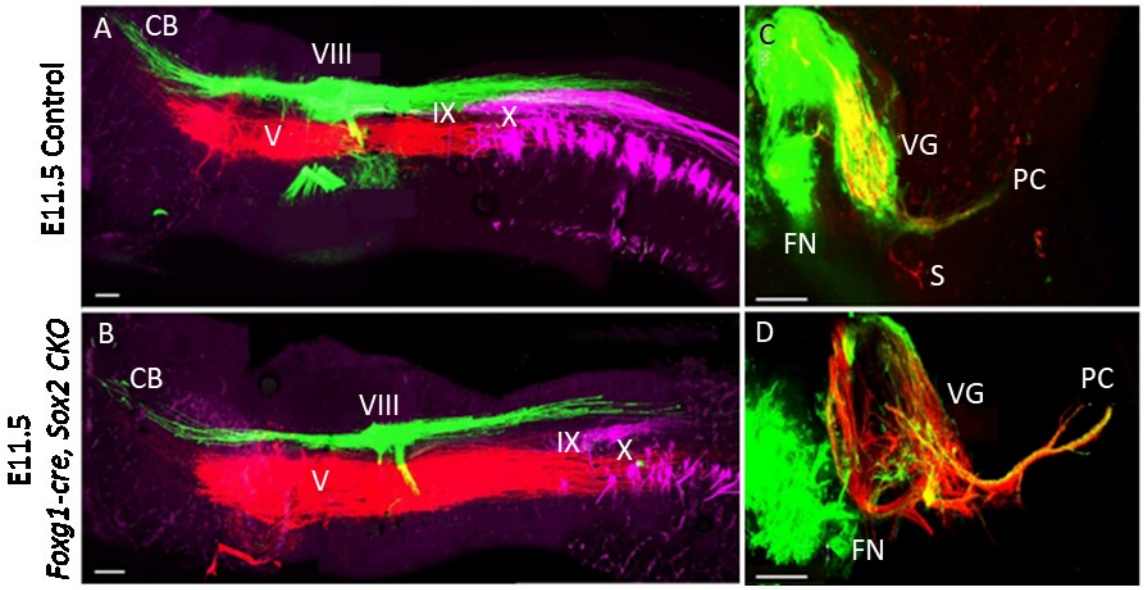

Figure 44: The peripheral and central projections of the inner ear were analogous in controls and *Foxg1-cre, Sox2 CKO* at E11.5 (Dvorakova *et al.*, 2019): Lateral views of whole hindbrains showed comparable lipophilic dye labelling in the control and mutant (A, B). Vestibular afferents of the VIIIth cranial nerve (green), projecting to the cerebellum, were comparable between control and mutant. Trigeminal afferents (red) of the trigeminal nerve (V), glossopharyngeal (IX) and vagal (X) afferents (magenta) of the control were comparable to the mutant (A, B). However, mutants showed fewer vestibular afferent fibers than controls but at the same time, these fibers extended as far rostral and caudal as afferents in control littermates (A, B). Figures of inner ear innervation showed green labelling of the facial nerve and inner ear efferents that extended to the posterior crista region (C, D). Vestibular ganglion neurons and vestibular afferents (red) extended to the region of the posterior crista in both control and mutant mice and to the saccule in controls (C, D). It is worth mentioning that at this age both inner ear afferents (red) and efferents (green) innervated the region of the posterior crista despite the fact that no crista ever formed in the *Foxg1-cre, Sox2 CKO* mice. Cranial nerves: V trigeminal nerve; VIII vestibulocochlear nerve; IX glossopharyngeal nerve; X vagus nerve; CB cerebellum; FN facial nerve; PC posterior crista; S saccule; VG vestibular ganglion; scale bar 100 μm

Central projections of the vestibular ganglion neurons remained almost identical between control and *Foxg1-cre, Sox2 CKO* littermates until at least E12.5 (Figure 45). Furthermore, at E12.5 the earliest central projections from spiral ganglion neurons to the cochlear nucleus could be traced. Targeted labelling of vestibular and cochlear afferent fibers depicted the normal segregation of the central axons of spiral ganglion neurons projecting to the cochlear nucleus from the vestibular nerve in control mice (Figure 45 C). In contrast, dye-labelled inner ear afferent fibers showed no detectable segregated projection from the cochlea in *Foxg1-cre, Sox2 CKO* mice. This indicates that the central projection of spiral ganglion neurons was missing.

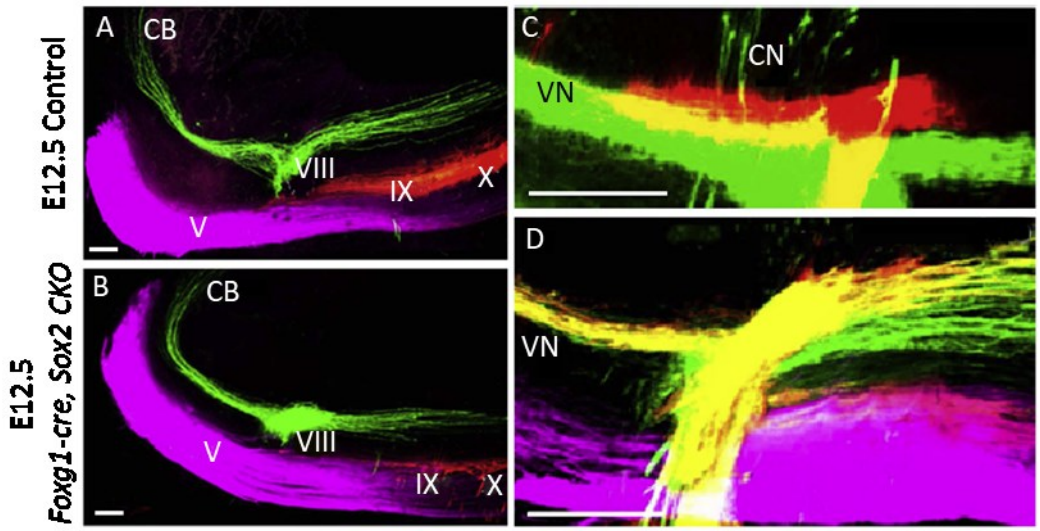

Figure 45: Near-normal vestibular projection at E12.5 but no cochlear projection in *Foxg1-cre, Sox2 CKO* (Dvorakova *et al.*, 2019): Lateral views of whole hindbrains showed almost indistinguishable central projections of the vestibular afferents (green) in the control and mutant littermates, although the number of afferents was reduced in the *Foxg1-cre, Sox2 CKO* (A, B). To analyze the earliest central projections from spiral ganglion neurons to the cochlear nucleus at E12.5, lipophilic dye was inserted into the cochlear duct (red). Vestibular afferent fibers were labelled by inserting the dye into the vestibular organs (green). Control animals showed cochlear projection (red) segregated from vestibular afferents (green) (C). No cochlear projection to the cochlear nucleus was detectable in *Foxg1-cre, Sox2 CKO*, only overlapping labelling of vestibular afferents (D). Cranial nerves: V trigeminal nerve; VIII vestibulocochlear nerve; IX glossopharyngeal nerve; X vagus nerve; CB cerebellum; CN cochlear nucleus; VN vestibular nerve; scale bar 100 μm

Applications of dye into rhombomeres 4 and 5 labelled projections to the posterior crista and to the basal turn of the cochlea in control animals. These applications in *Foxg1-cre, Sox2 CKO* mice labelled only vestibular afferents and efferents and showed no cochlear innervation (Figure 46).

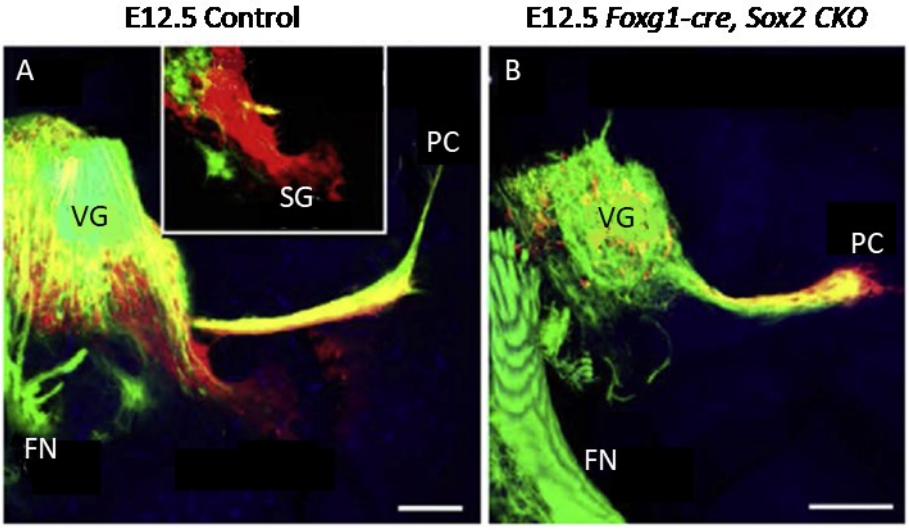

Figure 46: No cochlear innervation in *Foxg1-cre, Sox2 CKO* at E12.5 (Dvorakova *et al.*, 2019): Green dye labelled vestibular afferents and red labelled both vestibular and cochlear afferents. This labelling revealed spiral ganglia in the basal turn of the cochlea in the control (insert in A). No cochlear innervation or neurons were labelled in the mutant littermate (B). The vestibular ganglion was smaller in *Foxg1-cre, Sox2 CKO* mice compared to controls at E12.5 (A, B). FN facial nerve; PC posterior crista; SG spiral ganglion; VG vestibular ganglion; scale bar 100 μm

Selective dye tracing of efferent and afferent neurons at E18.5 revealed huge differences between control and *Foxg1-cre, Sox2 CKO* mice. In control mice, efferents and afferents formed a network of cells and fibers in both vestibular and spiral ganglia with the facial and intermediate nerves passing across the vestibular ganglion (Figure 47 A, B). In *Foxg1-cre, Sox2 CKO* mice, only facial and intermediate nerves, including geniculate ganglion, were labelled by similar dye applications as in controls (Figure 47 B, D). No vestibular or spiral ganglion neurons were labelled in mutants and the contralateral inner ear efferents formed a meshwork of fibers in the place of former vestibular ganglion.

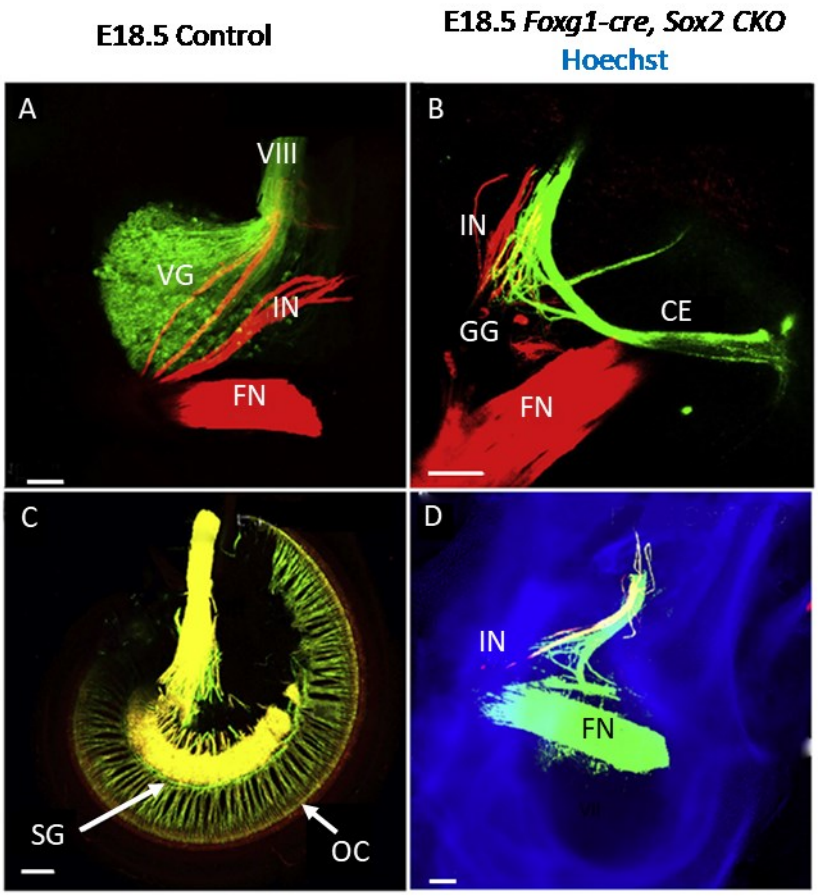

Figure 47: Only efferent fibers projected to the *Foxg1-cre, Sox2 CKO* ear at E18.5 (Dvorakova *et al.*, 2019): Facial and intermediate nerves (red) were labelled in both controls and mutants (A, B). Vestibular ganglion and vestibular afferents (green) were found only in controls, whereas in mutants, only some contralateral inner ear efferents remained until this stage and formed a meshwork of fibers where the vestibular ganglion used to be (A, B). Distribution of efferent (green) and afferent (red) fibers in the cochlea and spiral ganglion neurons of controls are shown (C). No cochlea or spiral ganglion neurons were found in *Foxg1-cre, Sox2 CKO*, only reduced residual ear vesicle (blue background) was present (D). VIII vestibulocochlear nerve; CE contralateral inner ear efferents; FN facial nerve; GG geniculate ganglion; IN intermediate nerve; OC organ of Corti; SG spiral ganglion; VG vestibular ganglion; scale bar 100 µm

These data indicate that at least some inner ear efferents could overcome the loss of vestibular ganglion neurons and remained in a projection pattern toward the residual ear at least until E18.5.

4.3. Deletion of *Sox2* in neurons of the inner ear

To distinguish the direct effects of SOX2 elimination on the development of inner ear neurons from the secondary effects of missing inner ear sensory epithelia, we decided to use *Neurod1-cre* driver to eliminate *Sox2* specifically in inner ear neurons. Generated *Neurod1-cre, Sox2 CKO* mice were viable, without any external abnormalities. At first, we wanted to see the effect of *Neurod1-cre* mediated deletion of *Sox2* on neurosensory cells of the inner ear at P0. The inner ear innervation, vestibular and spiral ganglion formation and sensory hair cell formation and distribution were indistinguishable from controls at P0 (Figure 48)

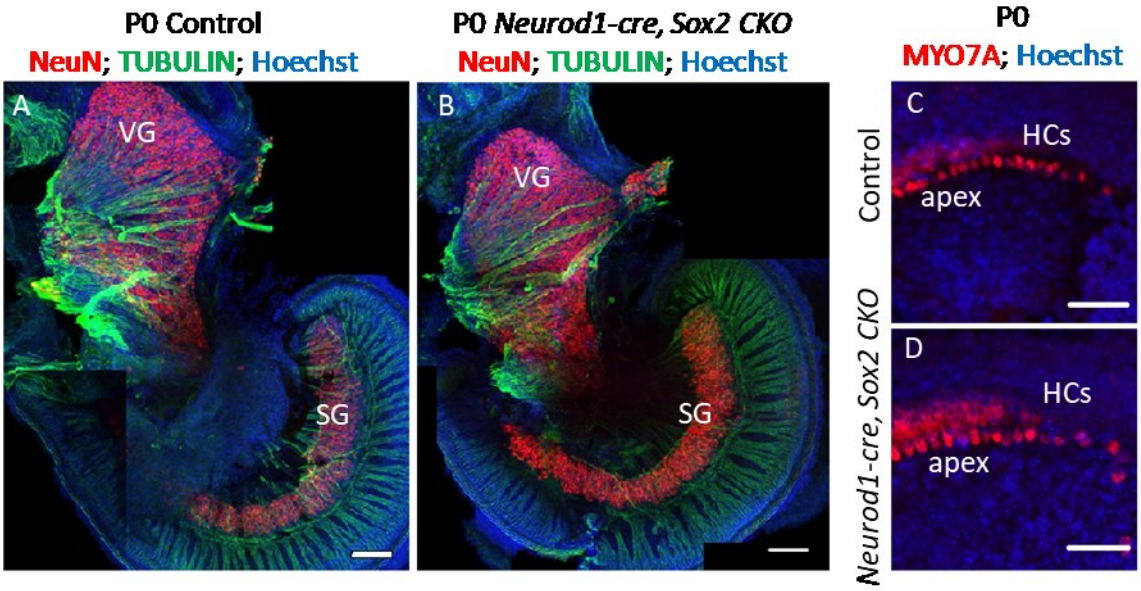

Figure 48: *Neurod1-cre, Sox2 CKO* inner ears were indistinguishable from controls (Dvorakova, unpublished data): Immunohistochemistry of whole inner ears for neuronal marker NeuN and TUBULIN showed identical staining in controls and mutants (A, B). Hair cells in the mutant cochlea formed normally. Depicted here is the detail of apical hair cells in control and mutant littermates (C, D). HCs hair cells; SG spiral ganglion; VG vestibular ganglion; scale bars: 200 µm (A, B), 50 µm

Next, we compared hearing functions of adult *Neurod1-cre, Sox2 CKO* mice to control littermates. Recording of ABR thresholds and otoacoustic emissions (DPOAE) did not show any hearing abnormalities in mutant mice (Figure 49).

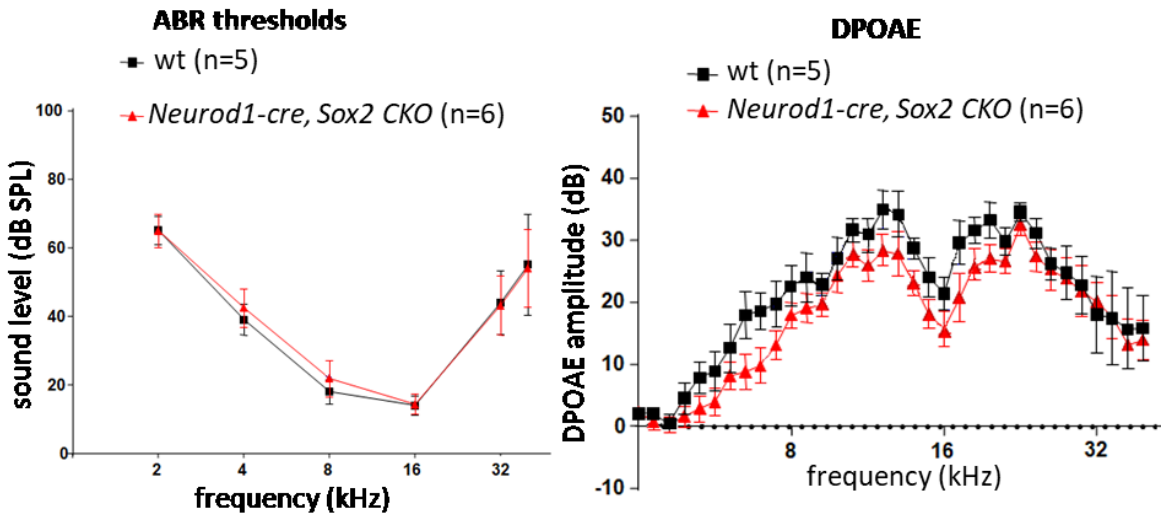

Figure 49: Hearing functions of *Neurod1-cre, Sox2 CKO* mice were not altered (Pysanenko, unpublished data): ABR thresholds and otoacoustic emissions of adult mice were comparable between controls and mutants. ABR auditory brainstem response; DPOAE distortion product otoacoustic emission; SPL sound pressure level; wt wild type

These data indicate that deletion of *Sox2* by *Neurod1-cre* caused neither morphologic nor functional difference in the inner ear.

5. DISCUSSION AND SUMMARY

This thesis investigated the role of SOX2 in inner ear neuronal and sensory development. We used mice as a model organism for all experiments due to its similarity of the genome and inner ear to humans. To determine the requirements of SOX2 for inner ear development, we generated three different conditional deletions of *Sox2* gene using *cre-loxP* strategy. Our data contribute to our understanding of the complexity of SOX2 regulation during inner ear development. To elucidate the molecular interactions underlying inner ear development is an essential basis for implementation of new therapeutic strategies of the hearing loss.

The first part of the thesis is focused on the delayed and incomplete deletion of *Sox2* in inner ear neurosensory precursors. Our conditional deletion of *Sox2* using *Isl1-cre* offered the first mouse model to test *in vivo* the function of SOX2 in the formation of inner ear neurons and sensory cells. In summary, our first study on delayed and incomplete deletion of *Sox2* showed a deep involvement of SOX2 transcription factor in neurosensory development of the ear at several levels:

First, *Isl1-cre, Sox2 CKO* mutant indicated that neuronal development depends directly on SOX2, as the latest-forming neurons never formed.

Second, the differentiation of hair cells depends on the level and duration of SOX2 expression, as in the mutant, hair cells differed in their number, size and stereocilia formation and showed incomplete segregation of neuronal and hair cell phenotype.

Third, *Sox2* deletion affected supporting cells, as shown by the variable distribution and unusual shape of P75-positive IPCs.

Fourth, the formation of boundaries between the organ of Corti and GER was affected by the loss of SOX2.

The inner ear changes in our *Isl1-cre, Sox2 CKO* mutant are summarized in Figure 50.

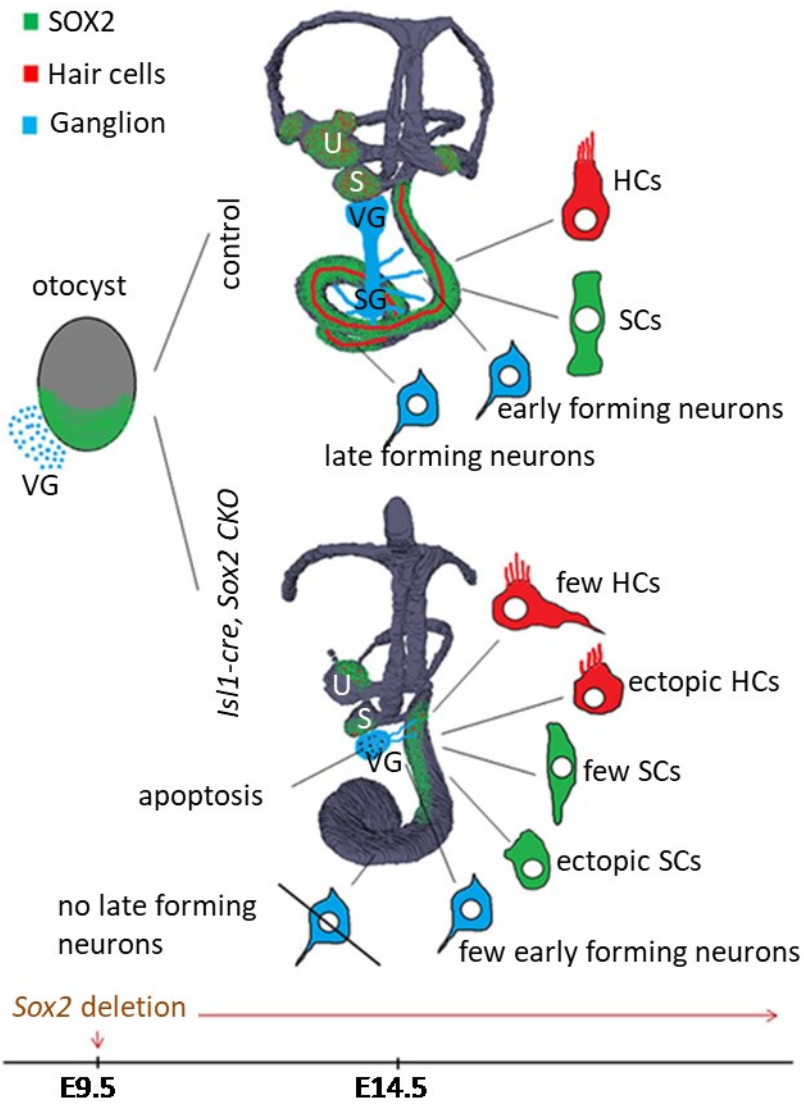

Figure 50: Summary of changes in *Isl1-cre, Sox2 CKO* inner ear (Dvorakova *et al.*, 2016): *Sox2* deletion resulted in considerable morphological changes at E14.5. All three cristae of the semicircular canals were missing; all remaining sensory organs were smaller and had decreased sensory area. The apex of the cochlea lacked neuronal formation, whereas vestibular and basal cochlear neurons died due to reduced or missing sensory epithelia. Loss of innervation toward all epithelia except for the apex of the cochlea was secondary to the lack or reduction of hair cells in the cristae, cochlear base, utricle and saccule. Many hair cells had an unusual phenotype. Similarly, supporting cells had aberrant characteristics, altered expression of markers and altered topology. HCs hair cells; S saccule; SCs supporting cells; SG spiral ganglion; U utricle; VG vestibular ganglion

Inner ear neurogenesis requires a series of transcription factors. Expression of the bHLH genes *Ngn1* and *Neurod1* is needed at the beginning of sensory neuron formation and is followed by several other factors necessary for the full differentiation of neurons (Ma *et*

al., 1998; Kim *et al.*, 2001). “All inner ear sensory neurons derive from the otocyst” (Yang *et al.*, 2011). Vestibular neurons delaminate from sensory epithelia or areas adjacent to sensory epithelia (Yang *et al.*, 2011; Fariñas *et al.*, 2001). Cochlear sensory neurons delaminate most plentifully from the area close to the basal tip and the middle turn and later from the apex of the cochlear duct. Spiral ganglion neurons undergo the last cell division in a base to apex progression (Matei *et al.*, 2005). In the *Isl1-cre, Sox2 CKO*, all early forming neurons seem to develop normally. However, the formation of late-forming apical spiral ganglion neurons is absent (Figure 22 D, F, Figure 50). This fact indicates a dependency of spiral ganglion neurons formation on the continuous expression of SOX2. We suggest that neuronal precursor expansion depends on SOX2, as apical spiral ganglion neurons, which are missing in *Isl1-cre, Sox2 CKO*, are the last neurons of the ear to exit the cell cycle and the basal spiral ganglion neurons, which are present in *Isl1-cre, Sox2 CKO*, are the first to exit the cell cycle at E10.5 (Matei *et al.*, 2005). This corresponds with the timing of *Isl1* expression and subsequent *Isl1-cre*-mediated elimination of SOX2 at E10.5 (Radde-Gallwitz *et al.*, 2004). *Ngn1* expression, and thus neuronal precursor specification, begins in the otic placode at E9.0 (Ma *et al.*, 1998). We hypothesize that the purpose of SOX2 protein is to stabilize early neuronal development by interacting with bHLH genes, as previously suggested (Evsen *et al.*, 2013). Kempfle, Turban and Edge used an inducible *Sox2-creER* line showing the effect of a delayed loss of SOX2 on cochlear development (Kempfle, Turban and Edge, 2016). However, the condition of inner ear neurons was not reported and therefore, our hypothesis could not be validated.

The viability and correct outgrowth of sensory neurons depend on two neurotrophins: BDNF and NTF3 expressed by inner ear sensory epithelia (Fariñas *et al.*, 2001). The targeted innervation of vestibular neurons to the area of cristae of the semicircular canals was initially formed in our *Isl1-cre, Sox2 CKO* mutant even in a complete absence of target hair cells and their neurotrophic support (Figure 22). One possibility is, that the neuronal migration could be guided by glial cells and thus, the target sensory cells are not required (Edmondson and Hatten, 1987). However, later in development neurons perished and the fibers retracted after the loss of sensory epithelia (Figure 22), as in other mutants without cristae formation (Pauley *et al.*, 2003). Our data suggest that the loss of neuronal fibers in the absence of sensory epithelia is delayed in the vestibular system. Vestibular neurons differentiated and formed the comparable vestibular ganglion to controls up to

E11.5 but later many vestibular neurons died presumably due to missing or significantly reduced sensory epithelia. In contrast, spiral ganglion and innervation in the cochlea was not formed in *Isl1-cre, Sox2 CKO* mutant with the exception of neurons innervating the base. The cochlear base was the only area of the auditory sensory epithelium with a few surviving sensory cells. Accordingly, the early forming neurons were present in the cochlear base but showed an unusual innervation pattern dependent on the density and distribution of hair cells, illustrated by neuronal fibers being directed towards the remaining hair cells (Figure 22 D, F, Figure 25 B). Our data on *Isl1-cre, Sox2 CKO* suggest a biphasic loss of neurons. Late-forming neurons of the spiral ganglion never formed due to an absence of SOX2, which is necessary to initiate their differentiation, whereas early-forming neurons died after differentiation due to the reduced number of hair cells to support them. This might presumably be true also for the reported absence of neurons in *Lcc* mutants at E15.0 (Puligilla *et al.*, 2010).

Many studies have demonstrated that SOX transcription factors are necessary to maintain pluripotency, but also to start differentiation through the upregulation of other transcription factors, in particular bHLH factors, which later form a negative feedback inhibition of *Sox2* for normal differentiation to proceed (Graham *et al.*, 2003; Pevny and Nicolis, 2010; Evsen *et al.*, 2013; Taranova *et al.*, 2006). Previous work has exhibited a crucial dependence of hair cell development on SOX2 (Kiernan et al., 2005). SOX2 becomes downregulated by increased expression of *Atoh1* in progenitor cells that will develop as hair cells but on the other hand, *Sox2* expression is needed for ATOH1 upregulation (Dabdoub *et al.*, 2008; Kempfle, Turban and Edge, 2016). Our data support these findings, since ATOH1 was expressed only in areas with SOX2 expression in the cochlea of *Isl1-cre, Sox2 CKO* (Figure 27). We showed, for the first time, that some yet uncertain level and time of *Sox2* expression is needed for normal hair cell development, since in *Isl1-cre, Sox2 CKO* different sensory epithelia formed variable numbers of variably differentiated hair cells. Some epithelia never formed (cristae of the semicircular canals, apical turn of the organ of Corti), other were variably reduced (utricle, saccule, basal turn of the organ of Corti) (Figure 24, Figure 25).

Various degree of sensory epithelia loss could be possibly caused by *Isl1-cre* that could considerably affect some but not other epithelia precursors. As a result, different epithelia would be completely or partially lost. However, this option is ruled out by our survey of the inner ear of *Isl1-cre, Atoh1*$^{f/f}$ mutants manifesting a uniform effect of *Isl1-cre* in all

sensory epithelia with no differentiated hair cells in the inner ear (data not shown), suggesting that incomplete recombination of *Sox2* by *Isl1-cre* is not the explanation of the patchy presence of some hair cells in *Isl1-cre, Sox2 CKO* mice. The simple delay in *Sox2* recombination is therefore a more probable reason of the differential loss of hair cells.

The alternative explanation could possibly be that, since only epithelia with confirmed or suspected common neuronal and sensory progenitors retain hair cells, only hair cells derived from such common neurosensory progenitors formed, whereas epithelia without such common precursors (cristae of the semicircular canals, apical turn of the organ of Corti) developed no hair cells (Satoh and Fekete, 2005; Matei *et al.*, 2005; Raft and Groves, 2015). The expression of neuronal markers in some of the present hair cells supports this notion (Figure 28).

The level and duration of ATOH1 expression is crucial for hair cell differentiation and survival (Bermingham *et al.*, 1999; Pan *et al.*, 2012). We found limited expression of *Atoh1* mRNA, which would probably lead to a differential loss of hair cells, as previously reported (Pan *et al.*, 2012) (Figure 27). Normal level of ATOH1 is important for the proper development of stereocilia and their polarity. Profound variability among remaining hair cells in *Isl1-cre, Sox2 CKO* inner ears summarized the compounding effect of *Isl1-cre* expression pattern, delay of effective *Sox2* recombination and alteration in *Atoh1* expression.

The organ of Corti has only two types of hair cells but a range of supporting cell types expressing multitude of diffusible factors (Fritzsch *et al.*, 2015). Formation of the precise pattern of hair cells and supporting cells in the organ of Corti is controlled by Delta-Notch lateral inhibition interactions between hair cells and supporting cells (Haddon *et al.*, 1998). Thus, hair cell defects could result in supporting cell defects, as reported (Jahan *et al.*, 2015). However, the unusual morphology of IPCs or the unusual distribution of *Bmp4* in the organ of Corti indicate a more direct role of SOX2 in cell fate execution of supporting cells (Figure 29 B, Figure 30 C–D'').

The second part of this thesis focuses on the early deletion of *Sox2* at the otic placode stage by *Foxg1-cre*. The early deletion of *Sox2* was needed to clarify the function of SOX2 in early neuronal development of the inner ear. Additionally, this mutant allowed

comparing differences in placode development of ear, eye and olfactory system. Our analyses revealed:

First, deletion of *Sox2* by *Foxg1-cre* caused impairment of the early eye and olfactory development, whereas early inner ear development was not affected.

Second, the early vestibular innervation in the mutant was comparable to controls suggesting that SOX2 is not necessary for the early stages of neuronal development.

Third, later stages of neuronal development in the inner ear were disrupted by massive apoptosis due to missing neurotrophic support from sensory hair cells.

Fourth, deletion of *Sox2* by *Foxg1-cre* caused severe inner ear dysmorphology.

The changes of *Foxg1-cre, Sox2 CKO* inner ears are summarized in Figure 51. The *Sox2* deletion caused residual ear structure at E14.5 with only rudimental cochlear duct and saccule. The initial formation of the vestibular ganglion and central projections to the brain were comparable to controls. In contrast, no distinct spiral ganglion structure was formed in mutants.

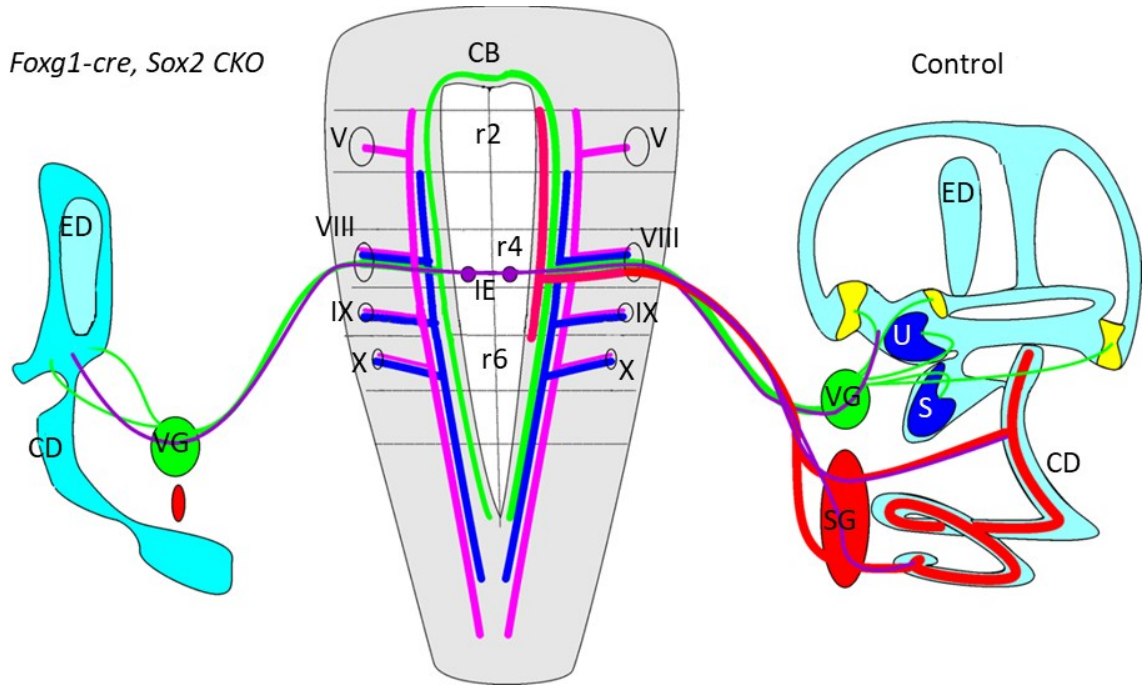

Figure 51: Overview of the inner ear defects and ear projection changes in *Foxg1-cre, Sox2 CKO* (Dvorakova *et al.*, 2019): Control inner ear (right) contain six sensory epithelia, five vestibular: the maculae of the utricle and saccule (blue) and the cristae of three semicircular canals (yellow) and the auditory

sensory organ of the cochlea, the organ of Corti (red). Neurons of vestibular ganglia (green) and spiral ganglia (red) send afferent fibers from the ear to the brain. The ear is also innervated by the inner ear efferents (lilac) ending on the sensory cells. In *Foxg1-cre, Sox2 CKO* (left), *Sox2* deletion resulted in malformations of the inner ear with only rudimental cochlear duct and saccule and all other structures being unrecognizable. The absence of SOX2 did not change the initial formation of the vestibular ganglion and neuronal projections to the brain (green). Dye tracing of trigeminal (magenta) and glossoparyngeal/vagal nerves (blue) showed near-normal central projections in *Foxg1-cre, Sox2 CKO* embryos. In contrast to control embryos, no afferent innervation from the cochlea (red) could be detected in *Foxg1-cre, Sox2 CKO*. The red dot in the mutant shows the possible temporary appearance of some spiral ganglion neurons. Cranial nerves: V trigeminal nerve; VIII vestibulocochlear nerve; IX glossopharyngeal nerve; X vagal nerve; CB cerebellum; CD cochlear duct; ED endolymphatic duct; IE inner ear efferents; r2, r4, r6 rhombomere 2, 4 ,6; S saccule; SG spiral ganglion; U utricle; VG vestibular ganglion

Significant abnormalities in lens and olfactory placode development after *Sox2* deletion correspond with the common origin of olfactory and lens placodes (Bhattacharyya *et al.*, 2004). Furthermore, anterior lens and olfactory placodal cells differ from posterior otic placodal cells in gene expression patterns. Anterior lens and olfactory placodes express *Six3*, *Pax6* and Orthodenticle homeobox 2 (*Otx2*), whereas posterior placodal cells express Iroquois homeobox 3 (*Irx3*), Gastrulation brain homeobox 2 (*Gbx2*), *Pax2* and *Pax8* (Bouchard *et al.*, 2010; Maier *et al.*, 2014). Therefore, the effect of SOX2 seems to be affected by different molecular pattern of these placodes. In particular, the previously reported cooperation of SOX2 and PAX6 in the olfactory and lens induction process supports our results of SOX2 requirement in this process (Quinn, West and Hill, 1996; Kamachi *et al.*, 2001; Panaliappan *et al.*, 2018). Furthermore, disruption of lens and olfactory placode development has been reported when PAX6 or SOX2 is lost (Quinn, West and Hill, 1996; Panaliappan *et al.*, 2018). Together, these results suggest that SOX2 and PAX6 transcriptional regulation is necessary for correct formation of lens and olfactory placodes.

Our results show that unlike the lens and olfactory placodes that failed to invaginate, the ear (otic) placode invaginated and formed the otic vesicle in *Foxg1-cre, Sox2 CKO* mice. The expression of *Sox9* overlaps with *Sox2* in inner ear development. Deletion of *Sox9* by *Foxg1-cre* showed failure of the ear placode to invaginate (Mak *et al.*, 2009; Barrionuevo *et al.*, 2008). Using the same *cre* mouse line, we, for the first time, showed that SOX2 is not needed for otic placode invagination and otocyst formation.

Moreover, our data revealed that SOX2 loss has no effect on early neuroblast delamination and expression of NEUROD1 (Figure 38, Figure 39). The capacity of the otic placode to generate neurons after deletion of SOX2 is in strong contrast to the olfactory system that showed lack of significant NGN1 and NEUROD1 expression and consequently, absence of neurogenesis (Panaliappan *et al.*, 2018). Moreover, our *Foxg1-cre, Sox2 CKO* mutant formed the proper vestibular ganglion with peripheral and central projections comparable to controls (Figure 44, Figure 51). This conclusion is in line with the results in our *Isl1-cre, Sox2 CKO*, where the vestibular ganglion was initially formed without any abnormalities. In contrast to *Isl1-cre, Sox2 CKO*, no SOX2 expression was detected in the developing cochlea of *Foxg1-cre, Sox2 CKO* mutant and accordingly, only a few transient spiral ganglion neurons were detected but neither their peripheral nor central projections were formed in *Foxg1-cre, Sox2 CKO*. Cochlear neurons exit the cell cycle in a base to apex progression (Matei *et al.*, 2005). It is thus possible that some early forming spiral ganglion neurons in the base could be only short-lived when SOX2 was eliminated from the development as we showed already with *Isl1-cre, Sox2 CKO* mutant.

Removing SOX2 from inner ear development may have more prominent consequences on the formation of spiral ganglion neurons than vestibular ganglion neurons because of the early dependency of spiral ganglion neurons on neurotrophin support. Neurotrophins affect fiber navigation and neuronal survival during development. Spiral ganglion neurons depend exclusively on NTF3 produced by cochlear sensory epithelium, whereas vestibular ganglion neurons are predominantly dependent on BDNF (Fariñas *et al.*, 2001; Bianchi *et al.*, 1996). However, vestibular ganglion neurons and vestibular projections do not require BDNF for their survival of up to E12.5 (Bianchi *et al.*, 1996). In contrast, cochlear neurons are wholly reliant on NTF3 produced by sensory epithelium (Fariñas *et al.*, 2001). No spiral ganglion innervation is detected in the absence of NTF3 in newborns. Consistently, we found no cochlear innervation at E12.5 in contrast to near-normal projections of vestibular ganglion neurons in *Foxg1-cre, Sox2 CKO* embryos (Figure 45, Figure 46). Despite the initially intact development of vestibular neurons, all inner ear neurons of *Foxg1-cre, Sox2 CKO* eventually died by apoptosis because of the absence of neurotrophic support from undifferentiated sensory epithelia. Interestingly, some efferent fibers remained at least until E18.5 as signs of previous development in

Foxg1-cre, Sox2 CKO, consistent with previous reports (Ma, Anderson and Fritzsch, 2000) (Figure 47).

We confirmed that after early elimination of *Sox2*, no sensory epithelia were established and general ear morphogenesis was extensively affected, even more than in *Lcc* mutant (Kiernan *et al.*, 2005).

Since spiral ganglion neurons in *Lcc* mutant at E15.5 were absent, it was suggested that no neurons ever form in this mutant (Kiernan *et al.*, 2005; Puligilla *et al.*, 2010). However, no evaluation of early neurogenesis and initial innervation similar to our data were performed in the inner ear of *Lcc* embryos. The loss of innervation observed in older *Lcc* embryos can thus be reconciled with our results of a postponed loss of neurons in *Foxg1-cre, Sox2 CKO* mutant. Another study of *Sox2* deletion in the inner ear used tamoxifen inducible *Sox2-creERT2* with tamoxifen injected daily from E8.5 until E11.5 (Steevens *et al.*, 2017). This study demonstrated about 70% smaller inner ear ganglion at E11.75. However, this publication showed the loss of SOX2 only at E11.75 without any data from earlier stages. In contrast, our results on *Foxg1-cre, Sox2 CKO* mutant presented a thorough elimination of SOX2 in the invaginating otic placode at E8.5 (Figure 32). Additionally, we showed delaminating NEUROD1-positive neurons from the SOX2-negative ear epithelium at E9.5, comparable number of neurons in the vestibular ganglion of controls and mutants at E10.5 and well developed peripheral and central projections of vestibular neurons in *Foxg1-cre, Sox2 CKO* mutants at E11.5 (Figure 39, Figure 44). Based on our data, an intense apoptosis of vestibular ganglion neurons occurred before E11.75 in SOX2-deficient inner ears. Thus, Steevens *et al.* may have completely missed the early stages of neurogenesis in the inner ear (Figure 41). Moreover, unlike Steevens *et al*., we used the whole-mount fiber tracing method that effectively verified the characteristics of inner ear neuronal projections that may have been missed with techniques used by them (Steevens *et al.*, 2017).

Our data confirmed that SOX2 is required for normal morphogenesis of the inner ear. Our results support the suggestions that early loss of SOX2 impairs otic epithelial volume and results in non-sensory tissue dysmorphogenesis, as SOX2 is highly expressed in non-sensory tissues besides its expression in sensory progenitors of the inner ear (Gu *et al.*, 2016; Steevens *et al.*, 2019).

The third part of this thesis investigates the effects of the elimination of *Sox2* specifically in the inner ear neurons of *Neurod1-cre, Sox2 CKO* mutants. In this mutant, unlike the previous *Foxg1-cre* and *Isl1-cre, Sox2 CKO*s, inner ear sensory epithelium was formed. We found no morphological or functional differences between *Neurod1-cre, Sox2 CKO* and their control littermates. Thus, the elimination of SOX2 by *Neurod1-cre* did not affect inner ear development. Therefore, we concluded that SOX2 is not necessary for ear neuronal development and that inner ear neurons lacking SOX2 can fully develop in the presence of normal sensory epithelium.

In summary, this thesis examined the role of transcription factor SOX2 in inner ear development. The critical dependence of sensory hair cell development on SOX2 was reported previously. We confirmed these results and showed that some level and time of *Sox2* expression is needed for normal hair cell development. Unusually shaped and topologically incorrect supporting cells in the absence of SOX2 suggest also the dependence of supporting cells development on SOX2. In *Isl1-cre, Sox2 CKO*, some epithelia did not form and some were variably reduced, whereas in *Foxg1-cre, Sox2 CKO*, no sensory epithelia ever formed.

In contrast, the otic placode invagination and otocyst formation does not require SOX2. Similarly, the development of early forming vestibular neurons was normal in both *Isl1-cre, Sox2 CKO* and *Foxg1-cre, Sox2 CKO* mutants, which indicates SOX2 is not necessary for the early ear neurogenesis. However, neurons died by apoptosis at later developmental stages in the absence of neurotrophic support from differentiated sensory epithelia, indicating a secondary effect of SOX2 loss on inner ear neurons.

Additionally, we showed the differences in SOX2 requirements for lens and olfactory placode development compared to the ear placode. In contrast to the ear, early eye and olfactory development did not proceed without SOX2.

In conclusion, we showed a direct dependency of inner ear sensory development on SOX2, but ear neuronal development can proceed without SOX2. Despite the expression of *Sox2* in both neuronal and sensory precursors, our results suggest that the role of SOX2 in the development of inner ear neurons is indirect, necessary for ear neuronal survival, which is dependent on the presence of sensory epithelium.

6. REFERENCES

Ahmed, M., Wong, E. Y., Sun, J., Xu, J., Wang, F. and Xu, P. X. (2012) 'Eya1-Six1 interaction is sufficient to induce hair cell fate in the cochlea by activating Atoh1 expression in cooperation with Sox2', *Dev Cell,* 22(2), pp. 377-90.

Anthwal, N. and Thompson, H. (2016) 'The development of the mammalian outer and middle ear', *J Anat,* 228(2), pp. 217-32.

Avilion, A. A., Nicolis, S. K., Pevny, L. H., Perez, L., Vivian, N. and Lovell-Badge, R. (2003) 'Multipotent cell lineages in early mouse development depend on SOX2 function', *Genes Dev,* 17(1), pp. 126-40.

Barrionuevo, F., Naumann, A., Bagheri-Fam, S., Speth, V., Taketo, M. M., Scherer, G. and Neubüser, A. (2008) 'Sox9 is required for invagination of the otic placode in mice', *Dev Biol,* 317(1), pp. 213-24.

Berglund, A. M. and Ryugo, D. K. (1987) 'Hair cell innervation by spiral ganglion neurons in the mouse', *J Comp Neurol,* 255(4), pp. 560-70.

Bermingham, N. A., Hassan, B. A., Price, S. D., Vollrath, M. A., Ben-Arie, N., Eatock, R. A., Bellen, H. J., Lysakowski, A. and Zoghbi, H. Y. (1999) 'Math1: an essential gene for the generation of inner ear hair cells', *Science,* 284(5421), pp. 1837-41.

Bhattacharyya, S., Bailey, A. P., Bronner-Fraser, M. and Streit, A. (2004) 'Segregation of lens and olfactory precursors from a common territory: cell sorting and reciprocity of Dlx5 and Pax6 expression', *Dev Biol,* 271(2), pp. 403-14.

Bianchi, L. M., Conover, J. C., Fritzsch, B., DeChiara, T., Lindsay, R. M. and Yancopoulos, G. D. (1996) 'Degeneration of vestibular neurons in late embryogenesis of both heterozygous and homozygous BDNF null mutant mice', *Development,* 122(6), pp. 1965-73.

Bok, J., Chang, W. and Wu, D. K. (2007) 'Patterning and morphogenesis of the vertebrate inner ear', *Int J Dev Biol,* 51(6-7), pp. 521-33.

Bouchard, M., de Caprona, D., Busslinger, M., Xu, P. and Fritzsch, B. (2010) 'Pax2 and Pax8 cooperate in mouse inner ear morphogenesis and innervation', *BMC Dev Biol,* 10, pp. 89.

Brooker, R., Hozumi, K. and Lewis, J. (2006) 'Notch ligands with contrasting functions: Jagged1 and Delta1 in the mouse inner ear', *Development,* 133(7), pp. 1277-86.

Burns, J. C., On, D., Baker, W., Collado, M. S. and Corwin, J. T. (2012) 'Over half the hair cells in the mouse utricle first appear after birth, with significant numbers originating from early postnatal mitotic production in peripheral and striolar growth zones', *J Assoc Res Otolaryngol,* 13(5), pp. 609-27.

Burton, Q., Cole, L. K., Mulheisen, M., Chang, W. and Wu, D. K. (2004) 'The role of Pax2 in mouse inner ear development', *Dev Biol,* 272(1), pp. 161-75.

Bylund, M., Andersson, E., Novitch, B. G. and Muhr, J. (2003) 'Vertebrate neurogenesis is counteracted by Sox1-3 activity', *Nat Neurosci,* 6(11), pp. 1162-8.

BYU-Idaho *Anatomy and Physiology, BIO 264 Textbook* https://content.byui.edu/file/a236934c-3c60-4fe9-90aa-d343b3e3a640/1/Textbook/Bio%20264%20Textbook.pdf.

Chang, W., Brigande, J. V., Fekete, D. M. and Wu, D. K. (2004) 'The development of semicircular canals in the inner ear: role of FGFs in sensory cristae', *Development,* 131(17), pp. 4201-11.

Chatterjee, S. and Lufkin, T. (2011) 'The sound of silence: mouse models for hearing loss', *Genet Res Int,* 2011, pp. 416450.

Cheah, K. S. E. and Xu, P.-X. (2016) 'SOX2 in Neurosensory Fate Determination and Differentiation in the Inner Ear', in Kondoh, H. and Lovell-Badge, R. (eds.) *Sox2: Biology and Role in Development and Disease*: Elsevier.

Chen, P., Johnson, J. E., Zoghbi, H. Y. and Segil, N. (2002) 'The role of Math1 in inner ear development: Uncoupling the establishment of the sensory primordium from hair cell fate determination', *Development,* 129(10), pp. 2495-505.

Choi, B. Y., Kim, H. M., Ito, T., Lee, K. Y., Li, X., Monahan, K., Wen, Y., Wilson, E., Kurima, K., Saunders, T. L., Petralia, R. S., Wangemann, P., Friedman, T. B. and Griffith, A. J. (2011) 'Mouse model of enlarged vestibular aqueducts defines temporal requirement of Slc26a4 expression for hearing acquisition', *J Clin Invest,* 121(11), pp. 4516-25.

Chumak, T., Bohuslavova, R., Macova, I., Dodd, N., Buckiova, D., Fritzsch, B., Syka, J. and Pavlinkova, G. (2016) 'Deterioration of the Medial Olivocochlear Efferent System Accelerates Age-Related Hearing Loss in Pax2-Isl1 Transgenic Mice', *Mol Neurobiol,* 53(4), pp. 2368-83.

Corwin, J. T. and Cotanche, D. A. (1988) 'Regeneration of sensory hair cells after acoustic trauma', *Science,* 240(4860), pp. 1772.

Corwin, J. T. and Oberholtzer, J. C. (1997) 'Fish n' Chicks: Model Recipes for Hair-Cell Regeneration?', *Neuron,* 19(5), pp. 951-954.

Croucher, S. J. and Tickle, C. (1989) 'Characterization of epithelial domains in the nasal passages of chick embryos: spatial and temporal mapping of a range of extracellular matrix and cell surface molecules during development of the nasal placode', *Development,* 106(3), pp. 493-509.

D'Amico-Martel, A. and Noden, D. M. (1983) 'Contributions of placodal and neural crest cells to avian cranial peripheral ganglia', *Am J Anat,* 166(4), pp. 445-68.

Dabdoub, A., Puligilla, C., Jones, J. M., Fritzsch, B., Cheah, K. S., Pevny, L. H. and Kelley, M. W. (2008) 'Sox2 signaling in prosensory domain specification and subsequent hair cell differentiation in the developing cochlea', *Proc Natl Acad Sci U S A,* 105(47), pp. 18396-401.

Delacroix, L. and Malgrange, B. (2015) 'Cochlear afferent innervation development', *Hear Res,* 330(Pt B), pp. 157-69.

Deng, M., Yang, H., Xie, X., Liang, G. and Gan, L. (2014) 'Comparative expression analysis of POU4F1, POU4F2 and ISL1 in developing mouse cochleovestibular ganglion neurons', *Gene Expr Patterns,* 15(1), pp. 31-7.

Dong, S., Leung, K. K., Pelling, A. L., Lee, P. Y., Tang, A. S., Heng, H. H., Tsui, L. C., Tease, C., Fisher, G., Steel, K. P. and Cheah, K. S. (2002) 'Circling, deafness, and yellow coat displayed by yellow

submarine (ysb) and light coat and circling (lcc) mice with mutations on chromosome 3', *Genomics,* 79(6), pp. 777-84.

Dvorakova, M., Jahan, I., Macova, I., Chumak, T., Bohuslavova, R., Syka, J., Fritzsch, B. and Pavlinkova, G. (2016) 'Incomplete and delayed Sox2 deletion defines residual ear neurosensory development and maintenance', *Sci Rep,* 6, pp. 38253.

Dvorakova, M., Macova, I., Bohuslavova, R., Anderova, M., Fritzsch, B. and Pavlinkova, G. (2019) 'Early ear neuronal development, but not olfactory or lens development, can proceed without SOX2', *Dev Biol*.

Edmondson, J. C. and Hatten, M. E. (1987) 'Glial-guided granule neuron migration in vitro: a high-resolution time-lapse video microscopic study', *J Neurosci,* 7(6), pp. 1928-34.

Evsen, L., Sugahara, S., Uchikawa, M., Kondoh, H. and Wu, D. K. (2013) 'Progression of neurogenesis in the inner ear requires inhibition of Sox2 transcription by neurogenin1 and neurod1', *J Neurosci,* 33(9), pp. 3879-90.

Faber, S. C., Robinson, M. L., Makarenkova, H. P. and Lang, R. A. (2002) 'Bmp signaling is required for development of primary lens fiber cells', *Development,* 129(15), pp. 3727.

Fariñas, I., Jones, K. R., Tessarollo, L., Vigers, A. J., Huang, E., Kirstein, M., de Caprona, D. C., Coppola, V., Backus, C., Reichardt, L. F. and Fritzsch, B. (2001) 'Spatial shaping of cochlear innervation by temporally regulated neurotrophin expression', *J Neurosci,* 21(16), pp. 6170-80.

Fettiplace, R. (2017) 'Hair Cell Transduction, Tuning, and Synaptic Transmission in the Mammalian Cochlea', *Compr Physiol,* 7(4), pp. 1197-1227.

Fornaro, M., Geuna, S., Fasolo, A. and Giacobini-Robecchi, M. G. (2001) 'Evidence of very early neuronal migration from the olfactory placode of the chick embryo', *Neuroscience,* 107(2), pp. 191-7.

Forni, P. E., Taylor-Burds, C., Melvin, V. S., Williams, T. and Wray, S. (2011) 'Neural crest and ectodermal cells intermix in the nasal placode to give rise to GnRH-1 neurons, sensory neurons, and olfactory ensheathing cells', *J Neurosci,* 31(18), pp. 6915-27.

Freyer, L., Aggarwal, V. and Morrow, B. E. (2011) 'Dual embryonic origin of the mammalian otic vesicle forming the inner ear', *Development,* 138(24), pp. 5403-14.

Friedman, L. M., Dror, A. A. and Avraham, K. B. (2007) 'Mouse models to study inner ear development and hereditary hearing loss', *Int J Dev Biol,* 51(6-7), pp. 609-31.

Fritzsch, B. and Beisel, K. W. (2004) 'Keeping sensory cells and evolving neurons to connect them to the brain: molecular conservation and novelties in vertebrate ear development', *Brain Behav Evol,* 64(3), pp. 182-97.

Fritzsch, B., Duncan, J. S., Kersigo, J., Gray, B. and Elliott, K. L. (2016) 'Neuroanatomical Tracing Techniques in the Ear: History, State of the Art, and Future Developments', *B. Sokolowski, Ed: Auditory and Vestibular Research: Methods and Protocols*: Springer Science+Business Media New York, pp. 243-262.

Fritzsch, B., Pan, N., Jahan, I. and Elliott, K. L. (2015) 'Inner ear development: building a spiral ganglion and an organ of Corti out of unspecified ectoderm', *Cell Tissue Res,* 361(1), pp. 7-24.

Fuchs, P. A. and Glowatzki, E. (2015) 'Synaptic studies inform the functional diversity of cochlear afferents', *Hear Res,* 330(Pt A), pp. 18-25.

Gill, G. N. (1995) 'The enigma of LIM domains', *Structure,* 3(12), pp. 1285-1289.

Goldsmith, T. H. (1990) 'Optimization, Constraint, and History in the Evolution of Eyes', *The Quarterly Review of Biology,* 65(3), pp. 281-322.

Graham, V., Khudyakov, J., Ellis, P. and Pevny, L. (2003) 'SOX2 functions to maintain neural progenitor identity', *Neuron,* 39(5), pp. 749-65.

Groves, A. K. and Fekete, D. M. (2012) 'Shaping sound in space: the regulation of inner ear patterning', *Development,* 139(2), pp. 245-57.

Gu, R., Brown, R. M., Hsu, C. W., Cai, T., Crowder, A. L., Piazza, V. G., Vadakkan, T. J., Dickinson, M. E. and Groves, A. K. (2016) 'Lineage tracing of Sox2-expressing progenitor cells in the mouse inner ear reveals a broad contribution to non-sensory tissues and insights into the origin of the organ of Corti', *Dev Biol,* 414(1), pp. 72-84.

Guo, Z., Packard, A., Krolewski, R. C., Harris, M. T., Manglapus, G. L. and Schwob, J. E. (2010) 'Expression of pax6 and sox2 in adult olfactory epithelium', *J Comp Neurol,* 518(21), pp. 4395-418.

Haddon, C., Jiang, Y. J., Smithers, L. and Lewis, J. (1998) 'Delta-Notch signalling and the patterning of sensory cell differentiation in the zebrafish ear: evidence from the mind bomb mutant', *Development,* 125(23), pp. 4637-44.

Heavner, W. and Pevny, L. (2012) 'Eye development and retinogenesis', *Cold Spring Harb Perspect Biol,* 4(12).

Heavner, W. E., Andoniadou, C. L. and Pevny, L. H. (2014) 'Establishment of the neurogenic boundary of the mouse retina requires cooperation of SOX2 and WNT signaling', *Neural Dev,* 9, pp. 27.

Hebert, J. M. and McConnell, S. K. (2000) 'Targeting of cre to the Foxg1 (BF-1) locus mediates loxP recombination in the telencephalon and other developing head structures', *Dev Biol,* 222(2), pp. 296-306.

Hemond, S. G. and Morest, D. K. (1991) 'Ganglion formation from the otic placode and the otic crest in the chick embryo: mitosis, migration, and the basal lamina', *Anat Embryol (Berl),* 184(1), pp. 1-13.

Hobert, O. and Westphal, H. (2000) 'Functions of LIM-homeobox genes', *Trends Genet,* 16(2), pp. 75-83.

Hume, C. R., Bratt, D. L. and Oesterle, E. C. (2007) 'Expression of LHX3 and SOX2 during mouse inner ear development', *Gene Expr Patterns,* 7(7), pp. 798-807.

Jaalouk, D. and Lammerding, J. (2009) 'Mechanotransduction gone awry', *Nature reviews. Molecular cell biology,* 10, pp. 63-73.

Jacques, B. E., Puligilla, C., Weichert, R. M., Ferrer-Vaquer, A., Hadjantonakis, A. K., Kelley, M. W. and Dabdoub, A. (2012) 'A dual function for canonical Wnt/β-catenin signaling in the developing mammalian cochlea', *Development,* 139(23), pp. 4395-404.

Jahan, I., Pan, N., Kersigo, J. and Fritzsch, B. (2010) 'Neurod1 suppresses hair cell differentiation in ear ganglia and regulates hair cell subtype development in the cochlea', *PLoS One,* 5(7), pp. e11661.

Jahan, I., Pan, N., Kersigo, J. and Fritzsch, B. (2015) 'Neurog1 can partially substitute for Atoh1 function in hair cell differentiation and maintenance during organ of Corti development', *Development,* 142(16), pp. 2810-21.

Kamachi, Y. and Kondoh, H. (2013) 'Sox proteins: regulators of cell fate specification and differentiation', *Development,* 140(20), pp. 4129-44.

Kamachi, Y., Uchikawa, M., Tanouchi, A., Sekido, R. and Kondoh, H. (2001) 'Pax6 and SOX2 form a co-DNA-binding partner complex that regulates initiation of lens development', *Genes Dev,* 15(10), pp. 1272-86.

Kanakubo, S., Nomura, T., Yamamura, K., Miyazaki, J., Tamai, M. and Osumi, N. (2006) 'Abnormal migration and distribution of neural crest cells in Pax6 heterozygous mutant eye, a model for human eye diseases', *Genes Cells,* 11(8), pp. 919-33.

Kandler, K., Clause, A. and Noh, J. (2009) 'Tonotopic reorganization of developing auditory brainstem circuits', *Nat Neurosci,* 12(6), pp. 711-7.

Kaplan, M. S. and Hinds, J. W. (1977) 'Neurogenesis in the adult rat: electron microscopic analysis of light radioautographs', *Science,* 197(4308), pp. 1092-4.

Karis, A., Pata, I., van Doorninck, J. H., Grosveld, F., de Zeeuw, C. I., de Caprona, D. and Fritzsch, B. (2001) 'Transcription factor GATA-3 alters pathway selection of olivocochlear neurons and affects morphogenesis of the ear', *J Comp Neurol,* 429(4), pp. 615-30.

Kempfle, J. S., Turban, J. L. and Edge, A. S. (2016) 'Sox2 in the differentiation of cochlear progenitor cells', *Sci Rep,* 6, pp. 23293.

Kiernan, A. E., Pelling, A. L., Leung, K. K., Tang, A. S., Bell, D. M., Tease, C., Lovell-Badge, R., Steel, K. P. and Cheah, K. S. (2005) 'Sox2 is required for sensory organ development in the mammalian inner ear', *Nature,* 434(7036), pp. 1031-5.

Kim, W. Y., Fritzsch, B., Serls, A., Bakel, L. A., Huang, E. J., Reichardt, L. F., Barth, D. S. and Lee, J. E. (2001) 'NeuroD-null mice are deaf due to a severe loss of the inner ear sensory neurons during development', *Development,* 128(3), pp. 417-26.

Kondoh, H. and Lovell-Badge, R. (2016) 'Historical Perspectives', in Kondoh, H. and Lovell-Badge, R. (eds.) *Sox2: Biology and Role in Development and Disease*: Elsevier.

Kopecky, B., Johnson, S., Schmitz, H., Santi, P. and Fritzsch, B. (2012a) 'Scanning thin-sheet laser imaging microscopy elucidates details on mouse ear development', *Dev Dyn,* 241(3), pp. 465-80.

Kopecky, B. J., Duncan, J. S., Elliott, K. L. and Fritzsch, B. (2012b) 'Three-dimensional reconstructions from optical sections of thick mouse inner ears using confocal microscopy', *J Microsc,* 248(3), pp. 292-8.

Králíček, P. (2004) *Úvod do speciální neurofyziologie.* Praha: Univerzita Karlova v Praze - Nakladatelství Karolinum.

Lam, E. W., Brosens, J. J., Gomes, A. R. and Koo, C. Y. (2013) 'Forkhead box proteins: tuning forks for transcriptional harmony', *Nat Rev Cancer,* 13(7), pp. 482-95.

Lanford, P. J., Lan, Y., Jiang, R., Lindsell, C., Weinmaster, G., Gridley, T. and Kelley, M. W. (1999) 'Notch signalling pathway mediates hair cell development in mammalian cochlea', *Nat Genet,* 21(3), pp. 289-92.

Lee, Y. S., Liu, F. and Segil, N. (2006) 'A morphogenetic wave of p27Kip1 transcription directs cell cycle exit during organ of Corti development', *Development,* 133(15), pp. 2817-26.

Li, H., Tierney, C., Wen, L., Wu, J. Y. and Rao, Y. (1997) 'A single morphogenetic field gives rise to two retina primordia under the influence of the prechordal plate', *Development,* 124(3), pp. 603-15.

Li, H. J., Kapoor, A., Giel-Moloney, M., Rindi, G. and Leiter, A. B. (2012) 'Notch signaling differentially regulates the cell fate of early endocrine precursor cells and their maturing descendants in the mouse pancreas and intestine', *Dev Biol,* 371(2), pp. 156-69.

Lim, D. J. (1986) 'Functional structure of the organ of Corti: a review', *Hear Res,* 22, pp. 117-46.

Litsiou, A., Hanson, S. and Streit, A. (2005) 'A balance of FGF, BMP and WNT signalling positions the future placode territory in the head', *Development,* 132(18), pp. 4051-62.

Liu, C., Glowatzki, E. and Fuchs, P. A. (2015) 'Unmyelinated type II afferent neurons report cochlear damage', *Proc Natl Acad Sci U S A,* 112(47), pp. 14723-7.

Liu, M., Pereira, F. A., Price, S. D., Chu, M. J., Shope, C., Himes, D., Eatock, R. A., Brownell, W. E., Lysakowski, A. and Tsai, M. J. (2000) 'Essential role of BETA2/NeuroD1 in development of the vestibular and auditory systems', *Genes Dev,* 14(22), pp. 2839-54.

Liu, Z., Walters, B. J., Owen, T., Brimble, M. A., Steigelman, K. A., Zhang, L., Mellado Lagarde, M. M., Valentine, M. B., Yu, Y., Cox, B. C. and Zuo, J. (2012) 'Regulation of p27Kip1 by Sox2 maintains quiescence of inner pillar cells in the murine auditory sensory epithelium', *J Neurosci,* 32(31), pp. 10530-40.

Luo, X. J., Deng, M., Xie, X., Huang, L., Wang, H., Jiang, L., Liang, G., Hu, F., Tieu, R., Chen, R. and Gan, L. (2013) 'GATA3 controls the specification of prosensory domain and neuronal survival in the mouse cochlea', *Hum Mol Genet,* 22(18), pp. 3609-23.

López-Elizalde, R., Campero, A., Sánchez-Delgadillo, T., Lemus-Rodríguez, Y., López-González, M. I. and Godínez-Rubí, M. (2018) 'Anatomy of the olfactory nerve: A comprehensive review with cadaveric dissection', *Clin Anat,* 31(1), pp. 109-117.

Ma, Q., Anderson, D. J. and Fritzsch, B. (2000) 'Neurogenin 1 null mutant ears develop fewer, morphologically normal hair cells in smaller sensory epithelia devoid of innervation', *J Assoc Res Otolaryngol,* 1(2), pp. 129-43.

Ma, Q., Chen, Z., del Barco Barrantes, I., de la Pompa, J. L. and Anderson, D. J. (1998) 'neurogenin1 is essential for the determination of neuronal precursors for proximal cranial sensory ganglia', *Neuron,* 20(3), pp. 469-82.

Madisen, L., Zwingman, T. A., Sunkin, S. M., Oh, S. W., Zariwala, H. A., Gu, H., Ng, L. L., Palmiter, R. D., Hawrylycz, M. J., Jones, A. R., Lein, E. S. and Zeng, H. (2010) 'A robust and high-throughput Cre reporting and characterization system for the whole mouse brain', *Nat Neurosci,* 13(1), pp. 133-40.

Maier, E., von Hofsten, J., Nord, H., Fernandes, M., Paek, H., Hébert, J. M. and Gunhaga, L. (2010) 'Opposing Fgf and Bmp activities regulate the specification of olfactory sensory and respiratory epithelial cell fates', *Development,* 137(10), pp. 1601-11.

Maier, E. C., Saxena, A., Alsina, B., Bronner, M. E. and Whitfield, T. T. (2014) 'Sensational placodes: neurogenesis in the otic and olfactory systems', *Dev Biol,* 389(1), pp. 50-67.

Mak, A. C., Szeto, I. Y., Fritzsch, B. and Cheah, K. S. (2009) 'Differential and overlapping expression pattern of SOX2 and SOX9 in inner ear development', *Gene Expr Patterns,* 9(6), pp. 444-53.

Maklad, A., Kamel, S., Wong, E. and Fritzsch, B. (2010) 'Development and organization of polarity-specific segregation of primary vestibular afferent fibers in mice', *Cell Tissue Res,* 340(2), pp. 303-21.

Masui, S., Nakatake, Y., Toyooka, Y., Shimosato, D., Yagi, R., Takahashi, K., Okochi, H., Okuda, A., Matoba, R., Sharov, A. A., Ko, M. S. and Niwa, H. (2007) 'Pluripotency governed by Sox2 via regulation of Oct3/4 expression in mouse embryonic stem cells', *Nat Cell Biol,* 9(6), pp. 625-35.

Matei, V., Pauley, S., Kaing, S., Rowitch, D., Beisel, K. W., Morris, K., Feng, F., Jones, K., Lee, J. and Fritzsch, B. (2005) 'Smaller inner ear sensory epithelia in Neurog 1 null mice are related to earlier hair cell cycle exit', *Dev Dyn,* 234(3), pp. 633-50.

MayoClinic *Parts of the ear*. https://www.mayoclinic.org/diseases-conditions/hearing-loss/multimedia/ear-infections/sls-20077144?s=1 (Accessed: 6.3.2020.

Milardi, D., Cacciola, A., Calamuneri, A., Ghilardi, M. F., Caminiti, F., Cascio, F., Andronaco, V., Anastasi, G., Mormina, E., Arrigo, A., Bruschetta, D. and Quartarone, A. (2017) 'The Olfactory System Revealed: Non-Invasive Mapping by using Constrained Spherical Deconvolution Tractography in Healthy Humans', *Front Neuroanat,* 11, pp. 32.

Mombaerts, P. (1999) 'Molecular biology of odorant receptors in vertebrates', *Annu Rev Neurosci,* 22, pp. 487-509.

Mui, S. H., Hindges, R., O'Leary, D. D., Lemke, G. and Bertuzzi, S. (2002) 'The homeodomain protein Vax2 patterns the dorsoventral and nasotemporal axes of the eye', *Development,* 129(3), pp. 797-804.

Muniak, M. A., Rivas, A., Montey, K. L., May, B. J., Francis, H. W. and Ryugo, D. K. (2013) '3D model of frequency representation in the cochlear nucleus of the CBA/J mouse', *J Comp Neurol,* 521(7), pp. 1510-32.

Najrana, T. and Sanchez-Esteban, J. (2016) 'Mechanotransduction as an Adaptation to Gravity', *Frontiers in Pediatrics,* 4, pp. 140.

NationalEyeInstitute (2012) *Drawing of the Eye*. https://www.flickr.com/photos/nationaleyeinstitute/7544457124/in/photostream/ (Accessed: 10.12. 2018).

Naya, F. J., Huang, H. P., Qiu, Y., Mutoh, H., DeMayo, F. J., Leiter, A. B. and Tsai, M. J. (1997) 'Diabetes, defective pancreatic morphogenesis, and abnormal enteroendocrine differentiation in BETA2/neuroD-deficient mice', *Genes Dev,* 11(18), pp. 2323-34.

Naya, F. J., Stellrecht, C. M. and Tsai, M. J. (1995) 'Tissue-specific regulation of the insulin gene by a novel basic helix-loop-helix transcription factor', *Genes Dev,* 9(8), pp. 1009-19.

Neves, J., Kamaid, A., Alsina, B. and Giraldez, F. (2007) 'Differential expression of Sox2 and Sox3 in neuronal and sensory progenitors of the developing inner ear of the chick', *J Comp Neurol,* 503(4), pp. 487-500.

Nieuwenhuys, R., Voogd, J. and van Huijzen , C. (1988) *The Human Central Nervous System: A Synopsis and Atlas.* Germany: Springer, p. 733-747.

Noden, D. M. and Van de Water, T. R. (1992) 'Genetic analyses of mammalian ear development', *Trends Neurosci,* 15(7), pp. 235-7.

Ohlemiller, K. K., Jones, S. M. and Johnson, K. R. (2016) 'Application of Mouse Models to Research in Hearing and Balance', *J Assoc Res Otolaryngol,* 17(6), pp. 493-523.

OpenWetWare (2006) *Olfactory receptor*. https://openwetware.org/wiki/BIO254:ORs (Accessed: 29.1. 2019).

Pan, N., Jahan, I., Kersigo, J., Duncan, J. S., Kopecky, B. and Fritzsch, B. (2012) 'A novel Atoh1 "self-terminating" mouse model reveals the necessity of proper Atoh1 level and duration for hair cell differentiation and viability', *PLoS One,* 7(1), pp. e30358.

Panaliappan, T. K., Wittmann, W., Jidigam, V. K., Mercurio, S., Bertolini, J. A., Sghari, S., Bose, R., Patthey, C., Nicolis, S. K. and Gunhaga, L. (2018) 'Sox2 is required for olfactory pit formation and olfactory neurogenesis through BMP restriction and', *Development,* 145(2).

Pandit, T., Jidigam, V. K. and Gunhaga, L. (2011) 'BMP-induced L-Maf regulates subsequent BMP-independent differentiation of primary lens fibre cells', *Developmental Dynamics,* 240(8), pp. 1917-1928.

Pauley, S., Lai, E. and Fritzsch, B. (2006) 'Foxg1 is required for morphogenesis and histogenesis of the mammalian inner ear', *Dev Dyn,* 235(9), pp. 2470-82.

Pauley, S., Wright, T. J., Pirvola, U., Ornitz, D., Beisel, K. and Fritzsch, B. (2003) 'Expression and function of FGF10 in mammalian inner ear development', *Dev Dyn,* 227(2), pp. 203-15.

Pevny, L. H. and Nicolis, S. K. (2010) 'Sox2 roles in neural stem cells', *Int J Biochem Cell Biol,* 42(3), pp. 421-4.

Pfaff, S. L., Mendelsohn, M., Stewart, C. L., Edlund, T. and Jessell, T. M. (1996) 'Requirement for LIM homeobox gene Isl1 in motor neuron generation reveals a motor neuron-dependent step in interneuron differentiation', *Cell,* 84(2), pp. 309-20.

Pieper, M., Ahrens, K., Rink, E., Peter, A. and Schlosser, G. (2012) 'Differential distribution of competence for panplacodal and neural crest induction to non-neural and neural ectoderm', *Development,* 139(6), pp. 1175-87.

Preibisch, S., Saalfeld, S. and Tomancak, P. (2009) 'Globally optimal stitching of tiled 3D microscopic image acquisitions', *Bioinformatics,* 25(11), pp. 1463-5.

Puligilla, C., Dabdoub, A., Brenowitz, S. D. and Kelley, M. W. (2010) 'Sox2 induces neuronal formation in the developing mammalian cochlea', *J Neurosci,* 30(2), pp. 714-22.

Purves, D., Augustine, G. J., Fitzpatrick, D., Katz, L. C., LaMantia, A.-S., McNamara, J. O. and Williams, S. M. (2001) *Neuroscience , 2nd edition. Central Vestibular Pathways: Eye, Head, and Body Reflexes*: Sunderland (MA): Sinauer Associates.

Quinn, J. C., West, J. D. and Hill, R. E. (1996) 'Multiple functions for Pax6 in mouse eye and nasal development', *Genes Dev,* 10(4), pp. 435-46.

Radde-Gallwitz, K., Pan, L., Gan, L., Lin, X., Segil, N. and Chen, P. (2004) 'Expression of Islet1 marks the sensory and neuronal lineages in the mammalian inner ear', *J Comp Neurol,* 477(4), pp. 412-21.

Raft, S. and Groves, A. K. (2015) 'Segregating neural and mechanosensory fates in the developing ear: patterning, signaling, and transcriptional control', *Cell Tissue Res,* 359(1), pp. 315-32.

Raphael, Y. (1992) 'Evidence for supporting cell mitosis in response to acoustic trauma in the avian inner ear', *J Neurocytol,* 21(9), pp. 663-71.

Remington, L. A. (2012) 'Visual Pathway', in *Clinical Anatomy and Physiology of the Visual System (Third Edition)*. pp. 233-252 [Online]. Version.

Rosowski, J. J. (2003) 'The Middle and External Ears of Terrestrial Vertebrates as Mechanical and Acoustic Transducers', in Barth, F.G., Humphrey, J.A.C. and Secomb, T.W. (eds.) *Sensors and Sensing in Biology and Engineering*. Vienna: Springer Vienna, pp. 59-69.

Rubel, E. W. and Fritzsch, B. (2002) 'Auditory system development: primary auditory neurons and their targets', *Annu Rev Neurosci,* 25, pp. 51-101.

Ruben, R. J. (1967) 'Development of the inner ear of the mouse: a radioautographic study of terminal mitoses', *Acta Otolaryngol*, pp. Suppl 220:1-44.

Sai, X. and Ladher, R. K. (2015) 'Early steps in inner ear development: induction and morphogenesis of the otic placode', *Front Pharmacol,* 6, pp. 19.

Satoh, T. and Fekete, D. M. (2005) 'Clonal analysis of the relationships between mechanosensory cells and the neurons that innervate them in the chicken ear', *Development,* 132(7), pp. 1687-97.

Schimmang, T. and Pirvola, U. (2013) 'Coupling the cell cycle to development and regeneration of the inner ear', *Semin Cell Dev Biol,* 24(5), pp. 507-13.

Schlosser, G. (2006) 'Induction and specification of cranial placodes', *Dev Biol,* 294(2), pp. 303-51.

Schwanzel-Fukuda, M. and Pfaff, D. W. (1989) 'Origin of luteinizing hormone-releasing hormone neurons', *Nature,* 338(6211), pp. 161-4.

Shaham, O., Smith, A. N., Robinson, M. L., Taketo, M. M., Lang, R. A. and Ashery-Padan, R. (2009) 'Pax6 is essential for lens fiber cell differentiation', *Development,* 136(15), pp. 2567-78.

Simpson, K. L. (2018) 'Chapter 23 - Olfaction and Taste', in Haines, D.E. and Mihailoff, G.A. (eds.) *Fundamental Neuroscience for Basic and Clinical Applications (Fifth Edition)*: Elsevier, pp. 334-345.e1.

Sjöqvist, M. and Andersson, E. R. (2019) 'Do as I say, Not(ch) as I do: Lateral control of cell fate', *Developmental Biology,* 447(1), pp. 58-70.

Steevens, A. R., Glatzer, J. C., Kellogg, C. C., Low, W. C., Santi, P. A. and Kiernan, A. E. (2019) 'SOX2 is required for inner ear growth and cochlear nonsensory formation before sensory development', *Development,* 146(13).

Steevens, A. R., Sookiasian, D. L., Glatzer, J. C. and Kiernan, A. E. (2017) 'SOX2 is required for inner ear neurogenesis', *Sci Rep,* 7(1), pp. 4086.

Streit, A. (2008) 'The cranial sensory nervous system: specification of sensory progenitors and placodes', *StemBook [Internet]*: Cambridge (MA): Harvard Stem Cell Institute.

Takahashi, K. and Yamanaka, S. (2006) 'Induction of pluripotent stem cells from mouse embryonic and adult fibroblast cultures by defined factors', *Cell,* 126(4), pp. 663-76.

Tao, W. and Lai, E. (1992) 'Telencephalon-restricted expression of BF-1, a new member of the HNF-3/fork head gene family, in the developing rat brain', *Neuron,* 8(5), pp. 957-66.

Taranova, O. V., Magness, S. T., Fagan, B. M., Wu, Y., Surzenko, N., Hutton, S. R. and Pevny, L. H. (2006) 'SOX2 is a dose-dependent regulator of retinal neural progenitor competence', *Genes Dev,* 20(9), pp. 1187-202.

Thompson, H. and Tucker, A. S. (2013) 'Dual origin of the epithelium of the mammalian middle ear', *Science,* 339(6126), pp. 1453-6.

Torres, M. and Giráldez, F. (1998) 'The development of the vertebrate inner ear', *Mech Dev,* 71(1-2), pp. 5-21.

UTHealth (2011) *Lab 6 - Auditory, Vestibular, Gustatory and Olfaction Systems*. The Vestibular System - Introduction. https://nba.uth.tmc.edu/neuroanatomy/L6/Lab06p04_index.html (Accessed: 8.3.2020.

Werner, M. H., Huth, J. R., Gronenborn, A. M. and Clore, G. M. (1995) 'Molecular basis of human 46X,Y sex reversal revealed from the three-dimensional solution structure of the human SRY-DNA complex', *Cell,* 81(5), pp. 705-14.

Wood, H. B. and Episkopou, V. (1999) 'Comparative expression of the mouse Sox1, Sox2 and Sox3 genes from pre-gastrulation to early somite stages', *Mech Dev,* 86(1-2), pp. 197-201.

Xuan, S., Baptista, C. A., Balas, G., Tao, W., Soares, V. C. and Lai, E. (1995) 'Winged helix transcription factor BF-1 is essential for the development of the cerebral hemispheres', *Neuron,* 14(6), pp. 1141-52.

Yang, L., Cai, C. L., Lin, L., Qyang, Y., Chung, C., Monteiro, R. M., Mummery, C. L., Fishman, G. I., Cogen, A. and Evans, S. (2006) 'Isl1Cre reveals a common Bmp pathway in heart and limb development', *Development,* 133(8), pp. 1575-85.

Yang, T., Kersigo, J., Jahan, I., Pan, N. and Fritzsch, B. (2011) 'The molecular basis of making spiral ganglion neurons and connecting them to hair cells of the organ of Corti', *Hear Res,* 278(1-2), pp. 21-33.

Zaghloul, N. A., Yan, B. and Moody, S. A. (2005) 'Step-wise specification of retinal stem cells during normal embryogenesis', *Biol Cell,* 97(5), pp. 321-37.

Zheng, J., Shen, W., He, D. Z., Long, K. B., Madison, L. D. and Dallos, P. (2000) 'Prestin is the motor protein of cochlear outer hair cells', *Nature,* 405(6783), pp. 149-55.

Zou, D., Erickson, C., Kim, E. H., Jin, D., Fritzsch, B. and Xu, P. X. (2008) 'Eya1 gene dosage critically affects the development of sensory epithelia in the mammalian inner ear', *Hum Mol Genet,* 17(21), pp. 3340-56.